BARC

HIGHLIGHTS

ENVIRONMENTAL SCIENCES AND ENGINEERING

BARC HIGHLIGHTS

ENVIRONMENTAL SCIENCES AND ENGINEERING

भारत सरकार
Government of India

भाभा परमाणु अनुसंधान केंद्र
BHABHA ATOMIC RESEARCH CENTRE

स्वर्ण जयंती वर्ष
GOLDEN JUBILEE YEAR
2006-2007

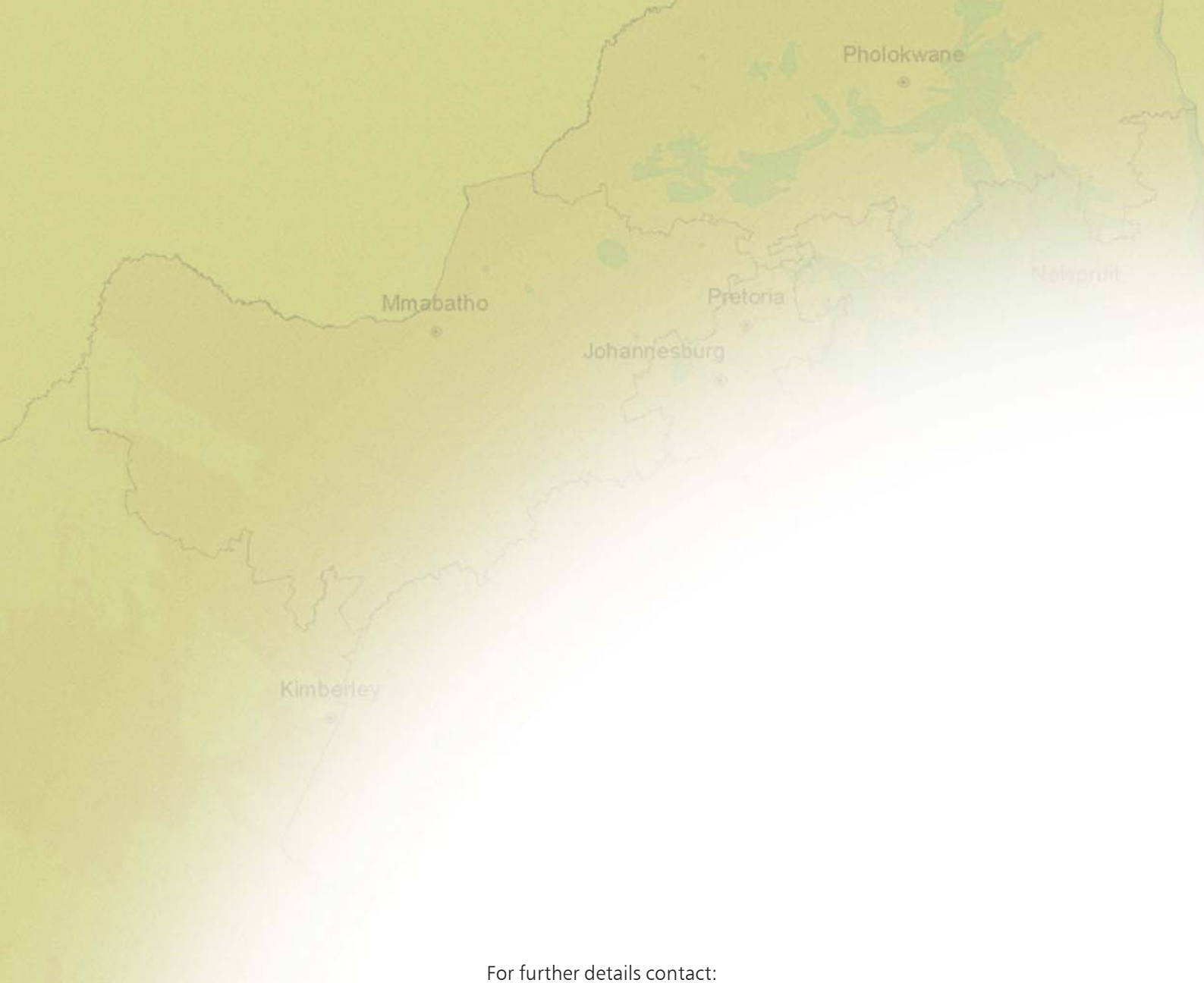

For further details contact:

Dr. Y. S. Mayya
Head, Aerosol, Monitoring and Simulation Section
Environmental Assessment Division
Bhabha Atomic Research Centre,Trombay, Mumbai - 400 085, India.

E mail: mayyays@barc.gov.in

Published by :

Dr. Vijai Kumar
Associate Director, Knowledge Management Group and
Head, Scientific Information Resource Division,
Bhabha Atomic Research Centre, Trombay, Mumbai - 400 085, India.

E mail: vijai@barc.gov.in

FOREWORD

Bhabha Atomic Research Centre (BARC) is celebrating its golden jubilee year during 2006-07. On 20th January, 1956, Pandit Jawaharlal Nehru formally inaugurated the Atomic Energy Establishment Trombay (AEET), which was renamed Bhabha Atomic Research Centre (BARC) on January 22, 1967. As a premier R&D centre of the Department of Atomic Energy (DAE), BARC has a mandate to provide R&D support to the nuclear power programme, to pursue all activities related to nuclear fuel cycle, to operate research reactors for supporting neutron beam research and supplying radioisotopes for various applications, to conduct frontline basic research in physical, chemical, biological and engineering sciences all of which lead towards improving quality of life of our people. The achievements BARC has made over the last 50 years are well known not only to the scientific community in the country but also to our people at large. Scientific achievements made by this premier research centre are well documented in various publications of DAE including the series "BARC Highlights". During this golden jubilee year, we have made an effort to bring out some glimpses of recent research and development accomplishments in the form of 8 volumes, highlighting the following areas:

1. Nuclear Fuel Cycle
2. Physical Sciences
3. Chemical Science and Engineering
4. Materials Science and Engineering
5. Life Sciences
6. Reactor Technology and Engineering
7. Electronics, Instrumentation and Computers
8. Environmental Science and Engineering

These volumes will showcase the latest work in the aforementioned areas and will demonstrate how each of these is directed towards achieving the overall goal of using nuclear energy for the benefit of our people.

Nuclear energy programme in India has now reached a level of maturity. Today, India is self-sufficient in building nuclear power stations of 540 MWe capacities and has gained sufficient mastery over the entire fuel cycle. We are at the threshold of entering the second stage of nuclear power programme, in which a rapid growth in installed capacity is expected through the fast reactor programme. In the area of basic research in science and engineering, BARC has been maintaining a lead position both in national and international scenarios. One of the strongest points of basic research in BARC lies in its capability in building in-house sophisticated research facilities. The core competence of the scientists and engineers in our centre covers a very wide range as is reflected in the 8 companion volumes released on the occasion of the golden jubilee year.

This volume highlights the achievements made during the last few years in the area of Environmental Sciences and Engineering. Measurement of radiation levels and of concentration of pollutants constitutes the most important component of environmental assessment. The techniques employed depend upon the type of parameters monitored and the objective behind monitoring. BARC scientists posted in a number of environmental survey laboratories located at nuclear power stations, reprocessing units and uranium mines, maintained a constant vigil on the environment in and around the areas where atomic activities are being pursued. The laboratories in association with the central unit at Trombay begin their work for collecting the lease line environmental data even before an activity starts in a new location and keep monitoring the impact of our activities on the environment. Study of long term impact also requires study of natural radiation environment in different regions of the country through large scale surveys. BARC's programme in Health, Safety & Environment has evolved in a unified risk assessment methodology through studies on radiation and conventional pollutants in an integrated manner.

BARC has adopted computational methods based on the atmospheric and aquatic dispersion models for estimating the environmental impact. These models requiring a host of meteorological parameters as input variables can map the spread of radioactivity and pollutants on real time basis.

Radiations and radioisotopes find important applications in industrial radiography, cancer treatment and medical diagnostics. In order to minimise unwanted exposures either to patients, their family members or to personnel handling these sources, appropriate shielding designs and dosimetric plans are evolved and these services are provided to the organisations to handle such radioactive sources.

Preparedness for the scenarios of probable nuclear and radiological emergencies in the country constitutes an important activity of the environmental safety programmes of BARC. As a first step, it is required to obtain online information on the radiation levels at various parts of the country through a well connected network of online radiation monitoring systems. It is also necessary to have an integrated decision support system and mobile monitoring facility to take countermeasures in case of nuclear and radiological emergency in the public domain. Safety assessment of Nuclear Power Reactors calls for laboratory scale studies for validating the computer codes used for source term prediction to the environment in the event of accidents. Apart from these, constant efforts are made in BARC to develop systems and techniques for scientific studies related to the assessment of the environment and application of nuclear techniques in other areas such as geological dating.

The present volume will provide an outline of the varied activities of BARC in Environmental Sciences and Engineering.

Srikumar Banerjee
Director

PREFACE

In recent years, environmental issues are playing an increasing role in considering the options available for energy production, a prerequisite for steering the course of national development. In the context of nuclear power, environmental protection and safeguards are inextricably linked to the setting up, operation and decommissioning of the entire fuel cycle facilities. Broadly speaking, these pertain to the protection of occupational workers, general public and the environment at large. In the occupational domain, the radiation exposures to workers should be controlled so as to meet the rigorous standards stipulated by regulatory agencies. This is achieved both at the level of design and at the level of operations. In the same manner, discharges from nuclear facilities to the public domain need to be controlled to within specified international standards. It is mandatory to ensure compliance to these standards by conducting regular environmental surveys, which in their totality, include studies on natural background radiation. In addition, one needs to address issues pertaining to the environmental consequences of extremely low probability reactor accidents as well as possible radiological emergencies. All these call for the setting up of elaborate programmes on field monitoring, predictive modeling, laboratory studies and emergency preparedness. These in essence form the activities being pursued in BARC in the area of environmental science and engineering.

The collection of articles in this "Highlights Volume" brings out the progress made in BARC in the areas mentioned above, over the last few years. The volume essentially intends to provide a flavour of the different facets of environmental studies, rather than present individual activities being carried out in various divisions. Keeping this in mind, the articles are arranged into four broad sections, namely,

I. Environmental assessment methodologies,
II. Modeling pollutant dispersion in the environment,
III. Safety in industrial and medical applications of radiation,
IV. Development of facilities, systems and techniques.

The first section deals with the methodologies used for monitoring radiation, radioactivity and other pollutants in the environment for carrying out impact assessment. The second section contains articles on the development of mathematical models and computer codes for understanding the processes and strengthening the prediction capabilities of pollutant behaviour in the environment. The third section deals with radiological safety aspects pertaining to the use of radiation sources in hospitals and in industries. The last section deals with the development of online systems as well as various other techniques for environmental applications. On the whole, the articles are written in a style that informs the reader on the motivation behind the studies and give essentially a glimpse of the depth involved in the subject. The references listed at the end of each article are intended to guide the interested reader to additional details.

I wish to thank all the contributors for their efforts in condensing their work in the form of short articles without compromising on the essence of the subject matter. I also acknowledge the help received from Dr. B.K. Sapra, EAD, in compiling this volume. I am grateful to Mr. H.S.Kushwaha, Director, Health, Safety and Environment Group for his guidance in bringing out this volume.

Y.S. Mayya

ENVIRONMENTAL SCIENCES AND ENGINEERING

CONTENTS

1. ENVIRONMENTAL ASSESSMENT METHODOLOGIES

INTRODUCTION

Measurement of radiation levels and concentration of pollutants constitute the most important component of environmental assessment. The techniques employed not only depend upon the type of parameters monitored, but also on the objective behind monitoring. In the context of environmental radioactivity, a quick assessment, using aerial survey techniques for meeting an emergency situation and long term assessment, using chemical/analytical techniques for understanding incremental changes due to discharges from nuclear facilities, provide striking examples of the two ends of the monitoring spectrum. Study of long term impact also requires the understanding of natural radiation environment in different regions of the country and this is obtained through large scale surveys. While pursuing excellence in these areas, one has also to keep one's vision open to the role of conventional pollutants and their effect on human health. Efforts are made in Health, Safety & Environment Programme of BARC to evolve a unified risk assessment methodology through studies on radiation and conventional pollutants in an integrated manner. This section highlights these perspectives by putting together a collection of nine illustrative articles in each of these areas.

1.1 AERIAL SURVEY TECHNIQUES FOR GAMMA RADIATION MONITORING

In the event of a nuclear reactor accident, there may be radioactivity deposited over a large area which is to be assessed quickly to initiate prompt counter and control measures including evacuation of public or restrictions of agriculture produce from the affected areas. Aerial gamma survey can be used as a reliable and effective technique to assess the ground contamination for demarking the affected areas. This technique can also be used for plume tracking, searching of radioactive sources and for mapping the background in EPZ around a NPP site periodically. For this purpose a compact Aerial Gamma Spectrometry System (AGSS) has been developed by Radiation Safety and Systems Division (RSSD) to strengthen the emergency preparedness program of DAE. The system can be deployed in any mobile platform including an aircraft. The other radiation monitoring systems based on mobile platform are Compact Aerial Radiation Monitoring System(CARMS), Compact Mobile Gamma Spectrometry System (CMGS) developed for similar applications as of AGSS.

Aerial Gamma Spectrometry System

■ System Configuration

The AGSS is a compact, light weight, easily upgradeable and vibration and shock-proof system configured around an industrial PC with LCD monitor. The system is fitted in a vibration and shock proof trolley. It consists of the following subsystems.

a) Detector: Uses either single or four NaI(Tl) scintillation detectors in detector enclosure.

b) MultiChannel Analyser (MCA): A 512 channel PHA designed around two PC Add-on cards for contiguous spectrometric data acquisition of shorter durations. The ADC is a flash type.

c) Global Positioning System (GPS): A six channel receiver that provides positional coordinates (Longitude/Latitude) and time through NEMA-183 port every alternate second.

d) Radio MODEM & VHF Set: Commercially available units for on-line data transmission from aircraft to ground.

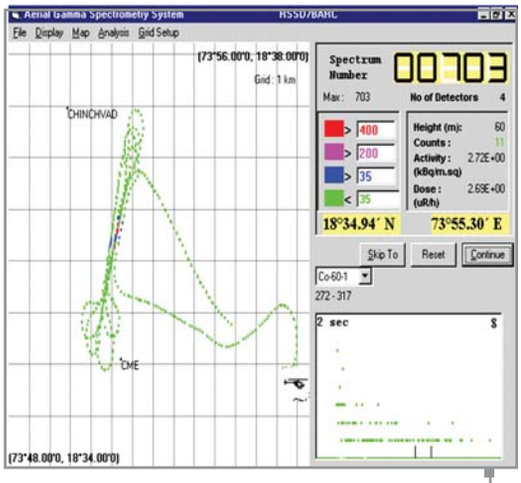

Screen Display

PCGS System with its detector in an enclosure and GPS receiver

System Software

The system software is developed in VB operating under MS Windows 95/98 and has the following features:-

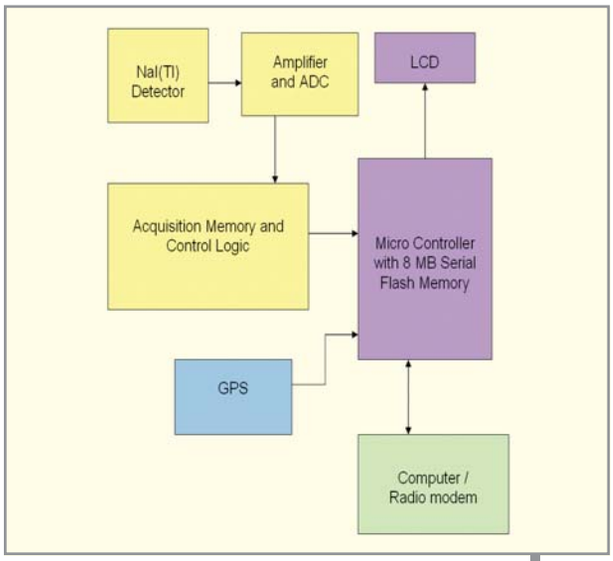

Block diagram of PCGS system

Compact Aerial Radiation Monitoring System (CARMS)

a) Real time transfer of spectral data from the MCA acquisition memory to hard disk.
b) Display of acquired gamma spectrum for deposited radionuclide identification.
c) On-line mapping of dose rates/contamination level in colour codes on the digitized map of the surveyed area.
d) On-line transmission of acquired data to Emergency Response Centre through radio modem and VHF.

D.N. Sharma, K.S. Pradeepkumar, G. Krishnamachari, Probal Chaudhury, N. Raman, M.S. Kale, M.M.K. Suri, S.K. Mehta, Anand Raman & Hari Kumar

<dnsharma@barc.gov.in>

1.2 ENVIRONMENTAL MONITORING AROUND NUCLEAR POWER PLANT SITES

As a mandatory requirement, a well-equipped Environment Survey Laboratory (ESL) is established at each Nuclear Power Plant Site by Health Physics Division, BARC well before the commissioning of the plant. In addition to carrying out environmental surveillance on a regular basis, ESLs are also identified as Emergency Response Centres (ERC) for quick response in case of large scale disasters. ESLs participate in On-Site Off-Site emergency exercises keep the required instruments in ready conditions as part of emergency preparedness.

The primary aim of the environmental monitoring programme is to demonstrate the compliance with the radiation exposure limits set for members of public. In pre-operational phase, ESLs generate baseline data on the levels of external radiation dose and concentration of natural radioactivity (U & Th and their daughter products, K-40 etc.) and radionuclides due to global weapon fallout (Sr-90, Cs-137 etc.). This requires a detailed measurement of these radionuclides in different environmental matrices (air, water, fish, silt, sediment, soil, vegetation, goat thyroid, vegetable, milk, grass, crops, fruits, meat and other dietary items) covering 30 km radial distance around the plant. The number and type of samples and sampling frequency is site specific and is optimized for each site on the basis of the nature of operating facilities, utilization of local natural resources, existence of population clusters and related demographic data. All the ESLs are equipped with state-of-the-art instruments such as Gamma spectrometers, Tritium counting units, whole body counters and met stations. Other activities of ESLs include public health and drinking water quality, sewage effluent monitoring for BOD and other parameters as per the requirement of pollution control board.

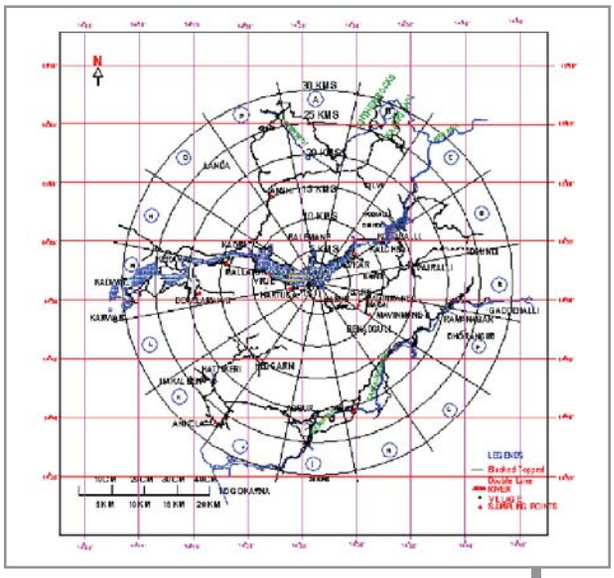

Environmental radioactivity monitoring

Mainly, three types of environmental samples are collected and analyzed. The first category of samples are directly relevant to the estimation of dose received by the members of public like drinking water, air and locally produced dietary items consumed by the public. The second category are trend indicators for build up of radionuclides, if any, such as weeds, sediment, soil, grass etc. The third category includes sensitive indicator organisms that accumulate specific radionuclides to a great extent and these serve as very sensitive detectors or markers; for example, goat thyroid for the detection of low levels of fresh radioactive fallout of Iodine–131.

Collection of water samples at NAPS

In the operational phase, the ESL continuously monitors the external radiation exposure levels in the environment, measures meteorological parameters and analyzes the distribution and concentration of reactor related radionuclides in samples of different environmental matrices to assess the contribution, if any, from the plant releases. About 1000-2500 samples per year from atmospheric, terrestrial aquatic environments are collected covering a radial distance of (0-1.6 km onsite) and (1.6 to 30 km offsite) as per the requirement of Atomic Energy Regulatory Board (AERB). The samples include storm water drain, bore wells, main out falls, soil samples and low level liquid effluents. The individual Fission Product and Activation Product concentrations in various matrices are detected using HPGe detector-based gamma spectrometry system.

HPGe Detector Gamma Spectrometry

Micro-meteorological Measurements

Data on Wind Speed, Wind Direction and Atmospheric Stability are collected using Meteorological Tower SODAR. Using this data, external gamma dose is computed using the atmospheric dispersion models. Annual averages are worked out by including persistence of weather categories.

Dose Estimations at NPPs

Experience of extensive environmental monitoring for the last five years has shown that even a hypothetical individual staying

Sodar At Kudankulam NPP Site

at plant exclusion boundary (1.6 km) received a maximum total dose of only about 6% of dose limits (1 mSv/y) prescribed for members of public, in case of Rajasthan Atomic Power Station (unit 1&2). The total dose due to Tarapur Atomic Power Station and Madras Atomic Power Stations was less than 2% of prescribed dose limit. In case of Narora Atomic Power Station, Kakrapar Atomic Power Station, Kaiga Generating Station and RAPS-3 & 4 due to improved design features; the total dose was less than 0.5%. At distances greater than 1.6 km, the doses to the members of public continuously get reduced and are negligible compared to doses received from natural sources.

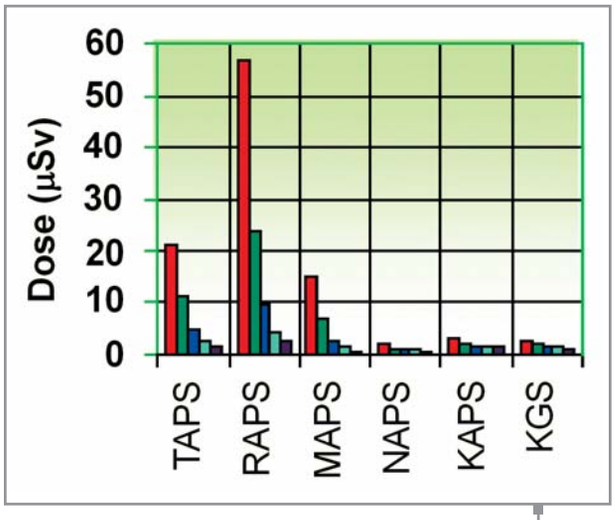

Mean total dose to the members of public during 2000-2004 at NPPs

Quality assurance programmes

ESLs routinely participate in various quality assurance programmes conducted by international bodies such as IAEA. ESLs at RAPS, TAPS and ESS at Trombay participated in IAEA proficiency test for determination of U Ra in water samples. Gamma spectrometry intercomparison exercise of HPGe detectors was arranged in collaboration with Radiochemistry Division, BARC using ^{152}Eu and ^{133}Ba point sources. The results of most of the laboratories agreed within 5% to that of the organizers value.

ESL, TAPS participated in whole body counting intercalibration exercise using IAEA phantoms of human body (BOMABII) and Thyroid (Thyroid II) during August 2003 and also in internal dose computation exercise IDEAS. ESL, KGS participated in modelling exercise on environmental distribution of tritium organised by EMRAS programme of IAEA. Apart from this, intercomparison exercises for environmental samples with IAEA, IRC WHO and also within DAE units in determination of radionuclides content, were also held.

Conclusions

Environmental survey laboratories cater to the need of demonstrating compliance of Nuclear power plant operations to environmental regulations. In addition, they also meet the requirement of acting as Emergency response centres to handle the eventuality of large scale disasters. The regular monitoring programmes have shown that even after 30 years of operation of nuclear power plants, the levels of radionuclides in terrestrial samples such as soil, crop, vegetation, milk, meat, egg etc. are at global weapon fallout levels and there is no observable increase due to power plant operations. Aquatic samples such as water, fish and sediments in the vicinity of discharge area of the NPP sites show a small increase in the levels of tritium and Cs-137, but the levels are insignificant to be of any concern from the point of view of health risks to general public.

A.G. Hegde, L.N. Sharma, S. Chandramouli, D.D. Rao, V. Matkar, P.C. Verma and M.P. Rajan <aghegde@barc.gov.in>

1.3 LONG-TERM RADIOLOGICAL IMPACT ASSESSMENT OF TROMBAY ENVIRONMENT

Trombay houses some of the oldest nuclear facilities of the Department of Atomic Energy. These include (i) Apsara, a 1 MW swimming pool type enriched uranium fueled research reactor commissioned in 1956, (ii) Cirus, a 40 MW heavy water moderated and cooled natural uranium fuelled research reactor commissioned in 1960 (iii) Dhruva, a 100 MW heavy water moderated research reactor commissioned in 1985 (iv) Radioisotopes research and production laboratories functioning since late 1950's (v) Fuel reprocessing facility for production of plutonium since 1964 (vi) Other facilities such as IRE Ltd., a thorium processing facility (dismantled in 2003), a Uranium Metal Plant for production of reactor grade uranium, Fuel fabrication facility for production of fuel pins.

Since the inception of these facilities, environmental radiological surveillance activities and research & development programmes are being carried out to understand the long term behavior of radionuclides in various environmental matrices. Initially, activities were aimed at establishing recipient capacity for the Bay waters, recommending discharge locations, dilution factor and maximum permissible concentrations. Monitoring activities in the bay started with gross alpha and beta measurement in 1959-60. However, regular rigorous surveillance activities were established by 1968. These facilities discharge effluents containing fission products, alpha wastes (mainly thorium, uranium and transuranic), tritium and noble gases.

The Environmental Monitoring Programme (EMP) aims to assess the environmental impact from various nuclear facilities at Trombay and to determine any public health impact that may be attributed to plant operations. This program also provides verification of the plant operated effluent monitoring system for each nuclear facility as well as its associated radiological environmental monitoring network and also serves as an in-place sampling network in the event of an accidental release. Atmospheric, terrestrial, aquatic and direct radiation pathways are monitored to determine the potential impact due to operations of nuclear facilities on the environment and public health.

■ Atmospheric Monitoring

The atmospheric monitoring network consists of four sampling stations (one fixed and two movable) at Trombay sites and a background reference station at Anushaktinagar. At each station a highly efficient, high volume sampler [PM-10] continuously draws ambient air at speed of 1.3 m^3/min. The air moisture samples are collected from thirteen different locations within Trombay, nineteen locations within Mumbai and twelve different locations from Mumbai Harbour Bay during off-shore sampling. External radiation levels are measured at 1 m above ground level at different locations using survey meter. The results show that the levels of H-3 in air moisture and long lived Gross α and β, Cs-137, Sr-90, I-131, Pu-239+240 in air particulate matter is within the statistical variations and are at the same levels as observed during earlier years.

■ Terrestrial Monitoring

The terrestrial monitoring network consists of fifteen sampling stations within Trombay and nineteen locations within Mumbai and its suburbs. Sampling stations at Trombay are scattered around various nuclear facilities while outside Trombay the sampling stations are scattered around Mumbai and its suburbs for geographical and population coverage. Samples of surface soil, vegetation, well waters, are collected from these locations. Milk samples are collected from local dairy at Deonar. All samples are analyzed for beta and gamma emitting radionuclides and some are analysed for alpha emitter radionuclides. Standard chemical procedures are followed for the analysis of beta and alpha emitting radionuclides. The observed concentration range of H-3, K-40, Cs-137, Th-232, U-238 Sr-90, Pu-239+240 in various environmental matrices does not indicate any build up of radioactivity.

■ Aquatic Monitoring

The aquatic monitoring network consists of three different categories namely well water, fresh water reservoir (lakes supplying drinking water to Mumbai and its suburbs, other small lakes) and sea water (onshore different coastal places around Mumbai of Arabian Sea and offshore sampling of Mumbai Harbour Bay). Aquatic organisms (fish, crab, arca) at

shore, bottom surface and core (0-60 cm from surface of the bottom) are also collected during these programs.

The ingestion dose to the members of the critical group (Fishermen at Trombay) by considering the median and upper bound values of Sr-90 and Cs-137 for the last 10 years, was in the range 0.04 - 4.76 μSv/y and 0.28 –13.33 μSv/y respectively. The computed external gamma doses due to Ar-41 at Trombay village gate are in the range of 5 – 45 μSv/y while the computed dose at BARC south site gate is 40 – 127 μSv/y.

Speciation studies

An assessment of speciation is important because the chemical/ radiological toxicity of an element or nuclide and its fate in the environment is governed principally by its physical (*size*) chemical (*oxidation state*) form. The potential exposure of a given radionuclide varies considerably depending upon the form of the species in which it occurs. The quantification of the various species of actinides in different environmental matrices is carried out by Anodic Stripping Voltametry in conjugation with alpha spectrometry and high resolution gamma spectrometry and Capillary electrophoresis.

Anodic Stripping voltammetry

Water may transport radionuclides either in suspension, bound to very small particles known as colloids or as a dissolved solid.

Capillary Electrophoresis with Photo diode array detector

Colloid particles can travel with flowing water through fractures and the matrix of the subsoil and also have the ability to bind radionuclides to their surfaces.

Stirred Ultra-filtration cells

Colloid transport of certain nuclides, such as plutonium, Cs-137 could result in relatively fast transport. Studies on colloids including determination of species concentrations and size distribution is carried out using Stirred Ultra-filtration Cells, operating in concentration mode.

The solution with colloidal particles in the range of 1.1 nm to 220 nm is concentrated and the Zetasizer nano Zs is used for the measurement of zeta potential and Nominal Molecular Weight cut-off Limit (NMWL). Simulated ground experiment in subsurface water shows that Pu-239+240 is preferentially attached to 10 k NMWL fraction while Cs is with 0.5k 10 k NMWL.

Zetasizer nano ZS

The importance of the complexation of actinides with naturally-present organic materials is well recognized in aquatic environment. The size distribution of actinides and hence their mobilities in natural waters depend on water chemistry (pH, ionic strength, inorganic organic components) and other complex physico-chemical interactions. Therefore, information on speciation is essential for predicting the mobility of these elements in aquatic environment.

Isolation of Pu/Am - soil humic substances

The studies focus on the association pattern of Pu and Am with Dissolved Organic Materials (DOM) in three types of organic-rich groundwaters: humus-rich terrestrial and saline groundwaters and humus-poor terrestrial groundwater containing protein-like materials. The soil humic substances are isolated and complexation of actinides in soil/aquatic system are compared. The association properties of Pu/Am/Cs/Sr are studied on the basis of molecular size of humic material. Fractionation in various NMWLs is carried out by using stirred ultrafiltration cell and analysis is performed by alpha and gamma spectrometry and for Sr-90 by gas flow proportional counter.

Conclusion

Results of the environmental surveillance around Trombay clearly demonstrate that there is no increase or build-up of radioactivity in the terrestrial or aquatic environment which can be attributed to operations of Nuclear facilities at Trombay. The total dose received by maximum exposed individual member of the public is only a small fraction of the annual dose limit prescribed by AERB (ICRP). At farther distances the doses are insignificant.

R.K.Singhal, N. Usha , J. Preetha and R.P. Gurg, **Dose re-evaluation to critical group based on habit survey undertaken to determine consumption and occupancy rates,** Proceedings of the Eighth National Symposium on Environment, IGCAR, Kalpakkam June 22-25, (1999).

R.K. Singhal, S.N.Joshi, A.G.Hegde, **Association of Uranium with Colloidal and Suspended Particulate Material in Arabian Sea near the West Coast of Maharashtra (India),** Journal of Radioanal. and Nuclear Chem., Vol.261 No.2 263-267, (2004).

R.K.Singhal, Ajay Kumar, Preetha J. Rupali Karpe, Madhuparana Datta, and A.G.Hegde, **Association of uranium with colloids of natural organic matter in subsurface aquatic environment,** Journal of Radioanal. and Nuclear Chem. Vol. 263 No.3 (2005).

1.4 COUNTRY-WIDE MAPPING OF RADON AND THORON USING TWIN CUP DOSIMETERS

An overwhelmingly large part of the radiation exposure to human population comes from natural sources, viz., the cosmic rays and the primordial radionuclides present on the earth's crust. Exposure from man-made sources arising from the applications of nuclear energy in industry and in medicine, constitute only a negligible part. It is thus important to generate comprehensive natural background radiation exposure profiles in different parts of the world. Such an assessment would need information on both the external gamma exposures as well as the inhalation exposures, the latter arising mainly from radon and thoron gases and their progenies present in the environment. In the Indian context, reports dealing with the mapping of the country for the distribution of naturally occurring radionuclides and the external gamma doses using Thermo Luminescent Dosimeters (TLD) covering quite a large number of locations scattered all over the country revealed that the average external gamma radiation dose for the country is about 775 μGy/y. Of the terrestrial component, 48.7 % of the contribution is from ^{40}K and the remainder is by the thorium (33.6 %) and uranium series (17.7 %). A database on the countrywide concentration levels of ^{238}U, ^{232}Th and ^{40}K in geological materials also exists.

However, data pertaining to the inhalation component due to radon and thoron and their progenies, especially in indoor environments were not available due to the complexities involved in their large scale measurements. To assess this component, a countrywide survey on radon and thoron levels has been carried out in Indian dwellings under a Coordinated Research Project (CRP) sponsored by the Board of Research in Nuclear Sciences (BRNS) of the Department of Atomic Energy (DAE) involving a large number of universities and other research institutions from different parts of the country. Environmental Assessment Division (EAD), BARC was the principal coordinator. The national survey has been carried out using Solid State Nuclear Track Detector (SSNTD)-spark counter based passive detector technique. A twin chamber radon-thoron dosimetric system was developed and used for this purpose.

■ Description of dosimeter

A twin chamber dosimeter based on SSNTD has been developed in Environmental Assessment Division, BARC for long-term and large-scale deployment for the measurement of radon, thoron and their progeny in ambient atmospheres. Each chamber has a length of 4.5 cm and a radius of 3.1cm.

Twin Cup radon/thoron dosimeter

The two chambers are fitted with a glass fibre filter and a membrane filter respectively. The different permeability constants of these filters allow for preferential diffusion of radon and thoron gases into the respective chambers. This dosimeter employs one SSNTD exposed in each chamber and a third placed outside the chamber. While the SSNTD in the membrane filter chamber registers the tracks due to radon gas, that in the glass fibre filter chamber records the tracks due to both radon and thoron gases. The SSNTD, placed outside the chamber in the bare mode, registers the tracks due to radon and thoron gases and their progenies. This information, in conjunction with that obtained from the SSNTDs in the chambers, is used to deduce the concentration of the progenies through a complex analysis. The SSNTDs used are 12 μm thick, LR-115 type II (Kodak cellulose nitrate), which after exposure of about 90 days, are etched with

10 % NaOH solution for 90 minutes at a bath temperature of 60^{0}C. Tracks developed are counted using a spark counter. These tracks are converted to the radionuclide concentrations by the use of appropriate calibration factors. These calibration factors are obtained by a series of experiments conducted in a calibration chamber under well-defined conditions of gas concentrations and aerosol concentrations.

Results of country-wide survey

These dosimeters have been widely used for the countrywide mapping of radon and thoron. About 1400 dwellings were monitored at different parts of the country by the participating institutions. The High Background Radiation Areas of Kerala are excluded from this study as these form special regions of interest and are being surveyed as part of epidemiological programmes. Results of the survey show that the Geometric Mean (GM) concentration value of radon is 23.0 Bq/m^3 (GSD 2.61); while that for thoron gas is 12.2 Bq/m^3 (GSD 3.22).

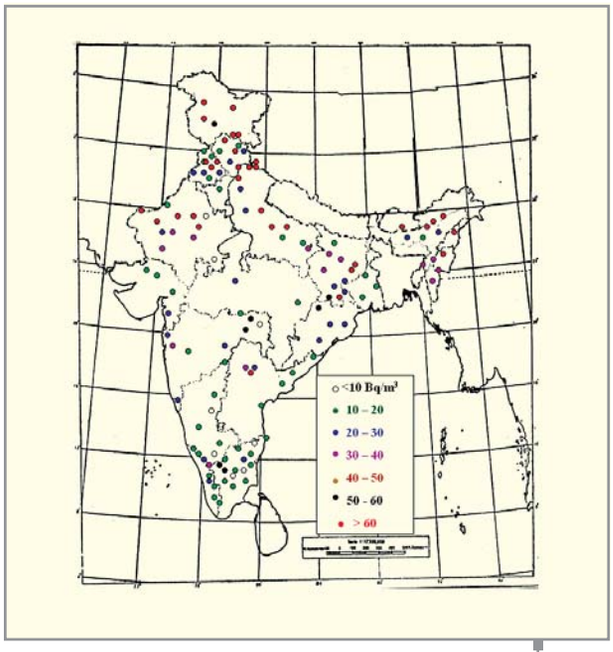

Indoor radon levels

Inhalation dose rates due to radon, thoron and their progeny gave a GM value of 0.97 mSv/y (GSD 2.49) for the country.

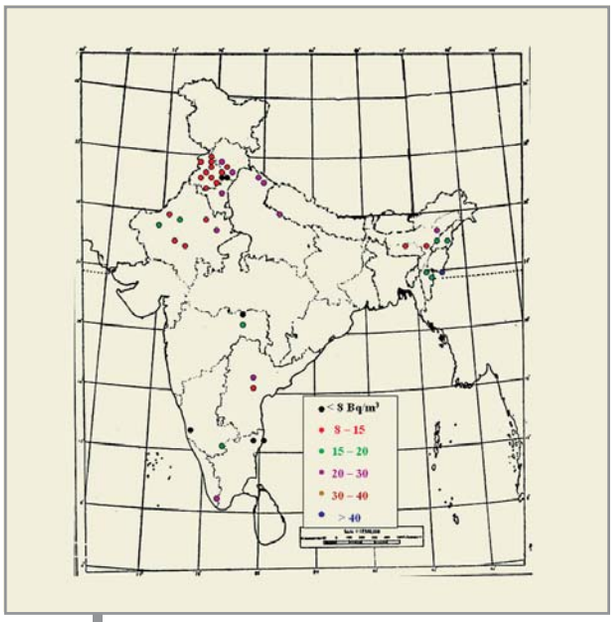

Indoor thoron levels

Geographical distribution pattern shows comparatively high inhalation dose rates (> 2.0 mSv/y) in the northeastern part of India, which is supported by observations of high concentration of uranium and thorium in soil and rocks in this region. The study reveals that most of the dwellings in India do not warrant any action levels with respect to indoor radon and thoron due to good ventilation prevailing in Indian dwellings.

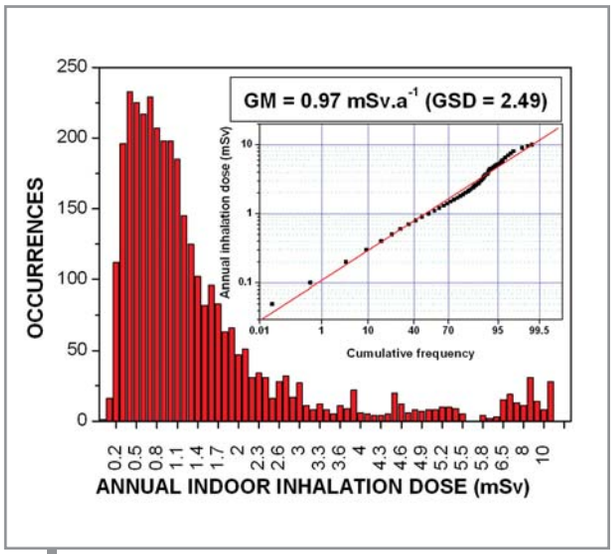

Distribution pattern of total indoor inhalation dose rates

Conclusions

The twin-cup dosimeter system developed for the national survey is a major development that has been widely used by Indian investigators for measuring radon and thoron in the environment. The country-wide survey indicated that the national average of the inhalation component is about 1 mSv/y. Although wide geographical variations are seen, the study reveals that unlike in the western countries, radon does not pose a major health hazard in Indian dwellings.

Y.S. Mayya, K.P. Eappen and K.S.V. Nambi - **Methodology for mixed field inhalation dosimetry in monazite areas using a twin-cup dosemeter with three SSNTDs.** Rad. Protect. Dosim. 77, 177-184 (1998).

T.V. Ramachandran, K.P. Eappen, R.N. Nair, Y.S. Mayya and S. Sadasivan, **Radon-thoron levels and inhalation dose distribution patterns in Indian dwellings,** BARC/2003/E/026 (2003).

K.P. Eappen and Y.S. Mayya, **Calibration factors for LR-115 (type-II) based radon-thoron discriminating dosimeters,** Rad. Measurements. 38, 5-17 (2004).

1.5 INDOOR DOSIMETRY IN HIGH BACKGROUND RADIATION AREAS IN KERALA

A natural background of ionizing radiation, due to the natural radioactivity of Thorium, Uranium, Potassium and their daughter nuclei has always been present on earth. All living organisms are inexorably exposed to it. In addition, the radiation originating from cosmic rays, which enter the earth's atmosphere from outer space also contribute to the background radiation levels. Although there exists a concern about man made sources of radiation, the dominant exposures are, in fact, almost always from the natural sources. The main exposure pathways from these sources are mainly from external gamma rays, inhalation of radon thoron and their progeny and to a small extent by ingestion through food consumption.

In the High Background Radiation Areas (HBRAs), where one or more of the radioactive nuclides are found naturally, the levels are found to be higher than those in the normal background radiation areas. In view of this, these areas are appropriate for examining the health effects of radiation on populations which have been living therein for centuries. An epidemiological analysis of the heath effects and the doses received by the populations can provide direct information on the low dose radiation risk coefficients on which direct information is lacking.

In the Indian context, the monazite bearing regions of Kerala are ideally suited for the above mentioned epidemiological studies. This area, mainly located in Dist. Kollam, Kerala, has high concentration of monazite, a mineral rich in radioactive thorium, of about 9% in the beach sand. Tazava, a village in the same region which contains negligible monazite concentrations shows lower radiation levels.

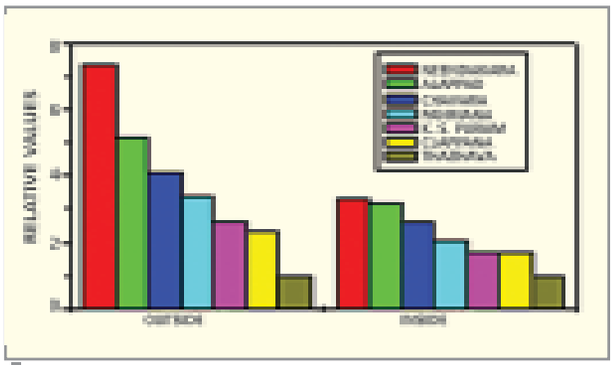

Comparison of radiation levels of different villages with Tazava

The dosimetric survey of external as well as inhalation doses, required for carrying out epidemiological analysis, was taken up by BARC. A sample survey, comprising of monitoring 100 houses every year in one village, has been conducted for obtaining the profiles of the dose distribution.

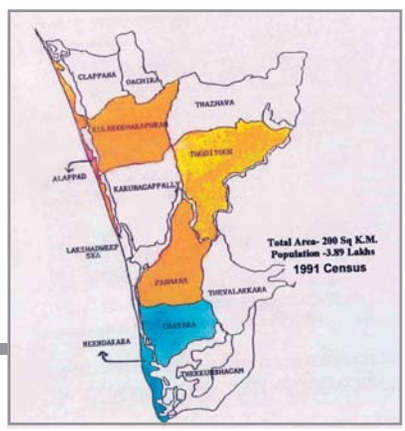

A schematic map of villages in Karunagapally Taluk monitored under indoor dosimetry programme.

Monitoring Methodology

The monitoring was carried out using GM-based gamma

radiation survey meters (for outdoor gamma radiation monitoring), TL Dosimeters (for indoor gamma radiation monitoring) and Solid State Nuclear Track Detector (SSNTD) based dosimeters (for indoor inhalation dosimetry).

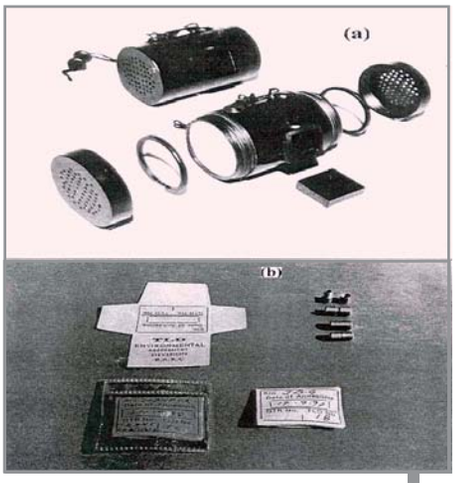

SSNTD and TLD-based dosimeters

It is well known that the concentration of radon gas that is mainly responsible for the inhalation dose, depends on the indoor ventilation and the radioactivity in the construction materials. The selection criteria for the houses, therefore, took into account aspects regarding types walls, roof and floor. The dosimeters were deployed inside the houses at about 1m height and were replaced by new dosimeters after a period of about 90-120 days. The exposed dosimeters were analysed at Mumbai and the doses were calculated. Considering the occupancy factors of 0.8 for indoor and 0.2 (UNSCEAR 2000) for outdoor and doses evaluated using TLDs, SSNTD-based inhalation dosimeters and survey meters, total doses in mSv/a were evaluated for each of the houses surveyed.

The results for the three villages that are compiled can be summarised as follows. The soil samples collected from the surrounding houses In Neendakara and Chavara villages under the programme, indicate that the ^{232}Th content in the soil varies from 75 to 9070 $Bq.kg^{-1}$ with a mean of 827.0 $Bq.kg^{-1}$. The data shows that the Th, U and K contents are 83%, 13% and 4% respectively.

These areas being situated near the seacoast are rich in monazite sand. The external gamma radiation levels are found to be high in Neendakara and Alapad and elucidate the deposits of

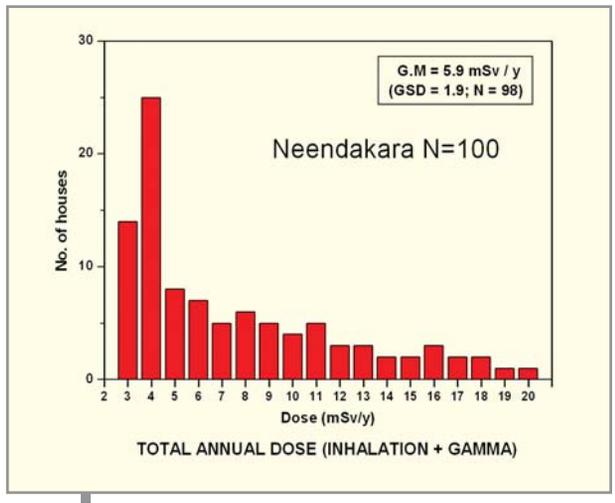

Dose distribution in Neendakara Village

monazite sand. Gas concentrations in dwellings seem to increase in the interior to the seacoast land areas. The lower levels of radon and thoron in dwellings in Alapad and Neendakara can possibly be explained as being due to the dilution that is seen at the seacoast areas because of high sea breeze.

It can be seen that the contribution of gamma dose (both external and internal components combined) is high in all the three panchayats. The distribution of dose to Neendakara, Chavara and Alapad are shown in figures. The value of the average annual exposure estimated from the three panchayats is 5 mSv.

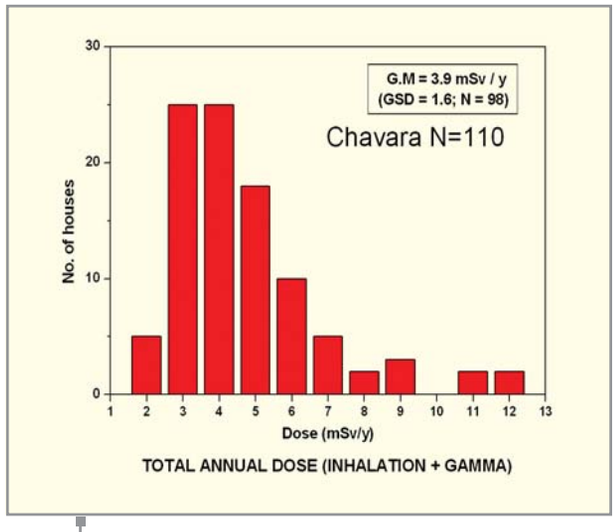

Dose distribution in Chavara Village

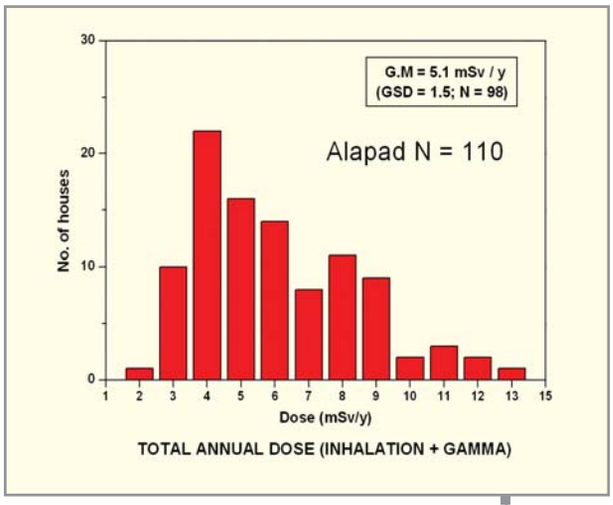

Dose distribution in Alapad Village

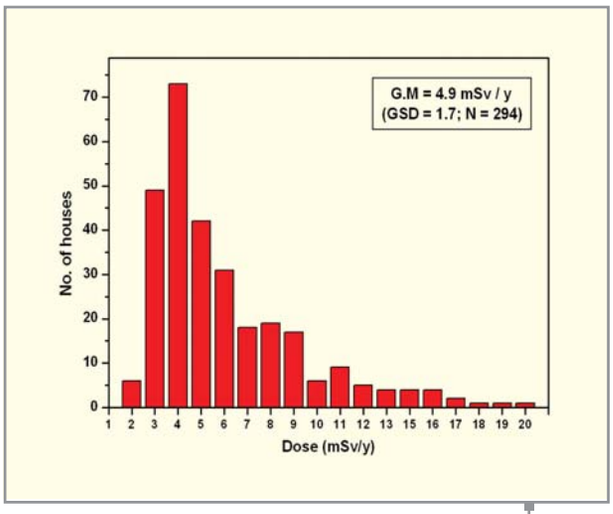

Overall dose distribution in all the three Villages together

Conclusions

The sample study reveals that inhalation doses due to radon/ thoron and their progeny constitute upto about 50% of the total dose received by the populations living in HBRAs. For epidemiological purposes, it is required to carry out these studies on a larger scale for assigning individual doses to the study populations.

Chougaonkar, M.P., Eappen, K.P., Ramachandran, T.V., Shetty, P.G., Mayya, Y.S., Sadasivan, S., and Venkat Raj, V., 2004. **Profiles of doses to the population living in the high background radiation areas in Kerala,** India., J. Env. Radioactivity. 71, 275 – 297.

Fareeduddin, S., Sethna, H.N., 1958. **Production of nuclear grade thorium compounds.** Second International Conference of the peaceful use of Atomic Energy (P/1670), Geneva.

Krishnan Nair, 2001. **Natural Background Radiation, Cancer Registry; Karunagappally, Kerala, India.** A report by Regional Cancer Centre, Trivandrum.

Kulkarni, VV., Pillai, T.N.V., Ganguly, A.K., 1974. **Distribution of natural radioactivity and trace elements in the soils and sands from high radiation coastal belt of India.** BARC report 702.

UNSCEAR, 2000. **United Nations Scientific Committee in the Effects of Atomic Radiation, Annex A: Exposure from Natural Sources.** United Nations. New York.

1.6 ASSESSMENT OF INTERNAL RADIOACTIVE CONTAMINATION IN HUMANS

A variety of radionuclides having different physical and chemical forms are handled during nuclear fuel cycle operations, use of radioactive sources in medicine, scientific research, agriculture and industry. There are built-in safety features and standard operation procedures to prevent internal contamination of person handling the radioactive materials. However, a possibility of release of radionuclides to the working environment and their subsequent intake by workers by different pathways such as inhalation, ingestion, injection or absorption through skin cannot be ruled out totally. Hence internal contamination monitoring of occupational workers handling the radioactive materials is carried out taking into account the nature of work and potential for internal contamination.

The estimation of internal contamination is carried out by (a) Whole Body Counting (in-vivo monitoring), (b) Excreta monitoring, also referred to as bioassay monitoring. The choice of measurement technique is determined by factors such as, the radiation emitted by the radionuclide, the metabolic behaviour of the contaminant and its retention in body.

A) Whole Body Counting

Whole body monitoring is used for estimation of radionuclides that emit X or γ radiation, positrons and energetic β particles. This covers most of the fission/ activation products such as ^{131}I, ^{137}Cs, ^{125}Sb, ^{95}Zr-^{95}Nb, ^{60}Co and other potentially important radionuclides such as Pu/Am, U and Th. In this

technique, X- or gamma ray photons coming out of the body are detected using appropriate detectors. The detector for High Energy Photon (HEP) emitters is either cylindrical NaI(Tl) or HPGe detector used singly or in array configurations. For Low Energy Photon (LEP) emitters special detectors such as Phoswich (sandwich of a thin NaI(Tl) and a thick CsI(Tl)) and an array of LOAX HPGe are used.

The photon detectors are positioned at selected points on or near the body. They are properly shielded using mild steel and lead to reduce interference due to natural ambient radiation. Signal from the detector is amplified, processed and corrected for the background to obtain the gamma-ray spectrum of the internal radionuclide of interest. This corrected response is used for assessment of the body or organ content through appropriate calibration procedures. The different types of whole body counters in use are briefly described below.

(i) Shadow Shield Moving Bed Whole Body Counter

Shadow shield whole body counters, installed at various nuclear facilities in India, are designed to shield the NaI(Tl) detector (10.2 cm dia. x 7.6 cm thick) all around except its viewing face. The design of the shield is such that no gamma ray from the environment can reach the detector directly. The scanning time from head to toe is about 15 min. This system can be used for locating the activity in the body at levels as low as 200 Bq of HEP emitters present in the body.

Shadow shield bed whole body monitor with IAEA BOMAB phantom in position

(ii) Shielded Chair Whole Body Counter

Used commonly for quick scanning of personnel, in this shield configuration, the subject sits in a chair, which is shielded with about 15 cm thick mild steel from all around except the front and the top. NaI(Tl) detector (10.2 cm dia x 7.6 cm thick), shielded with 5 cm lead all around except the face, is mounted on a plate hinged to the side of the shielded chair. The detector views the body from head to knees. This system cannot locate the activity in the body and has slightly lower sensitivity than the shadow shield whole body monitor. Using this, body activity of HEP emitters above 300 Bq can be measured.

Shielded Chair whole body monitor with subject in position

(iii) Steel Room Whole Body Counter

A totally shielded steel room whole body counter has 20 cm mild steel all around and is divided into two compartments separated by 15 cm thick steel wall (weight 150 tons). In the large compartment a linear scanning arrangement with a NaI(Tl) (20.4 cm dia. x 10.2 cm thick) detector is used for the measurement of body deposition of HEP emitters. The small compartment is specially designed for in-vivo detection of LEP

emitters and has graded lining inside. All detectors (Phoswich, HPGe etc.) used for measurement of organ contents of LEP emitters are operated inside this compartment. The measurement using whole body counting procedures gives the estimates of total body/organ contents of the contaminant radionuclides. These serve as inputs for assessment of internal radiation dose.

Steel room whole body monitor showing
Phoswich detector and IAEA BOMAB phantom in position

Calibration Procedures

For calibration of the whole body counter, a known amount of radioactivity is distributed inside the phantom and its count rate is recorded. Then the count rate per unit activity is calculated which is known as 'calibration factor'. The most suitable and popular method is based on the use of anthropomorphic phantoms. Phantoms are constructed from the tissue equivalent materials to closely approximate the human body and its various organs in terms of density, effective atomic number and their shapes and sizes. For HEP emitters, bottle mannequin absorber (BOMAB) phantom is most popular. This consists of 10 polyethylene containers of sizes which, when filled with water and assembled, roughly approximates a standard man in size, weight, height and shape.

Localized measurements may be required in situations where a radionuclide is known to concentrate in one particular organ, e.g. radioisotopes of iodine in the thyroid. In this case, a phantom representing the shape and size of the thyroid is used for calibration of thyroid monitor.

For calibrating in-vivo measurement systems for LEP emitters, a realistic anthropomorphic phantom for thorax, developed by Lawrence Livermore National Laboratory (LLNL) for Western Man or Japan Atomic Energy Research Institute (JAERI) phantom for reference Asian Man is used. For assessing contribution from HEP emitters, BOMAB phantom is used. Monte Carlo simulations are also used for deriving calibration factors using mathematical phantoms.

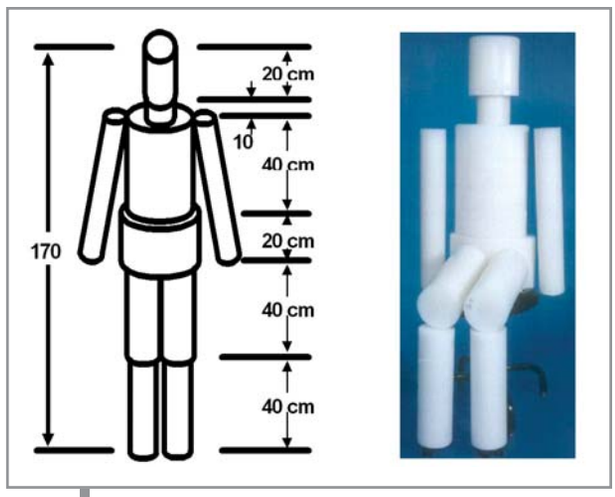

BOMAB phantom

B) Bioassay monitoring

Bioassay monitoring is based on the determination of activity content in biological samples such as urine, faeces, nasal smear and blood. This is most suitable for monitoring radionuclides that are pure β emitters (^{3}H, ^{90}Sr, ^{14}C etc.) or α emitters (Pu/Am, U, Th etc.). Normally, routine bioassay monitoring is conducted at annual frequency for most of the radionuclides such as ^{90}Sr, ^{232}Th, U(nat.), ^{239}Pu, ^{241}Am, etc. However, radionuclides with short biological half-life in the body e.g. ^{3}H are monitored on a weekly basis.

Urine samples are collected in polythene bottle (1.2 L capacity) with tight fitting lids. During collection of urine samples, care must be taken by the individual to avoid contamination of the sample. For most routine analyses, a 24 h collection is preferred.

The volume required for analyses depends upon the sensitivity of the analytical technique. Internal contamination monitoring of radiation workers is carried out under three categories viz. (i) routine (ii) operational/special or (iii) confirmatory monitoring.

In case of an accident of inhalation of radioactive materials (especially actinides), fecal samples are also collected in polythene containers lined with plastic bags.

Standard radiochemical separation procedures are used to separate the trace levels of radionuclides present in the urine samples. Suitable tracers / carriers such as ^{232}U for U, ^{242}Pu or ^{236}Pu for Pu, ^{229}Th or ^{234}Th for Th and ^{243}Am for Am are added, before wet or dry ashing, to determine the radiochemical yield. These tracers and standards are obtained from National Institute of Standards and Technology (NIST, US) and International Atomic Energy Agency (IAEA). The standard sources are also used for calibration and efficiency measurements of the detectors.

Evaluation of internal dose

For calculation of radiation dose from the measured body radioactivity, first the 'amount of radioactivity inhaled' (known as Intake) by the person is estimated by using biokinetic / metabolic models of radionuclides. The 'Intake' is multiplied by 'dose coefficient' (recommended by International Commission on Radiological Protection) to arrive at 'Committed Effective Dose' i.e., the total dose that will be received by the person in the coming 50 years. Various commercially available softwares like LUDEP (Lung Dose Evaluation Programme), MONDAL/ MONDES and IMBA (Integrated Modules for bioassay analysis) are available for dose evaluation.

Conclusion

Sensitive whole body counting facilities have been established for internal contamination monitoring of radiation workers. Elaborate bioassay monitoring services have been standardized. The radiation workers in different nuclear facilities are routinely monitored with these systems for assessment of internal radiation dose. If the expected radiation dose to the body is high, therapeutic measures are taken to accelerate removal of the radionuclide from the body by giving suitable chemical agents. Generally, no radioactive contamination is detected in the workers and therefore no radiation dose is received by them. However, in a small number of cases, sometimes, a small amount of radioactive contamination is detected but the corresponding radiation dose is insignificant.

Bhati, S, Sharma, R. C. and Venkatraj, V. **Assessing skull burdens of actinides using a mathematical phantom: A monte carlo approach.** Radiat. Prot. Dosim. 103(3) 247-254 (2003).

Garg, S. P., Singh, I. S. and Sharma, R. C. **Long term lung retention studies of ^{125}Sb aerosols in humans.** Health Phys. 84 (4) 457-468 (2003).

Haridasan, T. K., Surendran, T. and Sharma, R. C. **Calibration of lung monitoring systems for actinides using an Asian phantom.** Radiat. Prot. and Environ. 24(1-2) 141-148 (2001).

Jaiswal, D.D., Singh, I. S., Nair, Suma, Dang, H. S., Garg, S. P. and Pradhan, A. S. **Comparison of observed lung retention and urinary excretion of thorium workers and member of public in India with the values predicted by the ICRP biokinetic model.** Radiat. Prot. Dosim. 112(2) 237-243 (2004).

Sawant, Pramilla D., and Pradhan, A. S. **Bioassay monitoring of occupational workers in India. Proceeding of theme meeting on radiation protection activities and practices in Indian atomic energy program,** pp 102-109, August 18-20 (2004).

Singh, I.S., Suri, M.M.K., Vidhani, J.M., Garg, S.P., and Sharma, R.C. **Development of an automated shielded chair whole body monitor.** Radiat. Prot. Dosim. 102(2) 145-151 (2002).

1.7 FLUORIDE ESTIMATION IN GROUND WATER USING ISOTOPE TRACERS

Fluoride is a minor anion present in natural waters at the levels less than 1 mg/l. However, it is toxic for both animals and plants above a level of 1.5 mg/l. Occurrences of high fluoride concentrations in groundwater are reported in several parts of India and abroad. In recent times, cases of tooth mottling, a few skeletal and dental fluorosis among the residents have been noticed in and around Ilkal area of Bagalkot District. There are several small and large scale rock polishing industries situated in Ilkal, producing large amounts of liquid and solid wastes. These wastes are dumped into the mine pits and trenches, which subsequently dissolve in rain and contaminate surface water. There are two possible sources contributing to fluoride contamination in these groundwaters, they are, leaching of fluoride-bearing minerals present in the subsurface and

recharge of groundwaters from fluoride contaminated surface waters.

An isotope hydrochemical investigation was carried out to identify the source and origin of fluoride and to understand the factors responsible for fluoride release into groundwater. Water samples were collected from bore wells, dug wells, mine pit, infiltration gallery, lake, river and rain and analysed for physical parameters, fluoride content and other anions and cations. A few selected samples were also measured for environmental isotopes such as $\delta^{2}H$, $\delta^{18}O$ and ^{3}H.

[$\delta^{2}H$ or $\delta^{18}O = (R_{samp}.- R_{std}) \times 10^{3}/R_{std}$;
where R stands for $^{2}H/^{1}H$ or $^{18}O/^{16}O$]

Geology and Hydrogeology of the region

The area under study is covered by Archaean complex. The different rock types found in the area include pink granite, gneiss, sandstone and Dharwar schists. The weathering is noticed from 3 to more than 20m. The drainage pattern in Hungund taluk is dendritic and well developed. Ilkal halla basin and Hungund halla are the two main sub basins present in this area. Both the streams are ephemeral and confluence at Islampur before joining Krishna River. This area is semi-arid with an average rainfall of about 500-600mm. Groundwater in this area occurs in weathered, fractured, fissured and jointed formations. Groundwater table varies from 1 to 12m.

Results of study

Hydrochemical analysis

The chemical analyses data shows that the samples have conductivities in the range 130 to 10680 µS/cm (fresh to saline), pH ranges from 7.0 to 8.9 (neutral to moderately alkaline) and the fluoride levels range from 0.1 to 6.5 mg/l. An increasing trend of electrical conductivity is found in groundwater from recharge area to discharge area. In recharge area, the electrical conductivities are in the range of 500 to 1000 µS/cm which increases to above 6000 µS/cm in discharge zone. All the samples have sodium as dominant cation while calcium and magnesium are found in lower concentrations. Sulphate, bicarbonate and chloride are the dominant anions. Groundwater evolves from a Na-Ca-HCO_3 type in recharge zone, to a mixture of bicarbonate, sulphate and chloride type along the flow path and finally to Na-Cl-SO_4 type in discharge area.

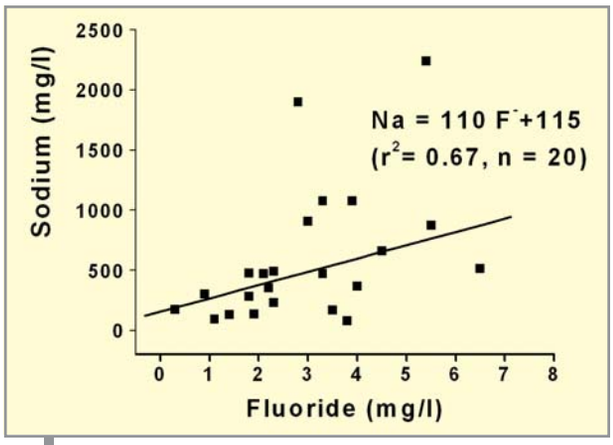

Correlation between Na^{+} and F^{-}

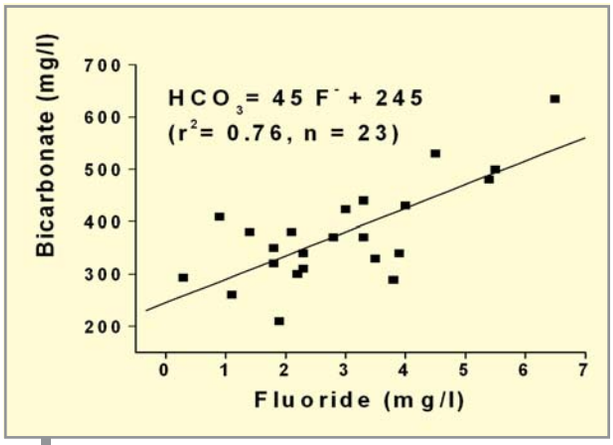

Correlation between HCO_3^{-} and F^{-}

The results show a positive correlation between sodium and fluoride. As it is known that sodium is released into the groundwater during chemical weathering, this correlation throws light on the contribution of fluoride from weathering. However, high sodium content at two locations indicates sources in addition to weathering. Also, leachability of fluoride from the minerals is mainly controlled by pH and dissolved carbon dioxide of the waters. A positive correlation between bicarbonate and fluoride indicates that waters with higher

bicarbonate content enhance the leaching of fluoride.

Environmental Isotope analysis

Water samples were collected from bore wells, dug wells after pumping out stagnant water for 10-15 minutes in order to get representative sample. The sample bottles/vials were filled completely and preserved airtight in order to avoid evaporation.Stable isotopes deuterium and oxygen-18 (δ^2H and $\delta^{18}O$) were measured using Mass Spectrometer. Environmental tritium was measured using Liquid Scintillation counter prior to electrolytic enrichment. The stable isotope results are expressed in d units (‰), where as tritium content of groundwaters is expressed in Tritium Units (TU). The precisions of δ^2H, $\delta^{18}O$ and ^3H measurements are ±1‰, ±0.2 ‰ and ± 0.5 TU respectively.

Plot of δ^2H versus $\delta^{18}O$ shows that bore-well and dug-well samples fall on the line with a slope of 4.6 indicating evaporation effect. A gradual enrichment in stable isotopes is seen in groundwater samples along the flow path. This clearly implies that surface waters have contributed to the groundwater. It is also observed that there is a good positive correlation between $\delta^{18}O$ and fluoride concentrations in groundwaters.

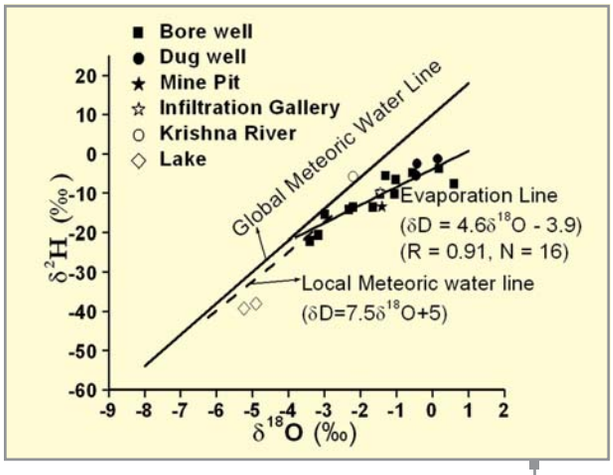

δ^2H vs $\delta^{18}O$ plot of samples

The environmental tritium content of most of the samples is in the range 4 to 7 TU. Comparison of fluoride versus tritium in the samples leads to three distinguished categories of samples. First category of samples contains low tritium content and low fluoride content. These waters are old and highly mineralized. Second category contains high tritium with fluoride levels < 1.8 mg/L, which are mostly from wells near recharge area or river/lake. These waters are modern and fluoride might have derived from geogenic sources without much contribution

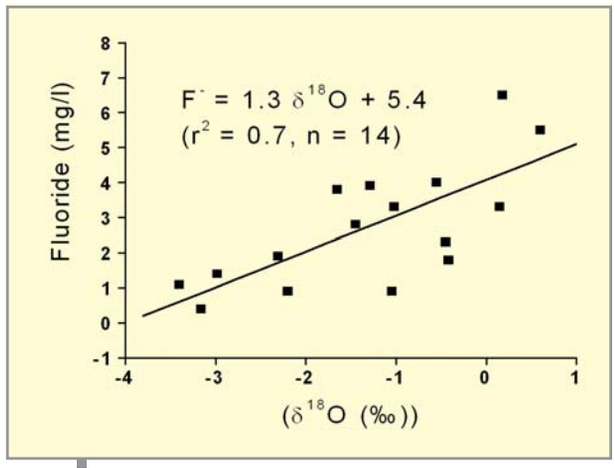

Correlation of F^- and $\delta^{18}O$

from contaminated surface waters. Third category includes high tritium with high fluoride concentrations i.e. above 2.8 mg/L, which are mostly from wells near mine pit and discharge area. These waters are modern and contribution of contaminated surface waters could be the source for high fluoride in addition to natural geogenic sources.

Conclusion

Fluoride contamination in the groundwaters of study area is mainly derived from fluoride rich minerals present in the subsurface. High degree of weathering and easy accessibility of modern fresh waters to weathered rocks could be responsible for the leaching of fluoride from the minerals present in the subsurface.

Surface water contribution to groundwater is observed all along the flow path and fluoride concentrations are found to be high in the places where there is surface water contribution. This contamination can be attributed to human activities. The release of the wastes that are rich in fluoride, into the surface waters by rock polishing industries plays a vital role in contaminating the surface water bodies and in turn groundwater. Fluoride contamination through this process

contributes a significant amount to total fluoride in groundwaters.

Handa, B.K. (1975) **"Geochemistry and genesis of fluoride containing groundwaters in India"** Groundwater 13, (3) 275-281

Suma Latha S., Ambika, S.R., and Prasad, S.J. (1999) **"Fluoride contamination status in Karnataka"** Current Science 76, (6) 730-734

Muralidharan, D., Anitha P. Nair, Sathyanarayana, U. (2002) **"Fluoride in shallow aquifers in Rajgarh Tehsil of Churu district, Rajasthan – an arid environment"** Current Science 83, (6), 699-702

K.Shivanna, Jalihal Adappa, K.Tirumalesh, Archana Deodhar, H.V.Mahokar, and Vinisha David. (2003) **"Isotope Hydrochemical Approach to study the Fluoride Contamination in Ground waters of Ilkal Area, Bagalkot District, Karnataka, India"** Proc. International Conference on Water and Environment (WE-2003), 15-18 Dec 2003, Bhopal, 332 – 346.

1.8 ASSESSMENT OF TOXIC ORGANIC POLLUTANTS IN THE ENVIRONMENT

Rapid industrialization, growth in energy demand and increase in vehicular density have brought about a sizeable increase in the anthropogenic emissions of various pollutants to the environment. These are often highly localized especially in urban and industrial areas. Many of these pollutants found in urban environment are organic in nature. Some of the organic pollutants are highly resistant to photolytic, chemical and biological degradation and remain in the environment for quite a long time. These pollutants are termed as Persistent Organic Pollutants (POPs) and they can be found in well measurable amount in air, water and soil. Organic pollutants, depending upon their vapour pressure, can be divided in three following categories: 1) Volatile Organic Compounds (VOCs) such as ethylene, propylene, benzene, toluene, xylenes etc. 2) Semi-Volatile Organic Compounds (SVOCs) such as organochlorine pesticides like Hexachlorocylcohexane (HCH) and Dichloro-diphenyl- trichloroethane (DDT), Polycyclic aromatic hydrocarbons upto 3 and 4 ring compounds such as naphthalene, anthracene, pyrene etc. and 3) Non Volatile Organic Compounds (NVOCs) such as 4 and 5 ring polycyclic aromatic hydrocarbons like benzo (a) pyrene, perylene, dibenzo (a, h) anthracene etc.

■ Estimation of Volatile Organic Compounds (VOCs) in air

Major urban sources of VOCs are releases from chemical industries, refinery operations, solvent evaporation and vehicular exhaust. Some of these VOCs, being carcinogenic are deleterious to human health while some are precursors to more toxic air pollutants such as aldehydes, oxidants including ozone. Extensive studies have been conducted on measurements of VOCs in different regions of Mumbai in indoor and outdoor air samples. Contribution of automobiles and industrial emissions to atmospheric levels of the VOC is evaluated by comparing the ratios of selected hydrocarbons such as ethylene/ acetylene, benzene/ toluene in ambient air samples.

Concentrations of Non-Methane Hydrocarbons (NMHCs) in atmospheric air were measured at six urban sites in Mumbai. Seventeen hydrocarbons, viz., ethane, ethylene, acetylene, propane, propylene, iso-butane, n-butane, iso-pentane, n-pentane, hexane, benzene, heptane, toluene, ethyl benzene, p-xylene, o-xylene and n-decane have been identified in 254 urban air samples using a cryogenic pre-concentration system attached to a Gas Chromatograph (GC) with Flame Ionization Detector (FID). Factor analysis (FA), a receptor modeling technique, has been used for quantitative source apportionment. Varimax rotated factor analysis identified five possible sources.

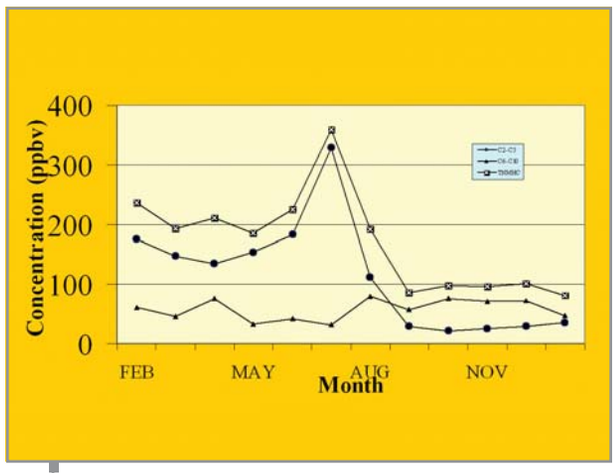

Monthly Variation of NMHCs in urban air

Studies on Polycyclic Aromatic hydrocarbons (PAHs)

Polycyclic Aromatic Hydrocarbons (PAHs) are released into the atmospheric air through incomplete combustion of fossil fuels. The urban sources are coal fired power plants, organic flares in petrochemical industries, automobile exhausts and organic refuse incineration. Releases from domestic cooking stoves and cigarette smoke are two indoor sources of these compounds. Many of the PAHs and their nitro derivatives are found to be carcinogenic and mutagenic. PAHs in atmospheric air are associated with small size particles (0.08 - 0.2 μm) which penetrate into the pulmonary region of the lung where the clearance mechanisms are slower and hence there is a greater risk due to prolonged exposure.

Reversed phase High Performance Liquid Chromatography (HPLC) with ultra violet detection was optimized for separation and quantification of PAHs in air particulate matter. Studies on monitoring of Total Suspended Particulate Matter (TSPM), benzene soluble organics and the PAHs in air samples collected in indoor environment of some tenements at Trombay where kerosene is used as cooking fuel have been carried out in relation to the concentration of the same in outdoor environment in near vicinity of the tenements.

The concurrent rain and air sampling conducted at Trombay showed that concentration of total PAHs varied from 84.25 ng/l to 777.49 ng/l in water and from 4.05 ng/m^3 to 34.42 ng/m^3 in air. In rainwater, the lower molecular weight PAHs (e.g. Phenanthrene, Fluoranthene, and Pyrene) were more prominent. The gas phase scavenging ratio (W_g) was found to increase with the molecular weight of the compound. The particle phase scavenging ratio (W_p) values for the more volatile PAHs were generally much higher than those for less volatile PAHs. The higher MW PAHs have W_g values equal to or larger than their W_p values.

The distribution of two to six ring PAHs on size fractionated aerosol samples has also been studied during the winter and in the absence of precipitation. Samples were collected over 72 h average sampling period using an eight stage cascade impactor. The filter paper samples were extracted ultrasonically. Total PAH concentrations (thirteen compounds) associated were in the range of 18.3 to 66.6 ng/m^3. The size

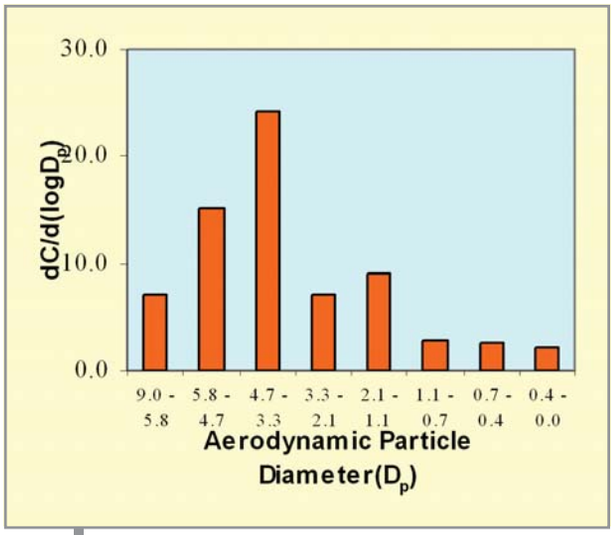

Size distribution of atmospheric PAHs

distribution was found to be bimodal with the two peaks at the particle size range 1.1 – 2.1 μm and at 3.3 – 4.7 μm.

These samples were also used for the estimation of the dry deposition rate of PAHs. The modeled deposition velocity ($V_{d,i}$) at the sampling site for the particle size ranges of 0 ~ 0.4 μm, 0.4 ~1.1 μm, 1.1 ~3.3 μm and 3.3 ~9.0 μm were found to be 0.004 cm/sec, 0.04 cm/sec, 0.3 cm/sec and 2.7 cm/sec respectively. The dry deposition flux for the individual PAHs was found to be in the range of 0.2 μg/m^2/day to 2.7 μg/m^2/day. The results indicate that the dry deposition of PAH is mainly due to the gravitational settling of coarse particulates.

Studies on OrganoChlorine Pesticide (OCP) residues

OrganoChlorine pesticides (OCPs) are potentially hazardous to living systems because of their bioaccumulation in lipid and their resistance to degradation. They are an important component of the Persistent Organic Pollutants (POPs) found in almost every compartment of the global ecosystem, especially in most human and animal adipose samples, milk and in all aquatic ecosystems.

In order to estimate the magnitude and direction of gas flux across the air-water interface, concentration of OCPs such as

hexachlorocyclohexanes (HCHs), Dichloro Diphenyl Trichloroethane (DDT) and its metabolite (DDE) and endosulfans were analysed in air and water samples collected at the creek adjoining Mumbai harbour. The HCHs revealed positive values of the fluxes indicating the tendency to transfer these contaminants from water to air. The flux for DDTs also follows the same pattern as HCHs suggesting the active transfer of these dissolved OCPs into the atmosphere due to volatilization.

Monitoring of OCP residues in human milk and blood samples collected from a hospital of Mumbai showed that the concentration of total HCH in human milk samples varied from 68.0- 959.5 ng/g milk fat and that for total DDT was 16.75- 1883.25 ng/g milk fat. In the blood samples, the total DDT was found to vary from 7.4-77.6 ng/ml and for total HCH it was 1.3-54.6 ng/ml. However, the levels of OCP residues in human milk were well below the tolerance limit of 1.25 mg/Kg for DDT and 0.075 mg/Kg for beta–HCH as prescribed by Food and Agricultural Organization/World Health Organization.

In order to estimate the risk posed by the presence of OCPs in milk and milk products a monitoring study was carried out in and around the Mumbai city along with a survey to determine the mean daily consumption of milk and milk products by different age groups. This data was used to evaluate the daily exposure to the public. Non-cancer effects were evaluated by comparing the predicted exposure distributions to the published guidance values. For carcinogens, cancer risk was evaluated using standard methodology. The study showed that current levels of the majority of OCPs in the samples do not pose unacceptable risks to the public. The alpha-HCH is the exception, for which the cancer risk estimated exceeds the U.S. EPA guidance value.

OCPs in sediment, water and biota samples were also analysed from coastal marine environment of Mumbai. High ratios of DDT to DDE in seawater samples were found. In sediment samples, gamma isomer contributed almost 55% to the total HCH indicating its high affinity towards the sediment. The levels in fish obtained from this study were found to be lower than those in fish of temperate regions.

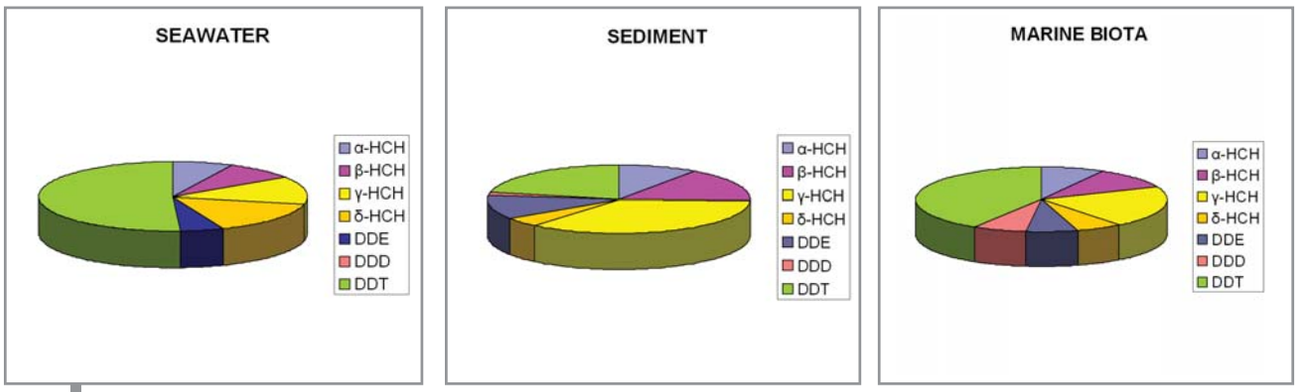

Distribution of mean values of organochlorine pesticide residues in seawater, sediment and marine biota

G.G. Pandit, S. K. Sahu, T.N. Mahadevan, V. D. Puranik and V. Venkat Raj (2003) **Source apportionment of atmospheric non-methane hydrocarbons at Mumbai.** Proceedings of the 12th National Symposium on Environment, Teheri, 518-522

G.G. Pandit and S. K. Sahu (2002) **Assessment of Risk to Public Health posed by Persistent Organochlorine Pesticide Residues in Milk and Milk Products in Mumbai, India,** Journal of Environmental Monitoring, 4 (1), 182-185.

G.G. Pandit and S. K. Sahu (2001) **Gas Exchange of OCPs Across the Air –Water Interface at the Creek Adjoining Mumbai Harbour, India,** Journal of Environmental Monitoring, 3, 635-638.

S. K. Sahu, G.G. Pandit and S. Sadasivan (2004a) **Precipitation Scavenging of Polycyclic aromatic hydrocarbons in Mumbai, India,** Science of Total Environment, 318 (1-3), 245-249.

S. K. Sahu, G.G. Pandit and V.D. Puranik (2004b) **Distribution of polycyclic aromatic hydrocarbons in urban aerosols of Mumbai**. IASTA Meeting and International Conference, IIT Kanpur, November 15-17.

S. K. Sahu, G.G. Pandit, R.S. Patil and V.D. Puranik (2004c) **Dry deposition of particle associated PAHs in an urban site, Mumbai.** Proceedings of the 13th National Symposium on Environment, Shillong.

1.9 ULTRA TRACE ANALYSIS OF ENVIRONMENTAL SAMPLES

Ultra trace analysis laboratory at EAD, BARC is equipped with state-of-the-art instruments for analysis of ultra trace levels of heavy metals, organometals and manmade as well as anthropogenic radionuclides in various environmental matrices. The laboratory houses sophisticated analytical instruments like Atomic Absorption Spectrophotometer (AAS), Hydride Generator Atomic Absorption Spectrophotometer (HG-AAS), Electro Thermal Atomic Absorption Spectrophotometer (ET-AAS), Differential Pulse Anodic Stripping Voltammeter (DPASV) and Gas Chromatography-Mass Spectrometer QP5050A. The Lab is a member of IAEA's Analytical Laboratory for Measuring Environmental Radioactivity (ALMERA) Network and well trained in determining radioactivity in the environment.

■ Trace metal analysis

Ultra Trace Uranium:

Considerable interest has developed in the determination of trace uranium in environmental sites as well as in facilities of the nuclear industry. Electro analytical techniques have frequently been used for the determination of uranium in various matrices. In particular, adsorptive stripping analysis is becoming a widely accepted tool for ultra trace measurements of uranium, using inexpensive and often portable instrumentation.

A method has been standardized for the estimation of uranium by adsorptive stripping voltammetry using chloranilic acid (CAA) as complexing agent. With these optimum parameters a sensitivity of 1.19nA/nM uranium was detected. Detection limit for this optimum parameter was found to be 0.1ppb. Using this method, uranium was estimated in different types of water samples such as seawater, synthetic seawater, stream water, tap water, well water, bore well water and process water. This method has also been used for estimation of uranium in sand, organic solvent used for extraction of uranium from phosphoric acid and its raffinate. Quality assurance of the standardized method is verified by analyzing certified reference water sample from USDOE, participation in intercomparison exercises and also by estimating uranium content in water samples both by differential pulse adsorptive stripping voltammetric and laser fluorimetric techniques.

Ultra trace lead:

Lead is a toxic metal which causes profound biochemical and neurological changes in human beings even at very low concentrations. Blood is a good indicator of the current exposure and body burden of lead and this has been used to discriminate between groups of individuals as regards to degree of exposure to lead. There is only a narrow tolerable region for this metal. Exposure assessment of Pb to Mumbai population was calculated taking into account both pathways such as ingestion and inhalation. Retention time of 20.3 days was observed for Pb in blood of 6-10 year old children. This is estimated from the measurement of Pb in air particulate, duplicate diet and blood of children residing in different locations in Mumbai. A good correlation (r=0.88) between blood lead of children and air lead was observed. The present study reveals that the blood Pb level in children could increase by 3.56 μg dl^{-1} for an incremental rise of 1.0 μg m^{-3} of air Pb concentration.

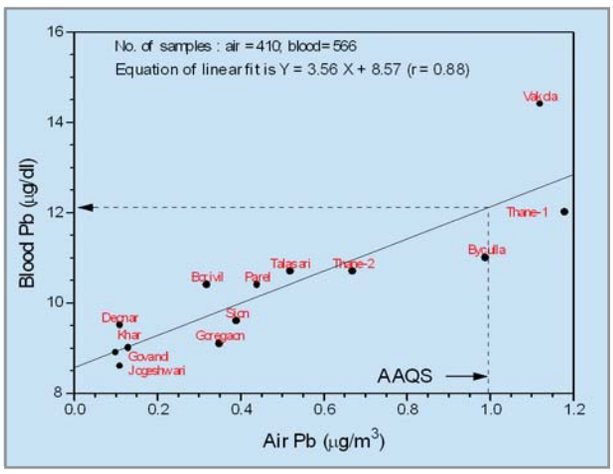

Antimony in environmental and biological samples:

Differential pulse anodic stripping voltammetric technique has been standardized for the determination of antimony in a variety of environmental and biological matrices. 6M HCl + 1M NH_2OH-HCl (1:1 v/v) and – 450 mV were found to be the most appropriate supporting electrolyte and initial potential, respectively. The detection limit using DPASV

was found to be 0.01 ng ml^{-1}. The reliability of estimation is assessed through the analysis of Standard Reference Materials (SRMs) such as Soil-7, SL-3 and (MA-A-2/TM) obtained from IAEA. The technique was applied for the estimation of Sb in air particulate, water, duplicate diet, sediment and blood samples collected from different parts of Mumbai.

***Aluminium in serum samples*:**

Normal concentration of aluminium (Al) in blood serum sample is very low of the order of <2 ng/ml. But in artificial kidney dialysis patients, the serum Al concentration will be high due to repeated dialysis. Hence a very sensitive method is required to estimate Al in serum samples. Electro Thermal Atomic Absorption Spectrophotometry (ET-AAS) has been standardized for the direct determination of Al in serum samples of artificial kidney dialysis patients. The advantage of this technique is that blank can be avoided since no pre-treatment of sample is required. The detection limit of Al using ET-AAS was found to be 0.1 ng/ml.

***Major elements in an industrial marine ecosystem at TTC area*:**

Concentrations of elements at three different locations i.e. site-1, site-2 and site-3 in trans-thane creek area were measured for trace and toxic elements in water, sediment and biota samples. The mean lead levels observed in Mumbai fish (0.15 µg g^{-1}) is well below the limits stipulated by several countries for lead in fish. The Cd, As and Hg levels observed in Mumbai fish during present study are also lower than the WHO permissible limits. The bio concentration factors for toxic elements like Pb, Cd, As, Hg for marine fish varied from 8-48, 105-152, 16-29 and 34-43, respectively. A good correlation between major elements i.e. Ca, Mg, Fe, Mn and Zn for suspended solids in water samples for site-3 region has been observed.

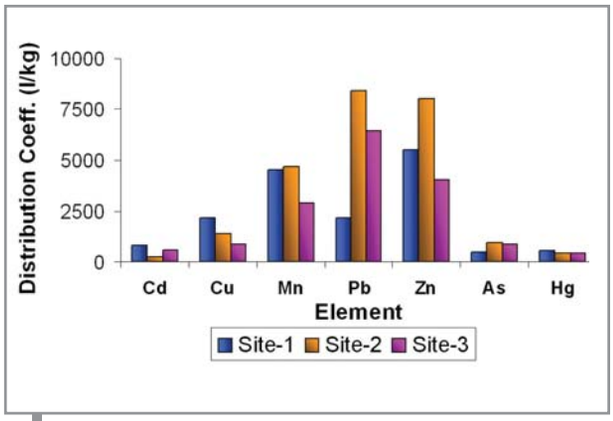

Distribution coefficient of industrially important elements in sediment at Thane Creek

***Intake of metals by adult population*:**

Daily intake of twelve metals (Na, K, Ca, Cu, Zn, Fe, Mn, Mg, Pb, Cd, Co and Ni) by Mumbai adult population were assessed by analysing duplicate diet samples. Daily dietary intake of 2.4 g Na and 1.2 g K were observed for Mumbai adults. Daily dietary intake of Ca, Cu, Zn, Fe, Mn and Mg were 367, 1.0,

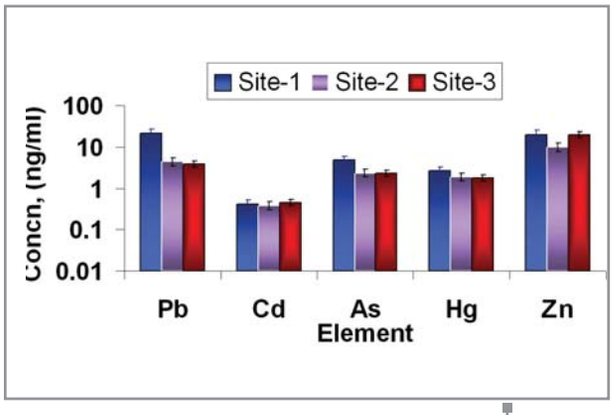

Concentrations of elements in sea water in Thane Creek

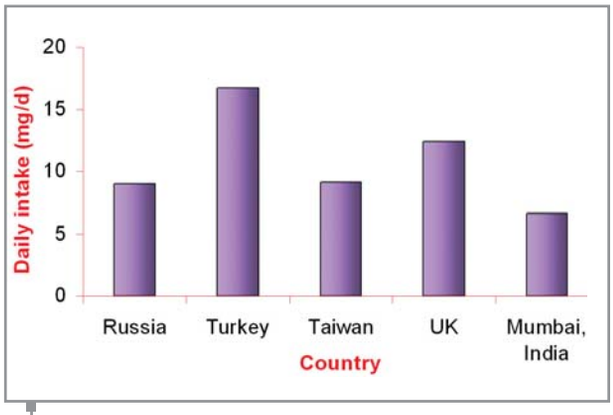

Daily dietary intake of iron in different countries

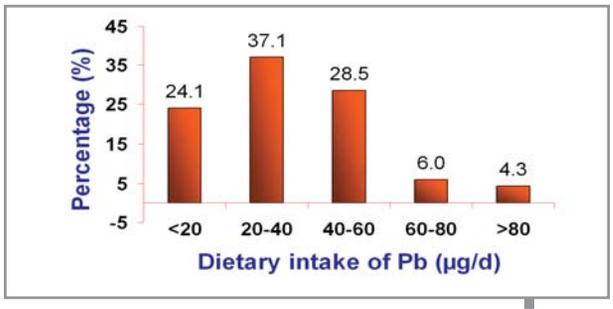

Distribution of dietary intake of Pb

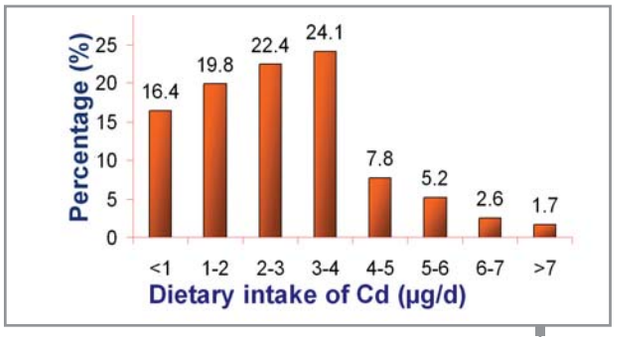

Distribution of dietary intake of Cd

6.3, 6.7, 2.0 and 304 mg respectively. Pb, Cd, Co and Ni intake by Mumbai adults were 32.3, 2.2, 2.2 and 108 μg/d respectively. From this study, it has been observed that the intake of toxic metals such as Pb, Cd and Ni are much lower than the tolerable daily intake derived from PTWI given by FAO/WHO and could not be considered harmful in this group of subjects. Daily intake of these metals were found to be higher in non-vegetarian diet as compared to the vegetarian diet ($P < 0.02, 0.01$).

***Selenium in Oral Cancer Patients*:**

Bio monitoring of Se in cancer patients is important because of its anti-carcinogenic behaviour. Low level of Se has shown increased oral cancer formation and there is a hypothesis that higher Se content in plasma can act as a cancer-preventing agent. The Se levels observed in blood, saliva and oral flesh tissues of cancer patients were analyzed by differential pulse cathodic stripping voltammetry and found to be 34 ng/ml, 0.27 ng/ml and 94 ng/g respectively, while the same for control subjects were 51 ng/ml, 0.22 ng/ml and 107 ng/g, respectively.

***Copper in liver biopsy samples*:**

Copper (Cu) content in liver is used as an index for the effective treatment of Wilson's disease. The line of treatment is based on the elimination of metals through chelating drugs and the elimination is monitored by urine analysis. The copper content in liver samples varied between 6.7- 7455 μg/g. Efficacy of the treatment was confirmed by excretion of Cu through urine.

***Lithium in serum samples*:**

A collaborative project with Psychiatric Department, BARC hospital is going on for estimation of Lithium (Li) in serum samples of psychiatric patients. As part of treatment Lithium carbonate is given to psychiatric patients and the level of Li in blood serum is to be monitored regularly.

■ Gas Chromatography Mass spectrometry techniques

The toxicity of an element depends largely on its physico-chemical form rather than its total concentration. For example, Tributyltin and other forms of organotins are extremely toxic to aquatic life at low concentrations. Similarly, it is well known that organomercury and organolead compounds have more toxicity even at very low concentration as compared to their metal counterparts. This calls for speciation studies of these compounds in environmental matrices.

Speciation of mercury in a marine ecosystem:

A solvent free solid-phase microextraction method has been developed to determine methyl mercury and Hg (II) in sediment, seawater and biota samples using Gas Chromatograph- Mass Spectrometer (GC-MS). The direct extraction of methyl mercury and Hg (II) by SPME after phenyl derivatization was studied and found to be suitable for the determination of trace levels of methyl mercury in above mentioned matrices.

***Speciation of butyltin compounds in marine environment*:**

The ionic butyltin compounds present in seawater and sediment

Sample	Total Mercury (ng/g)	Methyl mercury (ng/g)	Inorg. Mercury (ng/g)
Fish (n=5)	45 ± 5	40 ± 6	<12.0
Bivalves (n=3)	407 ± 22	224 ± 15	125 ± 11
Prawns (n=10)	82 ± 7	98 ± 9	14 ± 3.4
Crabs (n=6)	295 ± 17	208 ± 13	78 ± 9

Mercury Concentrations in biota collected from Trans-Thane Creek

samples were converted to their hydride forms using sodium tetrahydroborate ($NaBH_4$). These derivatized compounds were extracted using headspace SPME technique. A polydimethylsiloxane fibre was used to extract butyltin hydrides. The extracted analytes were then transferred to a GC-MS system for desorption, separation and quantification. The optimized method was applied to the speciation study of butyltin compounds in seawater and sediment from different part of the Thane Creek.

Speciation of organolead compounds in environmental matrices:

A method for the determination of organolead compounds and inorganic Pb^{2+} was standardised using GC-MS technique. The optimized analytical procedure was applied for the determination of organic and inorganic lead species in road dust and sediment samples. The ionic organolead compounds were extracted into hexane using chelating agent sodium diethyldithiocarbamate (NaDDTC) at pH 9 and in combination with EDTA. Derivatisation of ionic organolead species was performed with ethyl magnesium bromide. Ethyl derivatives of Me_3Pb^+, Et_3Pb^+ and Pb^{2+} were separated and quantified using a GC-MS system.

Man Made Radionuclides in the Environment

Plutonium and strontium in environmental samples:

Due to the nuclear reactor accidents, uranium nuclear fuel cycle and nuclear weapon production, actinides have been introduced into the environment. The mobilization of radionuclides in the environment has been studied for many years with the prime objective of tracing the routes by which they accumulate in the food chain and become available for human consumption. Therefore, it is necessary to have accurate, reliable and precise analytical method to determine actinides and fission products in environmental samples as well as their isotopic ratio to study environmental impact and risk assessment. Our laboratory is engaged in qualitative as well as quantitative analysis of Uranium, Plutonium, Americium and Strontium isotopes in different environmental samples and samples from nuclear fuel process (Depleted uranium, Ammonium nitrate samples, ore leachates etc.).

Quality Assurance/Quality Control for Nuclear Analytical Techniques:

The basis of economic, health care or environmental decision relies on analytical data and as it is well known, a decision based on incorrect analytical results can be extremely costly and detrimental. Therefore, it is essential that correct and reliable analytical data is used to make adequate decisions. To implement Quality Assurance/Quality Control for Nuclear Analytical Techniques, the laboratory has participated in various analytical quality control program and proficiency tests organized by IAEA (ALMERA, USDOE, MAPEP etc.) over the years. Our results compare very closely with the IAEA target values.

S. Bhalke, R. Raghunath, S. Mishra, B. Suseela, R.M. Tripathi, G.G. Pandit, V.K. Shukla and V.D. Puranik (2005). **Environmental Geochemistry,** Vol.8, N0.1&2, pp.180-185.

R.M. Tripathi, A. Vinod Kumar, S.T. Manikandan, Sunil Bhalke, T.N. Mahadevan and V.D. Puranik (2004). **Atmospheric Environment,** Vol. 38 (1), 135-146.

Radha Raghunath, R.M. Tripathi, Suchismita Mahapatra and S. Sadasivan (2002). **The Science of Total Environment**. 285, 21-27.

2. MODELING POLLUTANT DISPERSION IN THE ENVIRONMENT

INTRODUCTION

The routine environmental discharges from nuclear facilities are generally so low that it is often difficult to distinguish them from the natural background levels through monitoring methods. Moreover it may not be possible to monitor the pollutants at large number of locations over long periods of time, as required for obtaining long range and long term impacts. In view of these, computational methods based on the atmospheric and aquatic dispersion models provide alternative options for estimating the environmental impact of operating the Nuclear Fuel Cycle Facilities. Also, in order to be prepared for nuclear and radiological emergency situations, one requires reliable forecasting models that will predict the consequences in advance, if an eventuality takes place. These models are mathematically very complex and are solved through numerical computer codes requiring a host of meteorological parameters as input variables. The first few articles in this section are related to development and applications of these techniques. The remaining two articles relate to the formulation and validation of mathematical and chemical models to describe pollutant behaviour in the atmosphere, aquatic media and confined environments.

2.1 DEVELOPMENT OF ATMOSPHERIC POLLUTANT DISPERSION MODELS

The basic safety aspects of Nuclear Power Programme in India revolve around minimizing the release of radioactive effluents, both liquid and gaseous, to the environment to levels as low as reasonably achievable. In view of the safety systems involved in the operation of Nuclear Power Plants, the release of radioactive material to the environment is quite low and hence the resulting atmospheric concentration becomes difficult to measure. In case of accidental condition, even though with negligible probability, the emergency preparedness plan requires quick estimation of the affected zone, in order to take corrective actions for the protection of the environment and human beings. Thus, in both the cases modeling of the dispersion of released material becomes imperative.

For atmospheric route, conventionally the Gaussian Plume model is used for estimating the impact of normal release on the environment, on short-term as well as long-term basis. The Gaussian Plume model is quite simple and assumes homogeneous and stationary meteorological condition with constant source term data. The model is applicable for plain and homogeneous terrain conditions for distances in the range of tens of kms. However, in accidental conditions where source term can be time-dependent and/or for complex terrain conditions, such as hilly and/or coastal sites, the governing meteorological parameters for atmospheric dispersion vary significantly both in space and time and in such cases the treatment of atmospheric dispersion becomes complex. In order to address such complex situations, on the one hand we are developing the models that take care of such situations, and on the other hand we are also adopting available models to carry out state-of-the-science computations.

■ In-House Developed Models for Atmospheric Dispersion

a) EDPUFF- Equi_Distance PUFF Model

EDPUFF-Equi_Distance PUFF is a Gaussian dispersion code developed in the Environmental Assessment Division to study atmospheric dispersion of instantaneous or continuous point source release under time varying meteorological and source term conditions.

The model is developed in Visual Basic and has graphical user interface for data inputting as well as for post-processing the results. The figure given here shows the ground level concentration of Cs-137 after the source is switched off under changing meteorological conditions. The code is specifically designed to handle the atmospheric dispersion of Fission Product Noble Gases, I-131 and Cs-137 released from ground level as well as elevated sources. The code also has dose estimation module to assess the internal and external doses through various pathways. The plotting package of the code provides the facility to superimpose iso-contour curves

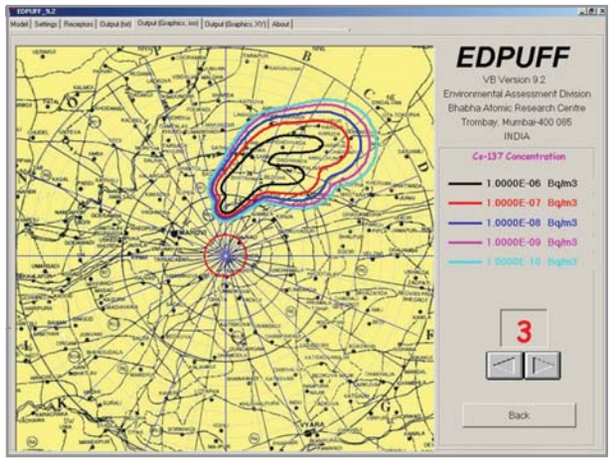

for ground level concentration, deposited activity or doses through various pathways on a site map. The package also contains facility to generate XY plot for all parameters mentioned earlier. Both the plotting facility has provision for animation. In addition to estimating the consequences of the released material on a pre-defined grid, the model also has a provision to assess the consequences of the released material at user defined receptor locations. The model was validated using SF6 tracer release experiment carried out at the Trombay site. At present the model is distributed to all the Environmental Survey Laboratories for their use.

b) Particle Trajectory Model

The EDPUFF model takes care of changing meteorological and source term conditions and has a capability to disperse ground level release and elevated release simultaneously with different wind speed, but with the same direction. However, it does not take care of vertical wind shear, which may become important

as puff grows in the size. The wind shear in vertical direction is expected to be significant even for a level and homogeneous terrain. In order to account for the vertical wind shear, Particle Trajectory Model is developed in the Environmental Assessment Division.

In the Particle Trajectory Model, the emitted gaseous material is characterized by a set of computational particles and each particle is moved at each time step by pseudo velocities, which takes into account (a) transport because of the mean velocities and (b) diffusion due to the turbulent velocities. The turbulent velocities are estimated using statistical method and mean velocities are obtained from the data collected by instrument like SODAR. The statistical method adopted for the estimation of turbulent velocities assumes that for a smaller time interval (few seconds), the turbulent velocities depend on its value at previous time step, plus some random component. After the displacement of the particles by pseudo velocities, the

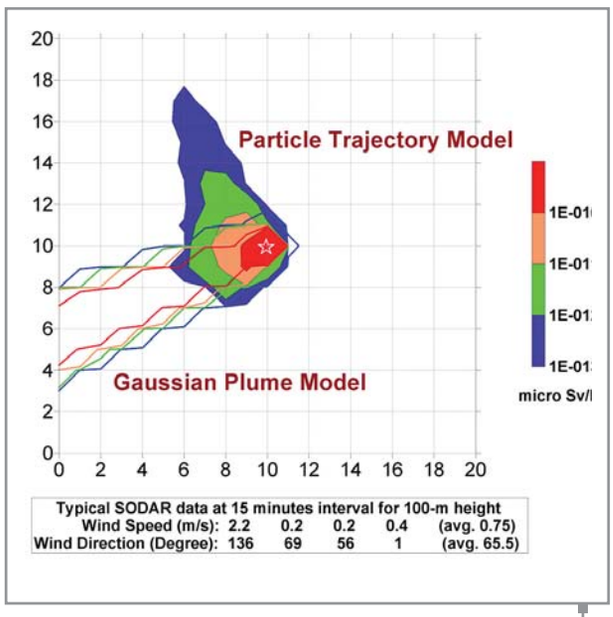

Estimation of gamma dose rate using
Particle Trajectory Model and Gaussian Plume model

concentration is then computed by descretizing the computational domain into grid cells and by counting the number of particles visiting the given cell and its residence time. A new methodology is also developed to compute gamma dose rate using particle trajectory model and it gives unique opportunity to estimate plume gamma dose under non-homogeneous and non-stationary meteorological conditions. The Figure presented below shows the gamma dose rate estimated using Particle Trajectory Model and Gaussian Plume model and as can be seen that the Gaussian Plume model may indicate wrong direction for the affected area, in view of the given meteorological data.

c) ADOCT- Atmospheric Dispersion Over Complex Terrain

In addition to vertical variation, meteorological parameters may vary significantly in horizontal direction also, especially for non-homogeneous and/or complex terrain conditions. The diagnostic models for complex terrain can be of use in such cases, however its accuracy of prediction depends on the density of meteorological measurements both spatially and temporally and in general fails to simulate circulatory flow pattern. To overcome these problems, the meteorological model ADOCT - Atmospheric Dispersion Over Complex Terrain is developed. ADOCT is a 3-dimensional mesoscale meteorological model in terrain following co-ordinate system for incompressible fluid with hydrostatic assumption and is coupled to the Particle Trajectory Model for dispersion computations. The flow model solves the momentum equations and the conservation equations for temperature and specific humidity in 3-dimensional computational domain. Meteorological module of the code is divided into two parts in vertical, namely, surface layer and transition layer. The surface layer module provides the boundary conditions at the bottom layer. The surface temperature, which is the most important boundary condition, is computed using standard astronomical formulae and Force-Restore method. The Force-Restore method makes use of the fact that diurnal variation of the temperature at one-meter depth is insignificant. This facilitates the assumption of two-layer approximation of the soil, where the top layer responds to the forcing term due to incoming solar radiation where as the bottom layer tries to restore the earth surface temperature. The 3-dimensional wind field generated by the meteorological module is passed onto the Particle Trajectory Model for the impact assessment, which is housed in the same code. A new methodology developed to estimate plume gamma dose rates using the Particle Trajectory Model is an integral part of the ADOCT code. The coupled

model ADOCT was applied to simulate typical sea-breeze condition observed at Kalpakkam. The time profile of wind speed and direction predicted by the model matched very well with that observed by Kalpakkam SODAR. The Figure given below shows the sea breeze simulation for Kalpakkam site at 15:00 hours. The Figure shows the flow field, surface temperature distribution and the distribution of released material.

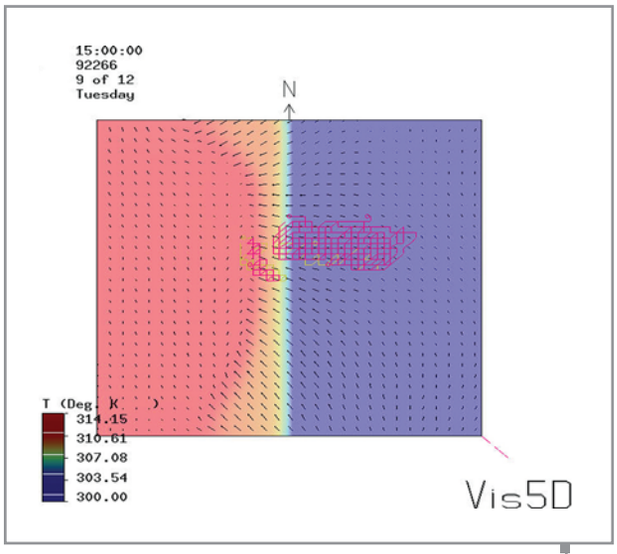

Sea breeze simulation for Kalpakkam site

Adopted Models

a) MM5

MM5 is a mesoscale meteorological model developed by Pennsylvania state university and National Centre for Atmospheric Research, USA. The model is used worldwide for the weather forecast over a regional scale. The model takes topographic and land use data in a standard format given by USGS. The initial and boundary condition data it takes from global weather forecast model and for that it supports many standard international formats. At BARC, the MM5 model is used with the global weather forecast model T80 from National Centre for Medium Range Weather Forecast, Noida, India, as well as with the AVN model output from NCEP, USA. The model has capability to have multiple nesting for getting forecast at finer scale. The MM5 model is being used to to drive CALMET/CALPUFF and RIMPUFF atmospheric dispersion models. The Figure given below shows typical MM5 output using initial and boundary condition data from NCEP USA.

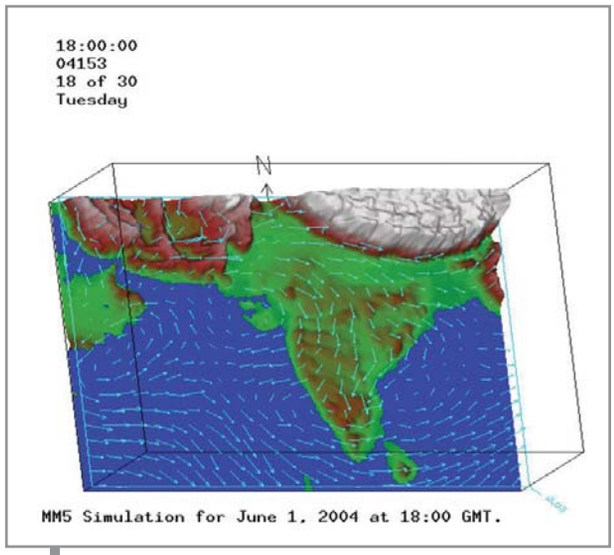

Simulation of wind field using MM5

b) CALMET/CALPUFF Model

CALMET/CALPUFF modeling system developed by Sigma Research Corporation is US-EPA recommended model for long-range transport and complex terrain modelling CALMET is a meteorological model that generates hourly wind and temperature fields on a 3 dimensional gridded modeling domain. CALMET uses terrain following vertical co-ordinate system. CALMET consists of a diagnostic wind field and micro-meteorological modules. The wind field is adjusted for kinematic effects and blocking effects of terrain. Optionally, prognostic wind fields can also be used as input to the met model. The advantage of using prognostic data is that the regional flows and sea breeze circulations are better captured which may not be the case while using surface met data. CALMET interpolates the coarse grid scale MM5 data to fine scale grid thus improving the spatial and temporal resolution of the dispersion model. CALPUFF is a multi species, multi layer, non-steady state Lagrangian puff dispersion model. It contains modules for complex terrain effects, over water transport, building downwash, wet and dry deposition and simple chemical transformation. The gridded output from CALMET is used to run CALPUFF. Hourly values of concentration and deposited activity are obtained as outputs from CALPUFF. A number of

methods to compute the dispersion coefficients are present. The model can also be used in a stand-alone ISCST3 single station mode. In addition to this, various pre-processors and utilities are provided to convert the input files and make it compatible with CALMET/CALPUFF. Post processors to analyse the results of the run are also provided. For test case, the CALMET/CALPUFF model was run with the MM5 data generated for India and the test result is presented here.

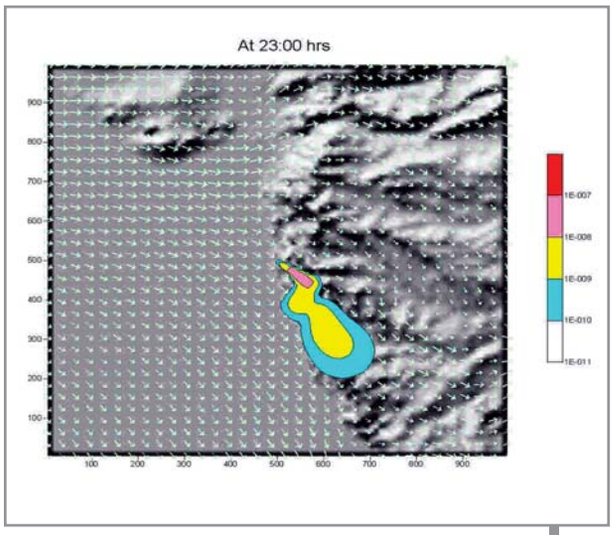

Atmospheric dispersion prediction using CALMET/CALPUFF coupled with MM5

c) RIMPUFF

RIMPUFF (Riso Mesoscale PUFF model) is a Lagrangian mesoscale atmospheric dispersion puff model designed for calculating the concentration and doses resulting from the dispersion of airborne materials. The model is developed by Riso National Laboratory, Denmark and is widely used in Europe for Emergency Preparedness Programme of their Nuclear Power Plants. The model can cope well with the non-stationary non-homogeneous meteorological situations, which are often of interest in connection with calculations used to estimate the consequences of the short term (accidental) release of airborne materials into the atmosphere. The model estimates ground level instantaneous concentration, time integrated concentration, gamma dose rate due to the plume passing over head as well as because of the deposited activity. At BARC the meteorological data required by the RIMPUFF model are supplied by the MM5 model. The necessary utility program required to generate input file from MM5 output was developed in-house. The Figure below shows a test output of the RIMPUFF model coupled with the MM5 model.

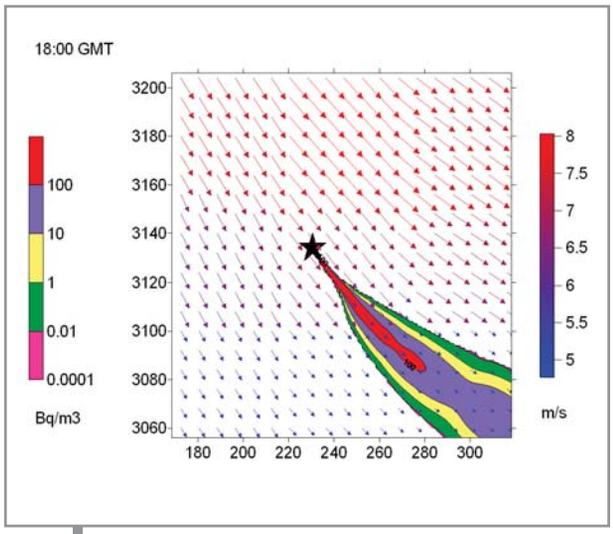

RIMPUFF coupled with MM5

d) PANEPR

In order to carry out atmospheric dispersion computations at a finer scale including the effects of terrain complexities as well as building structure etc., a CFD based modeling package FLUIDYN-PANEPR is obtained from Transoft, Bangalore. The PANEPR uses Computational Fluid Dynamics tools in a finite volume based approach to solve the differential equations governing mass, momentum and energy transfer. The conservation equations of each species are solved with the Navier-Stokes equations, which regulate the mixed flow and the energy conservation equations to take into account the heat phenomena. Fluidyn-PANEPR has a mesh generator tailor made for its requirements. In automatic mode, the software tries to adjust the mesh around the geometry of the source and of the obstacles. PANEPR uses a box-like computational domain of which the four vertical sides and the top are flat surfaces. The bottom face maps the ground. For a flat terrain, a Cartesian grid is used otherwise; the mesh is body-

fitted (bfc). The model can take into account the effects of presence of obstacles such as buildings and natural features of the landscape like fields, forests and water bodies and source effects. Fluidyn-PANEPR has built-in default values of simulation parameters, which are optimized for most of the cases and these can be altered as per user specifications. The fluidyn-PANEPR post-processor facility gives visual images of the flow field in the chosen computational domain. These images are mainly in the form of vector plots, contour plots surface plots and graph plots. The Figure below shows sample output obtained for a typical complex site.

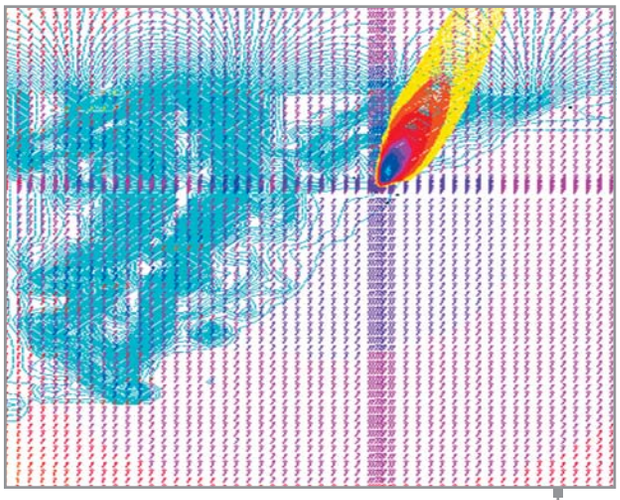

Atmospheric dispersion prediction for a complex site using PANEPR

Oza, R.B., Panchal, N.S., Nambi, K.S.V., Krishnammorthy, T.M., **Coupling of mesoscale meteorological model with particle trajectory model to study the atmospheric dispersion under sea breeze conditions,** Environmental Modelling & Software, 16, pp. 63-71, 2001.

Oza, R.B., **Application of ADOCT model to study atmospheric dispersion over peninsula,** IASTA Bulletin, 13, pp. 18-37, 2000.

Oza, R.B., Daoo, V.J., Sitaraman, V., Krishnamoorthy, T.M., **Plume gamma dose evaluation under non-homogeneous non-stationary meteorological condition using particle trajectory model for short term release,** Radiation Protection Dosimetry, 82 (3), pp. 201-206, 1999.

Oza, R.B., Bapat, V.N., Nair, R.N., Hukkoo, R.K., and Krishnamoorthy, T.M., **EDPUFF a Gaussian dispersion code for consequence analysis,** BARC/1995/E/001, 1995.

2.2 FLUID DYNAMIC MODELS FOR "INDIAN REAL TIME ONLINE DECISION SUPPORT (IRODOS)" SYSTEM

The Indian Real time Online Decision Support System (IRODOS) being developed at BARC caters to the off-site nuclear emergency of Nuclear Power Stations (NPPs).

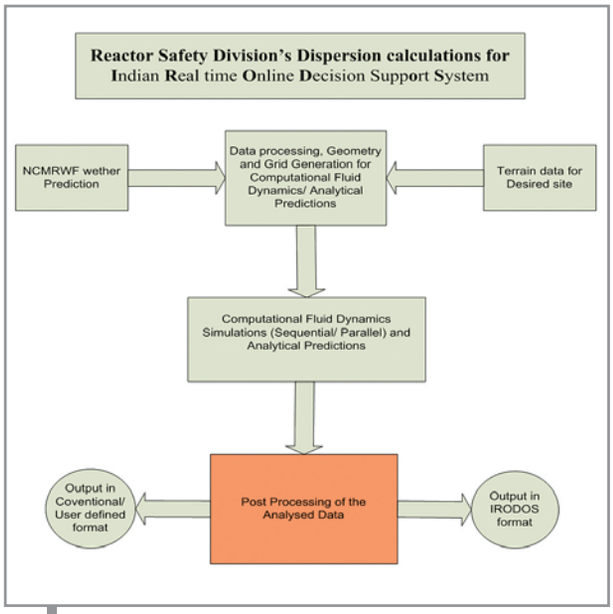

Dispersion modelling framework

The Reactor Safety Division of BARC is entrusted with the job of developing a framework for dispersion calculations using a) Computational Fluid Dynamics (CFD) software and b) Analytical models.

■ Analytical models

The differential form of the pollutant diffusion equation can be solved analytically with some appropriate approximation. There are different analytical models for vertical variation of concentration i.e. Source Depletion Model and Surface depletion model.These models evaluate height-distance profiles of the concentrations by considering various transport and removal processes. An example of Cs-137 concentration contours obtained using these models are shown in the figures for 24 hours of real time, reckoned 2 hours after stopping of the 24 hours release.

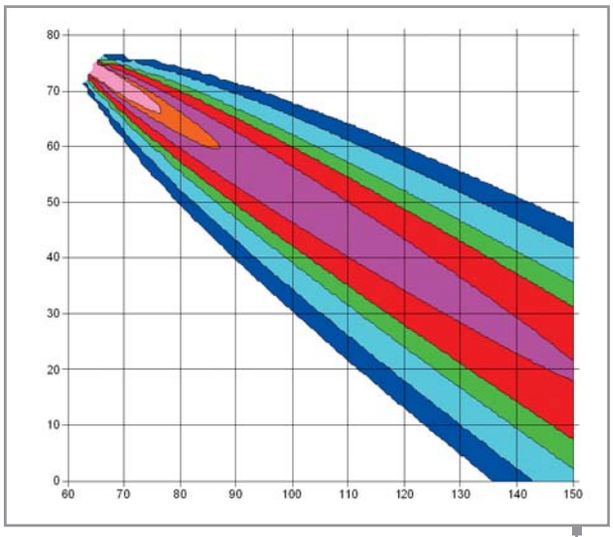

Cs-137 concentration (Bq/m^3)
Surface Depletion Model

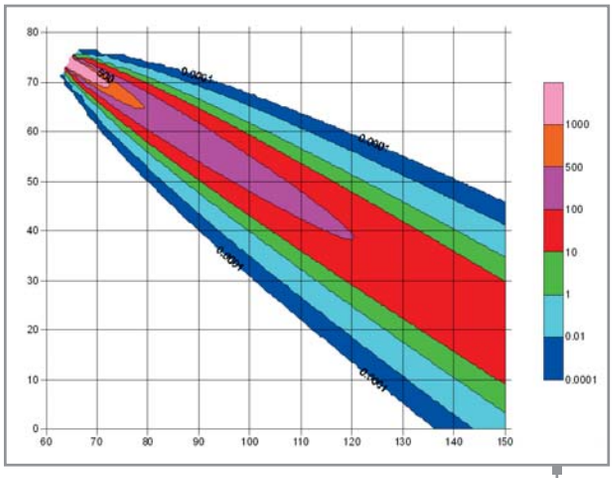

Cs-137 concentration (Bq/m^3)
Source Depletion Model

■ Computational Fluid Dynamics (CFD) simulation

CFD codes offer an opportunity of model development based on first principles of physics and hence such models have an edge over the existing models in terms of flexibility and accuracy. CFD techniques have been used for advanced large eddy simulation with multi-block cartesian mesh (both sequential and parallel computations). Case studies representing i) a simple terrain (150000 grid points for single block) and ii) complex Trombay site (325000 grid points in 7 blocks) terrain have been taken up before taking up the benchmark problem for the Narora NPP site.

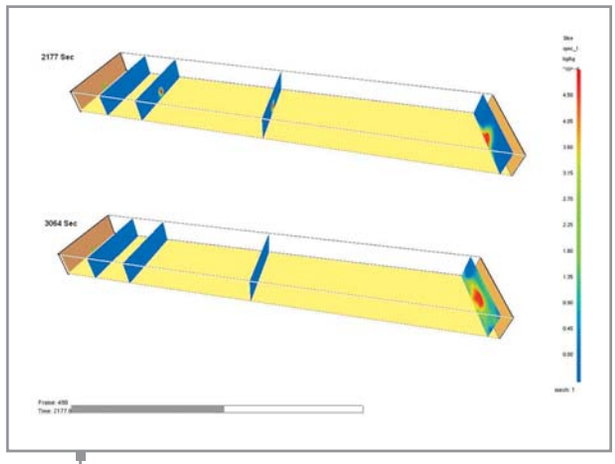

Dispersion in a Simple terrain

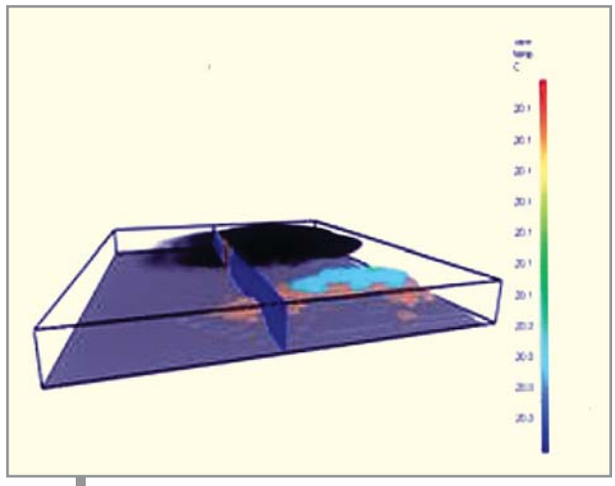

Dispersion in a Complex terrain

■ Narora benchmark problem

A continuous release of Cs-137 is assumed as the source term at a rate of 10^{10} Bq/Sec for 24 hours from a stack height of 145 m around Narora nuclear power plant. The actual meteorological data (about 50 MB data) was received from National Centre for Medium Range weather Forecasting (CMRWF), Delhi for 24 hours at IRODOS centre, BARC, Trombay through 2 Mbps internet data transmission line. The data contains meteorological parameters, such as atmospheric wind velocity, pressure and temperature distributions for a grid size of 1 km x 1 km over a calculation domain of 150 km x150 km around the site. This data was processed through a software and utilized as boundary and initial

conditions to simulate the prevailing climatic conditions in the CFD model and the mean atmospheric velocity profile and atmospheric stability condition required for analytical simulation. The CFD results have been compared with the analytical diffusion model. The predictions of the two are in reasonable agreement with each other.

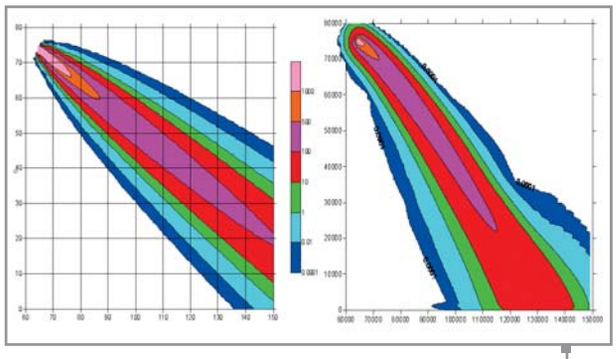

Comparison of Analytical and CFD Predictions

■ Conclusions

CFD and analytical results have been ported to IRODOS GIS platform to provide dispersion results in predictive mode. Developments are underway to integrate CFD and analytical computations with IRODOS in online manner.

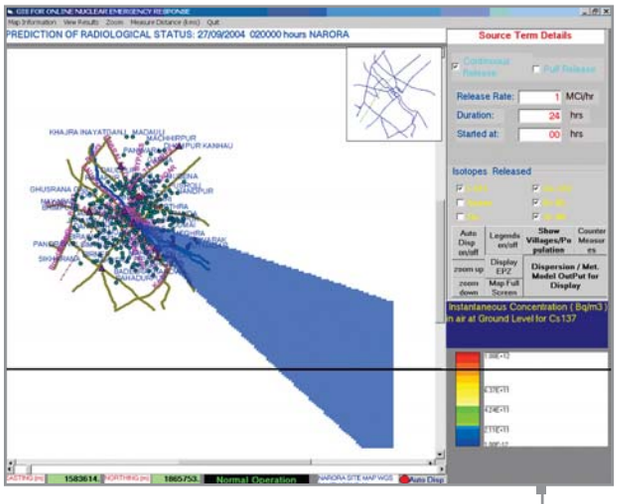

Dispersion results on IRODOS platform

Dr. A.K. Ghosh, <acss@barc.gov.in>

2.3 MODELLING THE DISPERSION OF POLLUTANTS IN AQUATIC SYSTEM

What is the sole method that can collectively assess the radiological impact of past, present and future releases in the hydrosphere? Answer is hydrological modeling. Over the years, the physical dispersion processes of pollutants have been studied mostly in the context of nuclear energy. As yet, there is less information about processes associated with the non-nuclear energy cycle releases than there is for the nuclear power cycle releases. Radioactive waste substances may enter the hydrological cycle either by direct release to surface and groundwater, or indirectly through contacts with the atmosphere and the soil. Direct releases to the hydrosphere may be part of the normal operation of nuclear fuel cycle facility. Releases, of course, may also take place under abnormal plant conditions. Hydrological models can describe the movement of radionuclides in the water bodies from a source mathematically. The use of hydrological models allows the establishment of relationships between releases, environmental levels of concentrations and resulting radiation doses to members of the public. This makes it possible to relate releases of radioactive substances into the environment to radiation protection requirements in terms of dose limits. The applications of hydrological models span over a wide range such as:

- Site evaluation for nuclear facilities
- Dose estimation for routine liquid releases from nuclear facilities
- Dose estimation for accident releases from nuclear facilities
- Radiological safety assessment of open cast uranium mines and tailing ponds
- Radiological safety assessment of radioactive waste disposal facilities
- Derivation of derived limits on discharge
- Derivation of waste acceptance criteria for radioactive waste disposal facilities
- Ensuring compliance with regulatory requirements on radioactive releases.

In this context, the Environmental Assessment Division has developed a number of hydrological models to evaluate the radionuclide concentrations in different aquatic media such as river, lake, coastal sea, deep ocean, sub-sea bed and

groundwater due to planned as well as accidental releases of radioactivity. The division is also in pursuit to explore the applicability of few commercial software like FEFLOW and POLLUSOL.

■ Surface Water Models

A two-dimensional surface water transport model has been developed for a tidally influenced sea with a view to derive the discharge rate limits for different groups of radionuclides. The main processes considered include advection by tidal currents, hydrodynamic dispersion and radioactive decay. This model can be used to evaluate the concentrations of radionuclides, which are released continuously into a tidally influenced coastal sea or bay. Models have also been developed to evaluate the concentrations of radionuclides in river, lake, deep ocean and sub-sea bed.

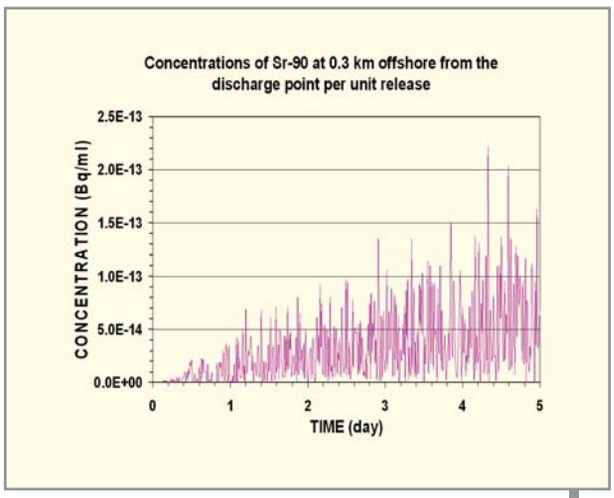

Concentrations of Sr-90 at 0.3 km offshore from the discharge point per unit release

■ Groundwater Models

a) Shallow Land Burial Model (SLBM)

It is a safety assessment model, which can be applied to near surface radioactive waste disposal facilities. The safety assessment model considers multiple disposal of radioactive waste into the facility, leaching of radionuclides from the waste form into the zone between the facility and the water table, migration of radionuclides through this zone towards the water table and finally migration through the geosphere (groundwater i.e. unconfined aquifer). It is assumed that the zone between the disposal facility and the water table is saturated for simplicity. The geosphere under consideration is assumed to be isotropic, homogeneous and saturated medium. The main processes considered in the migration of radionuclides are advection, hydrodynamic dispersion, linear sorption and radioactive decay. Since the dumping operation continues for a period of few years, it is required to evaluate the concentration of radionuclides during dumping period (disposal period) and post-dumping period (post-disposal period) in both the zones.

The SLBM can be used for different scenarios with respect to disposal facilities and type of sources. The figure given below shows the annual effective dose rates to members of the public through groundwater drinking water pathway due to near surface disposal of radioactive waste generated from 1 GW of nuclear energy at a typical site like Trombay.

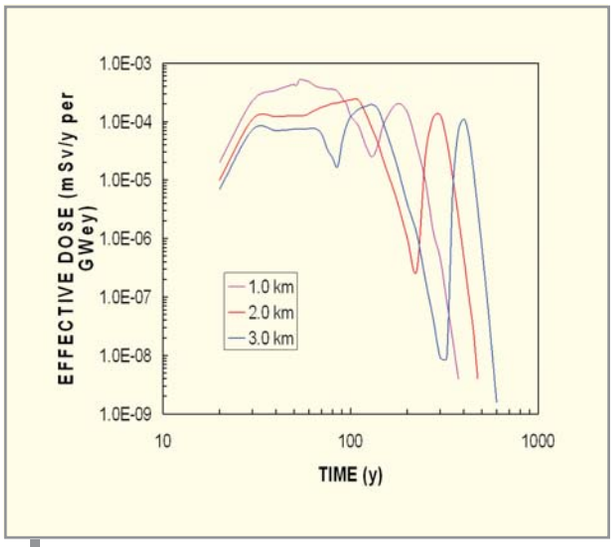

Committed effective dose rates to the members of the public

b) Risk Evaluation Model (REMS)

It is a probabilistic safety assessment model based on the failure rates of different natural and man-made barriers for Shallow Land Burial Facilities.

c) Migration of Radionuclides from Open Cast Mines (MIROC)

It is a two-dimensional solute transport model, which has been developed to assess the radiological impact due to the proposed exploration of uranium at Andhra Pradesh. The concentrations of natural uranium have been evaluated in the groundwater due to possible leaching of uranium from the open cast mines. These concentrations are translated into committed effective dose rates to members of the public using a radiological model.

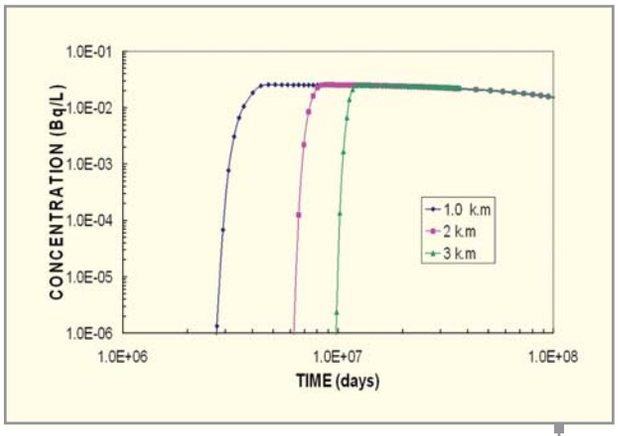

^{238}U concentration at different distances from the open cast mine.

d) Migration of Radionuclides from Tailing Ponds (MIRTAP)

It is a two-dimensional solute transport model, which has been developed to study the migration of radionuclides from uranium tailings ponds. This model has been applied for the proposed uranium tailings pond at Domiasiat, Meghalaya. For similar studies, a numerical groundwater flow and transport model has also been developed based on finite difference implicit scheme.

e) Multiple Area Source Model (MASOM)

It is an analytical groundwater transport model which has been developed to handle multiple sources, which are encountered in near surface radioactive disposal facilities. Since quantitative uncertainty analysis is required to quantify the degree of confidence in environmental models, computer programs have been developed based on Stochastic Response Surface and Fuzzy Logic.

f) Deep Geological Repository Model (DGRM)

It has been developed to study the migration of radionuclides through a single fracture from a high-level radioactive waste repository located in deep geological granite formations. The model utilizes two coupled equations; one for the fracture and the other for the host rock. The processes considered include advection, dispersion, surface sorption, diffusive loss to the host rock and radioactive decay for transport in the fracture; and radial diffusion, adsorption and radioactive decay for transport in the host rock. The source term to the model is provided as a two-component leach flux from the vitrified waste form stored in the repository. Results of the study indicate steep gradients in the concentrations within the first 50 m along the fracture axis. It is observed that about 99 % of the activity is retained by the host rock.

g) FEFLOW

It is a commercial interactive finite element groundwater modeling system for flow, mass and heat transport in subsurface environment. This model can be efficiently used to describe the spatial and temporal distribution of

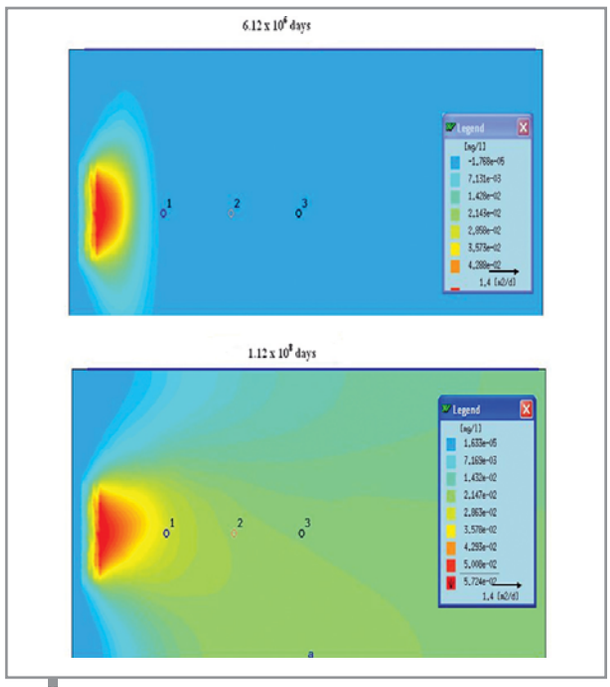

Profiles of U-238 concentrations in ground water for two time periods

groundwater contaminants, to model geothermal processes, to estimate the duration of travel times of pollutants in aquifers, to plan and design remediation strategies and interception techniques and to assist in designing alternatives and effective monitoring schemes. This software is used worldwide as a high-end groundwater modeling tool.

FEFLOW has been used to study the radiological impact of the proposed uranium tailings pond at Domiasiat at Meghalaya in the groundwater environment.

R.N.Nair, T.M.Krishnamoorthy and T.P.Sarma, **Tide induced mathematical model for coastal radioactive discharges and its application,** Indian J. Mar. Sci., 14 (1985) 9-14.

T.M.Krishnamoorthy, R.N.Nair and T.P.Sarma, **Migration of radionuclides from a granite repository,** Water Resour. Res., **28** (1992) 1927-1934.

T.M.Krishnamoorthy and R.N.Nair, **Groundwater models for safety assessment of low level radioactive waste repositories,** Nucl. Geophys., **8** (1994) 351-360.

R.N.Nair, Y.S.Mayya and V.D.Puranik, **A generic method to evaluate the reasonable upper bound dose from near surface radioactive waste disposal facilities through drinking water pathway,** Nuclear Technology, January 2006

2.4 ENVIRONMENTAL HEAT TRANSFER MODELS FOR THERMAL DISCHARGES FROM NUCLEAR POWER PLANTS

The efficiency of nuclear power plants, depends on the difference in the outfall and intake temperatures of the cooling water supply in addition to several other factors. Environmental heat transfer models thus have a major role in efficiently designing the intake and outfall locations of once-through cooling systems of power plants. Moreover, the concern about the environment in recent times has led to an increased interest in the convection and dispersion of thermal energy discharged from thermal and nuclear power plants. The biological impact of thermal pollution depends on the rise of temperature in the vicinity of the discharge outfall and the tolerance of different class of species existing in the region.

Heat transfer and related fluid flow processes encountered in the environment are generally very complex. They are usually turbulent and the mean distributions may vary with time. Many such flows involve mixed convection mechanisms because of buoyancy effects in the flows driven by wind shear. The radiation energy loss to the environment and the energy absorbed from the sun are also important in the analysis of environmental heat transfer. The natural temperature cycle of a water body is governed by this time dependent energy exchange at the surface. The energy loss at the surface can be expressed in terms of the heat transfer coefficient at the surface as a simplified assumption.

In fact, the energy exchange at the surface is coupled with the turbulent convective-dispersion processes. Because of the wind driven circulation, the convective heat transfer attains the stature of a three-dimensional turbulent problem.

In this context, the Reactor Safety Division (RSD) and the Environmental Assessment Division (EAD) are in the pursuit of developing environmental heat transfer models and applying them for thermal discharges from the nuclear power plants.

■ Fluid dynamic models

The Reactor Safety Division has developed an analytical model to predict the thermal plume behaviour in the Kadra reservoir at the Kaiga Atomic Power Station (KAPS) using a CFD code. After successful validation (against site data) of the model for the currently existing two operational plants at the Kaiga site,

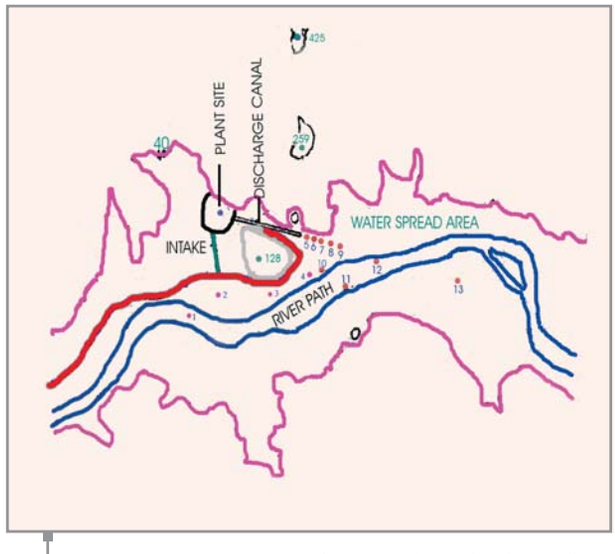

Important features of Kadra reservoir on the river Kali

the analysis was extended for the upcoming additional two units in the next phase and two more units in the final phase. It is understood that the existing discharge canal will be in use to discharge the hot water from all the six units proposed at the Kaiga site.

The analytical model was developed for the two units case by idealizing the Kadra reservoir as a simplified rectangular shaped geometry.

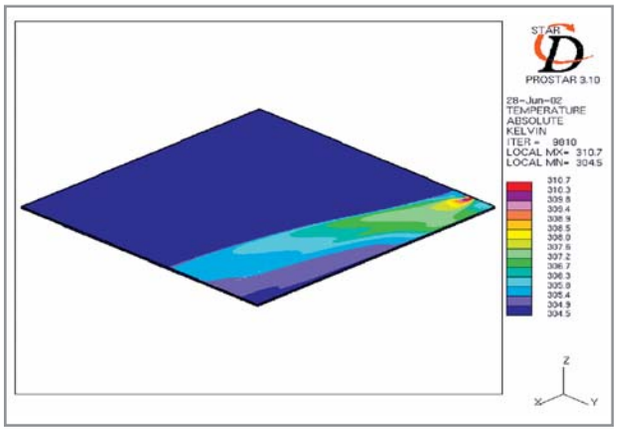

The same model has been extended for other cases. Some of the major input data for these analyses are the river flow velocity (0.2 m/s); hot jet velocity (0.4, 0.8 and 1.2 m/s for 2, 4 and 6 units respectively); temperature of hot water (310 K); temperature of reservoir water (304.6 K). The turbulence has been modeled using high Reynolds number k-ε model. The computational domain for all three cases is 1200 m (L) x 1200 m (W) x 8 m (D) and comprises of 3.8 lakhs cells.The total computational time required for each of these studies was of the order of 200 hours on Pentium-IV machine. The isometric contours of lake water temperature at the top surface (z = 0.0) for 2 units and 4 units are shown above. It can be clearly noted that the hot water jet, as it emerges from the discharge canal, tries to spread on both the left and right sides. However, due to close proximity of the river bank on its left side, the jet gets deflected from the left bank, thereby creating stagnant pockets in the reservoir near its left bank.The deflected jet then moves rightwards and spreads gradually along the width of the reservoir. The hot water spread is highest on the top surface due to buoyancy effects and the water temperature progressively decreases along the depth due to good mixing between hot jet water and the entrained cold water. The results of the analysis are presented in the table.

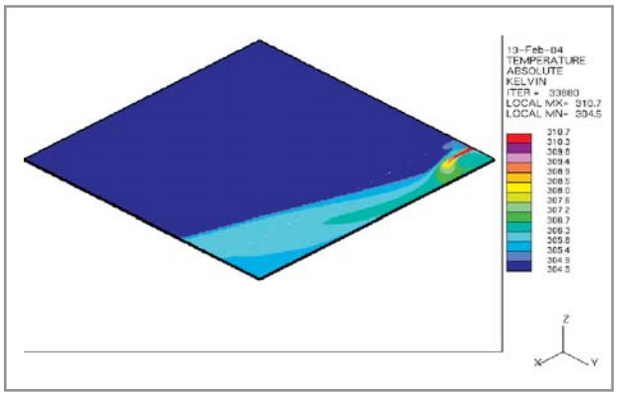

No. of Units in operation	Jet Spread (m)		
	Longitudinal	Transverse	
		Right	Left
2	500	110	220
4	700	60	110
6	900	50	100

The spread in the transverse direction is more or less same for both, the 4 units and 6 units cases and is almost 50 % smaller than that for the 2 units case.

Coastal Sea Heat Transfer Model

The Coastal Sea Heat Transfer Model (CHTM) has been developed in the Environmental Assessment Division to obtain the flow field and temperature field in the vicinity of thermal discharge outfalls located in coastal seas. It is a three-dimensional convective heat transport model. The model comprises of the flow equation to generate the velocity field in the coastal sea using wind stress at the sea surface as a forcing function and the energy equation to evaluate the temperature distribution with the discharge temperature at the outfall as the source term. A complete solar heat budget equation is also included in the energy equation. The coupled flow and energy equations are solved numerically using semi-implicit method with upwind scheme.

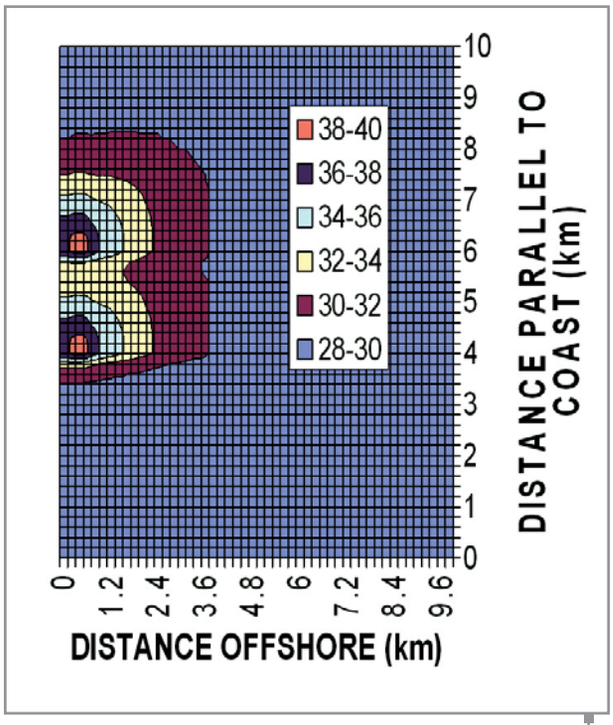

Temperature distribution in a coastal sea due to multiple thermal discharges obtained from CHTM

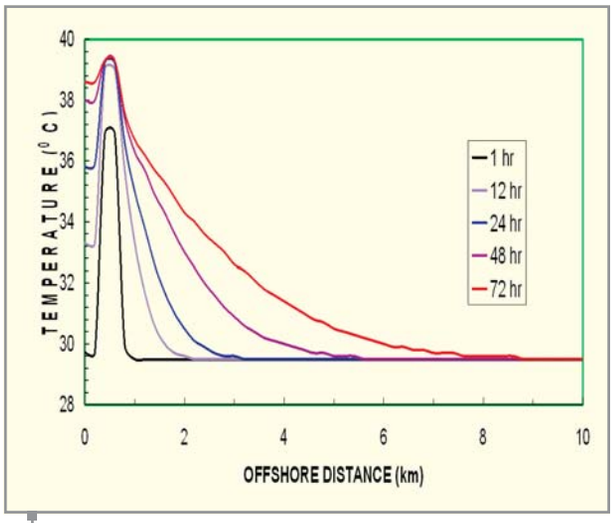

Temperature distribution as a function of offshore distance from the discharge outfall for different discharge periods

Steady State Heat Transfer Model

The Environmental Assessment Division has developed a three-dimensional steady state environmental heat transfer model for handling thermal discharge problems in rivers.

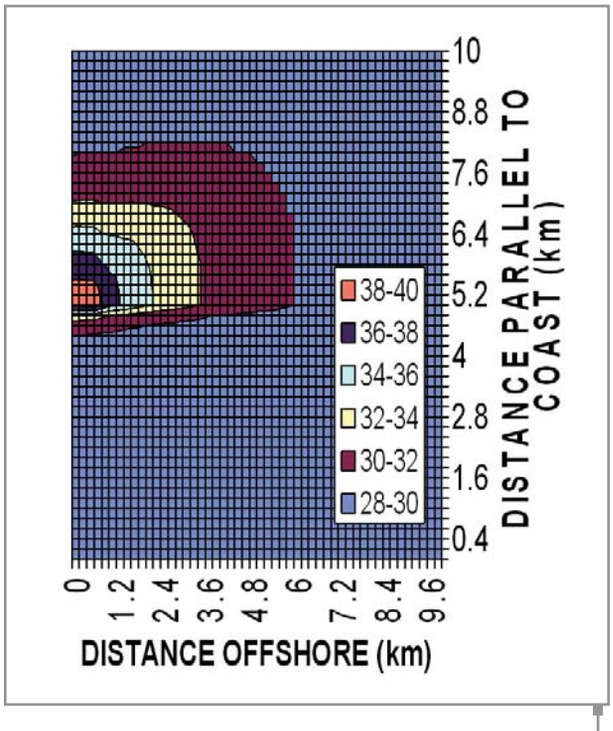

Thermal plume behaviour after 72 hours of thermal discharge

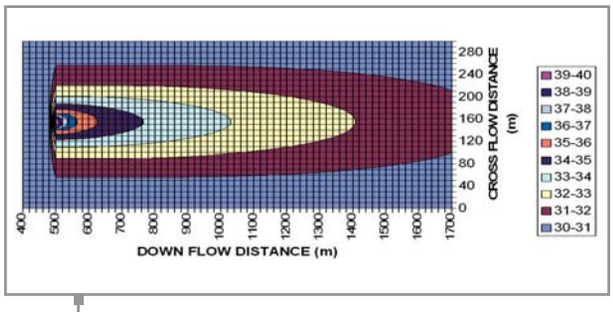

A typical thermal plume output of the model

Repository Heat Transfer Model

A three dimensional heat transfer model has been developed in the Environmental Assessment Division to predict the temperature distribution around high level radioactive waste repositories located in deep geological formations. The main processes in the model comprise of diffusion and decay in the waste form and in the surrounding environment. Spatial variation of diffusive and thermal properties with respect to

different material encountered in and around the repository such as granite, concrete and glass has been incorporated in the model. The effect of porosity in the surrounding host matrix is visualized by using an effective thermal diffusion and thermal conductivity in that region. The waste form includes a single canister having 1 kW decay heat energy.

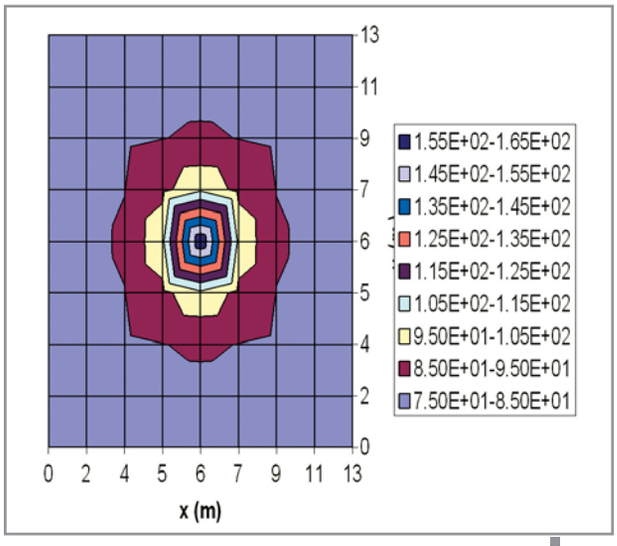

Temperature distribution around a hypothetical vitrified high level waste repository

Saurabhi Vadalkar, R.N. Nair and T.M. Krishnamoorthy, **Numerical simulation of environmental heat transfer from thermal discharge outfall,** Proc. 8th National Symp. on Environment (NSE), Kalpakkam, 1999, pp. 53-56.

R.N.Nair, S.Sadasivan and V.Venkat Raj, **Environmental heat transfer from thermal discharge outfall,** Proc. Fifth ISHMT/ASME and Sixteenth National Heat and Mass Transfer Conference, McGraw Hill Pub., 2002, 1211-1216.

2.5 PROBABILISTIC SAFETY ASSESSMENT LEVEL III FOR NUCLEAR REACTORS

Probabilistic Safety Assessment (PSA) is an effective tool for nuclear safety evaluation. Releases of radioactive material, which could cause major offsite consequences, are very unlikely for they arise only from accidents in which the reactor core is severely damaged and the containment fails. One major part of a full-scope PSA is the evaluation of the magnitude and probability of offsite consequences, alternatively called PSA Level III. The models developed for offsite consequence assessment describe the behaviour of released radioactive materials and predict the resulting interaction with and influence on the environment and man. Counter-measures are included for a realistic assessment. Predicted consequences may include early fatalities and injuries, latent cancer fatalities, the effect of counter-measures on people and agriculture and the magnitude of economic impacts.

The Reactor Safety Study published by USNRC in 1975, was the first comprehensive assessment of the consequences and risks to society from potential accidents at nuclear power plants. Since 1975 there has been a sustained development of consequence modelling techniques and many Probabilistic Consequence Assessment (PCA) models have been developed around the world to examine the risk posed by reactors and other nuclear installations to provide guidance for planning and decision-making. Besides use in risk evaluation, areas of application include assessment of alternative design features, evaluation of reactor siting recommendations, and development of safety goals.

■ Modeling Approach of PSA

The main elements of a consequence analysis are described in the figure below.

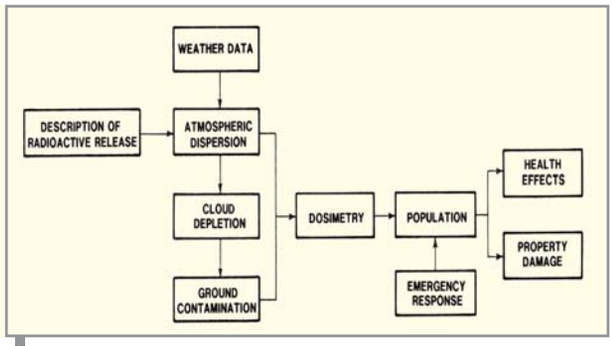

Basic elements of probabilistic consequence assessment

The major input data are: Accident source term, atmospheric dispersion and deposition, meteorological data and its sampling, exposure pathways and dose assessment, population, agricultural and economic data, countermeasures, health effects, economic consequences, sensitivity and uncertainty analysis.

Adopted Codes

CRAC2 [developed by Sandia National Laboratory] and COSYMA [developed by KfK and NRPB] are applicable for PSA level III as well as for deterministic calculations of the off-site consequences due to hypothetical accident releases of radioactive material to atmosphere from a nuclear facility. Another code RADTRAN IV [developed by Sandia National Laboratory] is used to estimate the risk of transportation of radioactive materials. These are briefly described below.

CRAC2 - Calculation of Reactor Accident Consequences

CRAC2 requires inputs on inventory of radionuclides released from the reactor containment to the environment and a description of the accident conditions. It models i) the meteorological dispersion of the cloud of radioactive material; (ii) the health effects of the material upon the surrounding population; and (iii) the cost of impact to the public from the accident. It samples specific meteorological conditions from a set of representative reactor locations and probabilistically combines the results to form frequency distributions of consequence from a reactor accident. In addition, CRAC2 models emergency planning procedures, such as evacuation. Detailed parametric and sensitivity studies can be simply accomplished in one computer run.

As an application of CRAC2, the NAPS site was considered for carrying out Level 3 PSA study for a typical Indian PHWR (235 MWe). Two scenarios of beyond design basis accident described below were the starting point for carrying out the consequence analysis:

LOCA + ECCS failure + Containment (inlet damper) failure

LOCA + ECCS failure + Containment (outlet damper) failure

Source terms for the triple failure were taken from the "Report of Task Force on Review of Indian Nuclear Power Plants in the Light of the accident at Chernobyl". One calendar year (1990) of hourly sequence of meteorological data of the NAPS site and population data around the site up to a radial distance of 16 km was used for carrying out the consequence accident analysis. Counter-measures were not considered for this accident sequence.

CRAC2 code has the capability to produce 84 different end points. The figure shows one end point namely the Cumulative Complimentary Distribution Frequency (CCDF) for the Whole Body Dose.

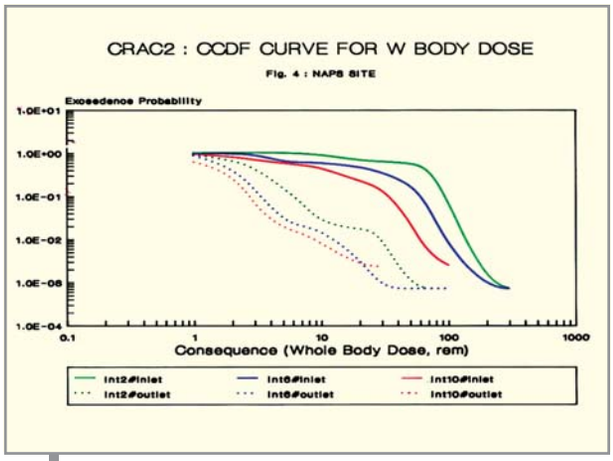

Cumulative Complimentary Distribution for Whole Body Dose at NAPS using CRAC2

COSYMA - Code System from MARIA

COSYMA consists of NE, NL and FL sub-systems. The NE (Near, Early) sub-system is limited to calculating early health effects and the influence of emergency actions to reduce those effects and is intended for use in the region near to the site. The NL (Near, Late) subsystem is limited to calculating late health effects and the associated counter-measures and is intended mainly for use in the region near to the site. The FL (Far, Late) sub-system is concerned with calculating late health effects and appropriate counter-measures at larger distances from the site.

The COSYMA code was adopted to estimate the early health effect due to a hypothetical release of radioactivity from Kakrapar Nuclear Power Plant. In this study, a triple failure i.e. LOCA+ECCS failure+Containment (Inlet damper) failure is considered as the accident scenario for a 235 MWe Indian PHWR. Noble gases and Iodines are the two-release groups of

radionuclides considered for estimation of doses in the population zone around the KAPS site up to 25km. The source terms for noble gases and iodine are estimated to be 55% and 13.75% of the core inventories, respectively.

Meteorological sampling is done from one calendar year's hourly data. In view of the very short duration of release, counter-measures were not simulated in the study. Cloud-shine, ground-shine, inhalation, resuspension from ground deposited activity, and skin doses from material deposited on skin are the exposure pathways considered for estimating acute health effects. Short-term dose is integrated to one month, except cloud-shine, which lasts for the duration of release.

Estimation of the dose for PSA level III is done using the PC version of the code. A comparison with the results of the mainframe version of COSYMA confirmed that there is only a small (< 2%) variation in the estimated mean doses provided the same weather sequences are employed.

This study was extended to finding the uncertainty caused by the meteorological sampling for assessment of off-site radiological consequences. Two different sampling schemes, namely cyclic and stratified sampling schemes, were considered for carrying out the uncertainty analysis. The number of weather sequences considered are, 8760, 400 and 300 in cyclic sampling, 147 in Stratified-1 and 114 in Stratified-2 samplings. Individual risk is considered as an endpoint. The results show that ranges of predicted risk arising from different sampling schemes are within a factor of two.

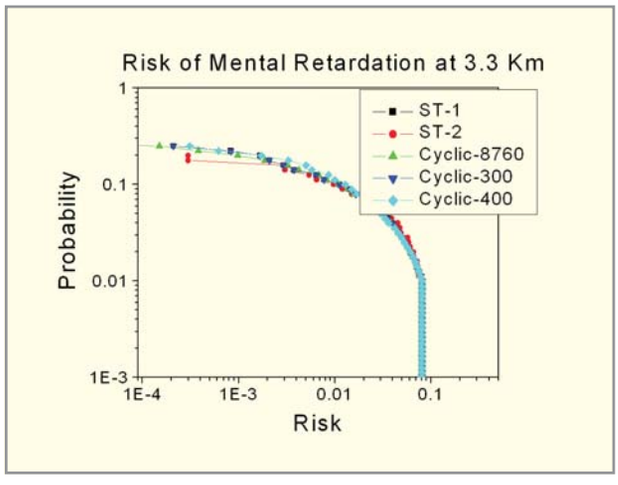

RADTRAN IV

RADTRAN 4 is a FORTRAN 77 computer code for the analysis of transportation risk. The code is used to estimate radiological risks associated with i) incident-free transportation of radioactive materials and ii) accidents that may occur during transportation. The code combines user-determined meteorological, demographic, transportation, packaging and materials factors with health physics data to calculate the expected radiological consequences and accident risk of transporting radioactive materials.

A full-scope PSA of transport of spent fuel by rail has been performed using this code to estimate the accident risk involved in the transport of spent fuel from the PHWR plant at Kota to the fuel reprocessing plant at Tarapur. The fuel considered was the low burn-up natural UO_2 fuel with a minimum cooling period of 485 d. The spent fuel is transported in a cuboidal, naturally-cooled shipping cask over a distance of 822 km by rail. For the computation of the accident risk, the basic rail accident frequency was obtained from the Indian rail accident statistics. The demographic data on rural, suburban and urban segments of the route were extracted from the1991 census report.

The meteorological data input for the analysis was based on the climatological study of the Tarapur site. Various accident environments like impact, puncture and fire were considered in the analysis. The possible ways in which a release of radioactive material could occur from the spent fuel cask were identified by the fault tree analysis.

The risk of potential severe accidents were computed using PSA methodology as shown in Table. Results of the study show that the radiological risk values are acceptably low and in the expected range of transport risks. Parametric studies carried out showed that the risk continues to be small even when the controlling parameters assume extreme adverse values.

Accident Severity Category	Total Population Risk in Person-Sv			Total Population Risk in Latent Cancer Fatalities		
	Rural	Suburban	Urban	Rural	Suburban	Urban
1	0.00	0.00	0.00	0.00	0.00	0.00
2	$1.12x1Q^{-15}$	$9.53x10^{-15}$	$1.35x10^{-14}$	$2.42x10^{-17}$	$1.94x10^{-16}$	$2.75x10^{-16}$
3	$2.84x10^{-11}$	$2.43x10^{-10}$	$3.44x10^{-10}$	$6.56x10^{-13}$	$5.32x10^{-12}$	$7.53x10^{-12}$
4	$1.49x10^{-9}$	$1.28X10^{-8}$	$1.82x10^{-8}$	$3.59x10^{-11}$	$2.95x10^{-10}$	$4.20x10^{-10}$
5	$1.85x1Q^{-9}$	$3.18x10^{-9}$	$2.26x1Q^{-9}$	$4.49x10^{-11}$	$7.44x10^{-11}$	$5.27x10^{-11}$
6	$4.88x10^{-12}$	$8.31 x 1Q^{-12}$	$5.93x10^{-12}$	$6.58 x 10^{-14}$	$1.09x10^{-13}$	$7.72 x 10^{-14}$
7	$1.27 x10-^{9}$	$2.17x10^{-9}$	$1.54x10^{-9}$	$1.92x10^{-11}$	$3.17x10^{-11}$	$2.25x10^{-11}$
8	$1.16x10^{-12}$	$1.98x10^{-12}$	$1.41x10^{-12}$	$1.59x10^{-14}$	$2.62 x10^{-14}$	$1.86x10^{-14}$
9	$2.14x10^{-13}$	$3.67x10^{-13}$	$2.60x10^{-13}$	$2.91 x 10^{-15}$	$4.82 x10^{-15}$	$3.41 x 1Q^{-15}$
Total	$4.64x10^{-9}$	$1.84x10^{-8}$	$2.24x10-^{8}$	$1.01x10^{-10}$	$4.07x10^{-10}$	$5.03 x10^{-10}$

Estimated Population Risk per Shipment for each Accident Severity Category

IAEA, **Procedures for Conducting Probabilistic Safety Assessments of Nuclear Power Plants (Level 3)**. Safety Series No. 50 P-12, IAEA, Vienna (1996).

V. Sitaraman, V.K. Sharma & K.D. Singh, **'An application of CRAC2 Model to NAPS site',** Internal Report, Health Physics Division, BARC, 1993.

Pradeep Bhargava, et al., **'Benchmarking of COSYMA and PC-COSYMA to estimate dose under postulated accident condition',** 1st National Conference on Nuclear Reactor Safety, November 25-27, 2002, Mumbai.

S. Chitra, V.K. Sharma and U.C. Mishra, **"Accident Risk Assessment of Transport of spent fuel by rail in India",** Nuclear Technology, Vol. 10, No. 4, pp 251-264 (1999).

2.6 MODELLING GRAVITY-INDUCED AEROSOL STRATIFICATION IN NUCLEAR AEROSOL TEST FACILITY

In a scenario involving low probability, severe accident in a nuclear reactor, radioactivity would be released into the atmosphere in the form of aerosols from any breach in the containment. The magnitude and nature of this release is assessed using several computer codes. These codes involve a host of interacting complex processes such as removal, coagulation, vapor condensation etc. To gain experience in the validation of these computer codes in the context of Indian power reactors, an experimental facility termed as the Nuclear Aerosol test Facility (NATF) has been set up in BARC. NATF houses a 9 m^3 test vessel, a Plasma Torch Aerosol Generator (PTAG) system and aerosol sampling instruments. Several aerosol behaviour experiments have been conducted in the test vessel by injecting metallic aerosols generated from the PTAG.

■ Problem statement

Aerosol behaviour codes generally assume spatial homogeneity of aerosols in the containment. This however need not be true if sufficiently strong mixing currents do not exist. Quiescent atmosphere forms the case of an extreme scenario in which much of the thermally and mechanically generated turbulence has died down after sufficient time has elapsed following aerosol release into the containment. As part of obtaining quantitative understanding of the aerosol characteristics under this situation, experiments were conducted in an undisturbed atmosphere in the test vessel. Also, quiescent conditions provide the appropriate environment to test gravitational sedimentation rate formulae used in the model. Aerosol concentrations were monitored at regular intervals for several hours at two heights of the vessel separated by about 1.7 m height. Results indicated that aerosol concentrations at the higher level decreased far more rapidly as compared to that at the lower level. This is

attributable to a gradual onset of gravity-induced stratification in which heavier particles elutriate to the bottom of the vessel at a faster rate than the lighter

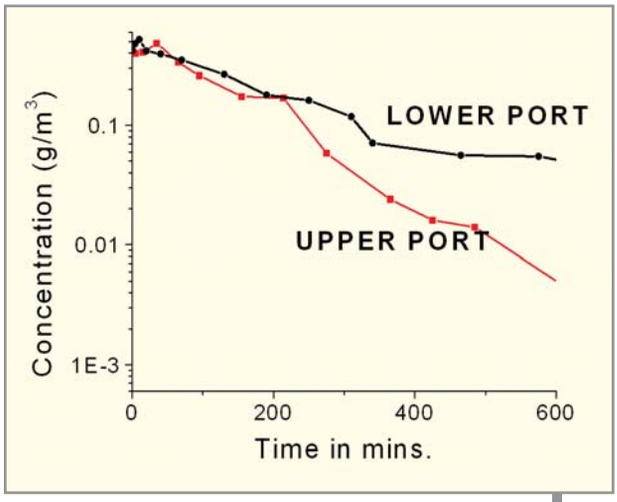

Observation of aerosol stratification at two heights of the vessel

particles. This generates local inhomogeneity in space thereby, altering other processes. Such a situation is not generally handled by available computer codes. In view of this, a new model, albeit approximate, was developed to account for stratification.

Model formulation

In the quiescent atmosphere, aerosol removal is essentially gravity-controlled modulated through evolution by coagulation. Hence, bulk diffusion as well as losses of particles to the top and side walls, may be set to zero. The problem is handled through the well known Smoluchowski coagulation equation modified to include gravity settling throughout bulk space:

$$\frac{\partial n(x,v,t)}{\partial t} = \frac{1}{2}\int_0^v K(v,v-v')n(x,v')n(x,v-v',t)dv'$$

$$-n(x,v,t)\int_0^\infty K(v,v')n(x,v')n(x,v',t)dv'$$

$$-v_g(v)\frac{\partial n(x,v,t)}{\partial x} \qquad (1)$$

where

$v=(4\pi/3)\,(r_a/\sqrt{\rho})^3$, is the volume of particles related to the aerodynamic radius r_a, $n(x,v,t)$=number concentration of particles at point (x,t) between volumes v and v+dv, $K(v,v')$=coagulation kernel,

$V_g(v) = k\,r_a^2 = c.\,v^{2/3}$ is the gravitational settling velocity where

$c=(2\rho g/9h)(3/4p)^{2/3}$ and $k=(2g/9\eta)$

(ρ=particle density, η=air viscosity).

We prescribe an initially homogeneous aerosol. i.e.

$n(x,v,0)=n_0\,g(v)$

where, g(v), normalized to unity, is the number concentration distribution function in volume variable v, and n_0 is the total number of particles /cc.

If coagulation were zero, (gravity induced drift were to be the only operating mechanism), the given polydisperse aerosol would have evolved according to the formula

$$n(x,v,t)=n_0 g(v).\,H(x-Vg)t) \qquad (2)$$

where H(z) is the Heaviside function, defined as 0 for z<0 and 1 for z>0. Then the fraction of the total airborne mass M(x,t) assumed to be proportional to the total air borne particle volume, may be given by

$$M(x,t) = \int_0^\infty vn(x,v,t)dv \Big/ \int_0^\infty vn(x,v,0)dv = \phi\left[\left(\frac{x}{kt}\right)^{3/2}\right] \qquad (3)$$

where,

$\phi\left((x/kt)^{3/2}\right)$ is the fractional cumulative initial mass lying for $0<r_a<(x/kt)^{3/2}$.

Eq.(3) implies that with only gravitational settling, the observed M(x,t) should be identical to the cumulative mass (as measured by a cascade impactor) below an aerodynamic radius $(x/kt)^{3/2}$. That is, the mass depletion is tantamount to a gradual unfolding of the mass-size spectrum. Then the temporal mass decay patterns at the two ports collapse into a single curve with scaled time t_s (= t/x). However, experiments showed a perceptibly faster decay at the lower port as compared to the upper port which may be explained by adding the coagulation term as a weak modifier over and above the

settling aerosol. Mathematically, it is equivalent to the ansatz

$$n(x,v,t) \approx n_0\, g(x,v,t).\chi(x,t) \qquad (4)$$

Upon substituting this and integrating over all v, the coagulation factor $\chi(x,t)$ satisfies the nonlinear, first order, partial differential equation

$$R_1(x/t)\frac{\partial \chi}{\partial t} = R_2(x/t)\chi^2 - R_3(x/t)\frac{\partial \chi}{\partial x} \qquad (5)$$

where, $R_1(x/t)$, $R_2(x/t)$ and $R_3(x/t)$ are the integrals of $g(v)$, $-(1/2)K(v,v')\,g(v)g(v')$ and $V_g(v)\,g(v)$ between $v,v' = 0$ and $(x/ct)^{3/2}$. Through a series of transformations one can solve the above equation in the form of a quadrature. We obtain

$$\chi(x,t) = \left[1 + x_1 \frac{t}{x}\left\{R_1\left(\frac{x}{t}\right) - \left(\frac{x}{t}\right)R_2\left(\frac{x}{t}\right)\right\}\int_1^2 \frac{R_2(u)du}{\{R_1(u) - (u)R_2(u)\}^2}\right]^{-1} \qquad (6)$$

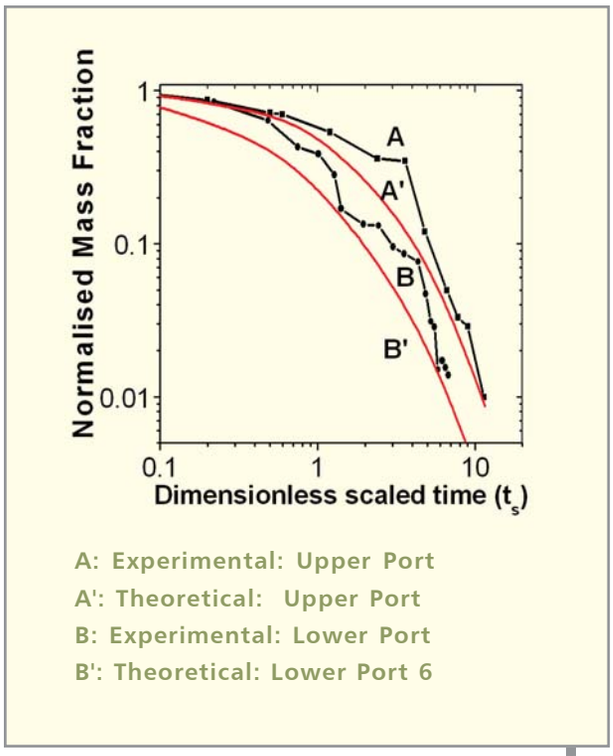

A: Experimental: Upper Port
A': Theoretical: Upper Port
B: Experimental: Lower Port
B': Theoretical: Lower Port 6

Comparison between observation and theory

Results and Discussions

If coagulation were negligible, the mass depletion curves at the two ports, when re-plotted w.r.t their respective scaled times (t_s), would have collapsed into a single curve. However, actually, the curve for the upper port appears above that for the lower port, thereby indicating a higher effect of coagulation at the lower port.

The size distributions generated by the 8-stage cascade impactor were used to estimate the coagulation correction factors at the two ports. This factor is larger at larger depths. The cumulative mass fractions, when multiplied by these factors for the two ports, are seen to follow the observed decay curves fairly well. This provides a validation of the stratification model.

Conclusions

Experimental studies conducted at low turbulence conditions have shown the gradual onset of aerosol concentration stratification in the test vessel. This has been modeled satisfactorily by introducing drift in the aerosol dynamics equations. The results have bearing on the behaviour of reactor containment aerosols at late times, in event of low turbulence in the containment.

Mayya Y.S, Sapra B.K., Arshad Khan, Faby Sunny and Venkat Raj V. (2002) **"Aerosol behaviour in BARC-Nuclear Aerosol Test Facility: Modelling gravity induced stratification and comparison with test facility data"** Indian Aerosol Science and Technology Association (IASTA) Bulletin, 14(1), 287-290.

Arshad Khan, Faby Sunny, Sapra B.K., Mayya Y.S., Anand S., Sharma V.K. and Venkat Raj V. (2002) **"Aerosol behaviour in BARC-Nuclear Aerosol Test Facility: Comparison with NAUA (MOD5) code calculations"** Indian Aerosol Science and Technology Association (IASTA) Bulletin, 14(1), 202-205.

Beonio-Broccheiri F.,Helmut Bunz, W. Schock et al. (1988): **Nuclear Aerosol codes,** Nucl. Technol. 81, 193-204.

2.7 MODELING INDOOR AIR-CLEANING EFFECTIVENESS OF UNIPOLAR IONIZERS

It is often said that the effect of air pollution is more significant in indoor air than in the outside environment. Human activities associated with indoor life as well as ingression from the

outside environment coupled with limited dispersive capability of the confined atmosphere result in the bottling up of chemical and biological pollutants in offices, workplaces and homes. To reduce the hazards associated with indoor pollution, several air-cleaning techniques have been developed. One such technique involves the use of air ionizers to charge the particles and precipitate them from air space. In recent years, experimental studies have demonstrated the reduction of air borne particulate concentrations in confined spaces using air ionizers. Several corona discharge based air purifiers are being

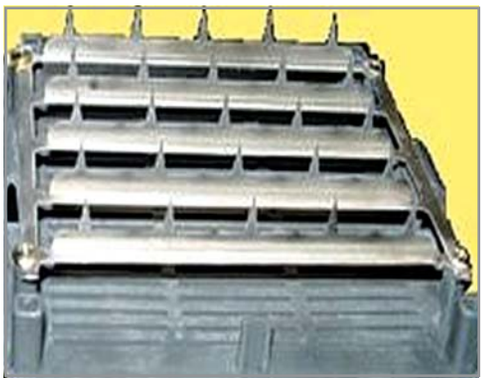

marketed world over. These systems consist of an array of sharp needles to which a potential of about -10 kV is applied. Ions are generated at the tips of the needles due to air breakdown and the negative ions are ejected into the air space. These attach to aerosol particles, causing them to migrate towards the wall surfaces due to the space charge generated electric fields. This article describes the experimental studies and the mathematical modeling of the air-cleaning efficiencies of ionizers by considering a host of particle transport processes in the indoor environment.

Illustration of ionizer action

In order to demonstrate the effectiveness of ionizers in reducing particulate pollution in confined spaces, experiments were conducted by placing an ionizer in a 0.5 m^3 stainless steel vessel. Aerosols were generated by burning an incense stick inside the vessel for a short time. In the first experiment, the normal depletion rate of the particles was studied with the ionizer off. Optical Particle Counter (GRIMM-Aerosol, GmBH) was used for counting the particle concentrations. In the next set of experiments, the ionizer was switched on soon after aerosol generation and the fall in concentration in various size classes was noted. The time variations of the normalized concentrations (i.e. the ratio of the concentrations at a given time with respect to their initial values) are shown in figure below for three size classes, viz., 1-1.6 μm, 1.6-2.0 μm, and 2-3 μm. It is clearly seen that when the ionizer is on, the aerosol depletion rate is enhanced by a large factor as compared to that without the ionizer. Although, this study is limited to a small chamber, it illustrates the effect of unipolar charging of particles in enhancing their removal rates.

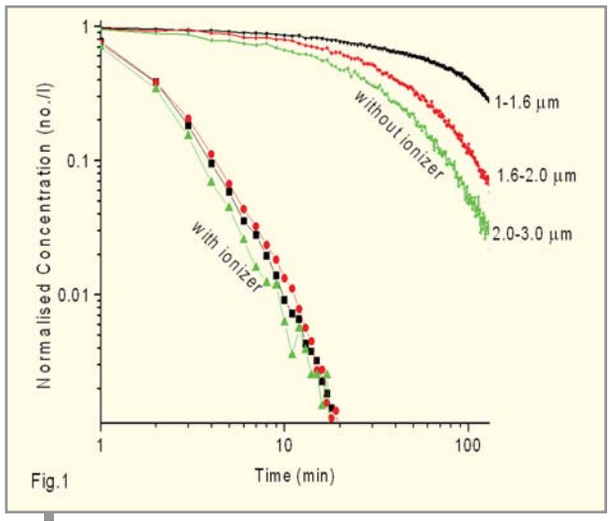

Fig.1 Time variation of Normalised concentrations

Formulation of the model

In order to quantify the air-cleaning efficiency of the ionizers in realistic indoor atmosphere, a model has been formulated for a negative ion generator located in a cubical enclosure having a certain air exchange rate due to ventilation. The ions are assumed to be dispersed in the room due to normal mixing currents. These attach to particles as a result of which space charge develops in space. This in turn drives the particles to the walls at a rate dictated by the size and concentration of particles, eddy diffusivity in the room and surface electric fields. The problem involves setting up of mutually coupled system of equations to describe the temporal evolution of the space charge induced electric fields, ion concentrations, particle concentration and charge build-up on particles. Particle removal processes include turbulent diffusion, gravitational sedimentation, electro-migration and external ventilation. This results in the following system of time-dependent nonlinear

coupled equations for the surface electric field $E_s(t)$, particle concentration C(t), particle charge $q_c(t)$ and ion concentration n(t):

$$E_g(t) - \frac{e}{\varepsilon_o}[n(t) + q_C(t)C(t)]\frac{V}{A}$$

$$\frac{\partial C}{\partial t} = -[(\lambda_p(t) + \lambda_v]C(t) + S_O$$

$$\frac{\partial q_C(t)}{\partial t} = K(q_C(t)n(t) - \frac{q_C(t)S_O}{C(t)}$$

$$\frac{\partial n}{\partial t} = Q_i - \{\lambda_i(t) + \lambda_o\}n(t) - K(q_C(t)n(t)C(t)$$

In the above, e is the electron charge, ε_0 is the permittivity of free space, V/A is the volume to surface ratio of the room, $\lambda_p(t)$ and $\lambda_i(t)$ are particle and ion removal rates, λ_v is the ventilation rate, Q_i is the ion generation rate density, S_0 is the aerosol injection rate and $K(q_c(t))$ is the ion-particle combination coefficient. The auxiliary expressions for $\lambda_p(t)$ and $\lambda_i(t)$ are based on Crump-Sienfeld type formulae and that for the $K(q_c(t))$ is based on ion-aerosol attachment theory. The system of equations are solved numerically through a FORTRAN Programme for various situations.

Computations and results

Numerical solutions have been obtained for the following typical parameters: Cubical room with volume, V = 80 m^3, A/V = 1.4 m^{-1}, coefficient of turbulence, k_e=6.3 s^{-1} and ion generator emission current 0.5 μA. Other parameters are: particle radii (R) in the range 0.01-1 μm, concentration (C) in the range ~0-10^4 cm^{-3} and ventilation rates, λ_v= 0 and 0.5 h^{-1}. At low particle concentrations, E_s ~16 V/cm and it increases drastically with concentration and size.

The *Concentration reduction factor (CRF)* attributable to ionizer seems to depend sensitively on the presence of preexisting ventilation in the room. This is illustrated in Figures given below for λ_v = 0 and λ_v = 0.5 h^{-1} respectively. It is seen that the CRF decreases by about a factor of 10 at all sizes even when a small ventilation is present. Other features are: CRF is higher at higher particle concentrations and also, for λ_v= 0, CRF increases with particle size attaining a peak at R~0.4 μm and decreasing thereafter. It may be safely assumed

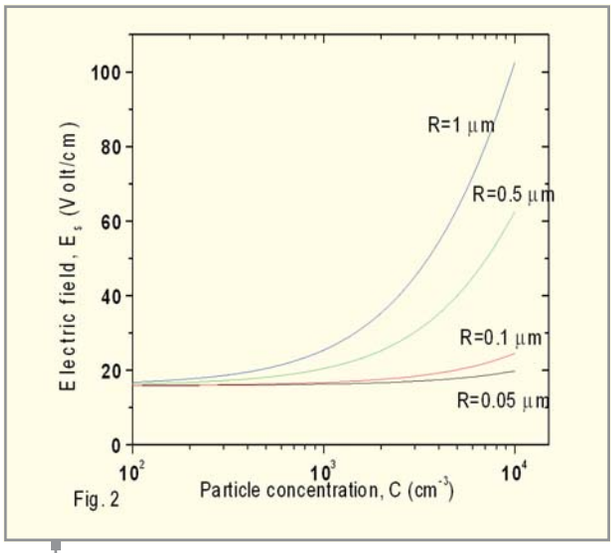

Fig. 2

Dependence of the induced surface electric field Es on aerosol concentration and size.

that a typical ionizer would yield a CRF value about 2-3 in the presence of small ventilation.

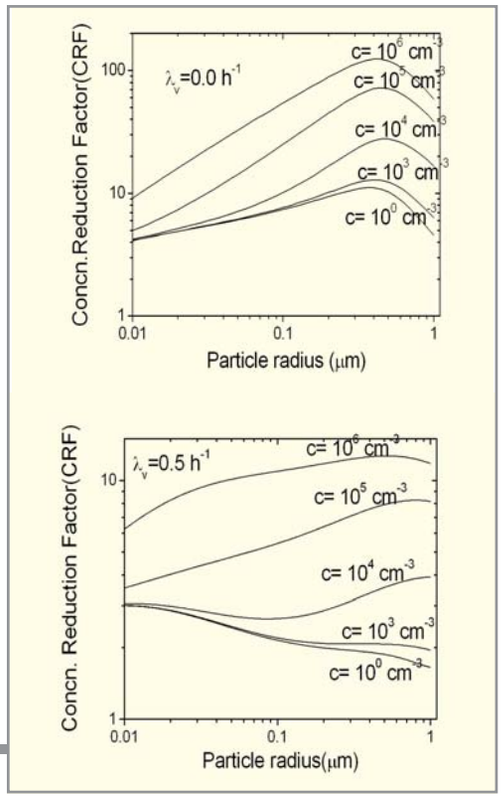

Variation of the concentraton reduction factor CRF under a steady-particle source as a function of particle radius for a ventilation rate of λ_v =0 and λ_v = 0.5 h^{-1}.

Simulations have been carried out for examining several other aspects such as the effect of room turbulence on temporal depletion rates, extent of charge build up on particles and dependency on room size and ionizer strengths. Essentially it is seen that ionizers are most effective in small rooms and under condition of low background removal rates.

Comparison with experiments

The model was subjected to validation tests with respect to the both published experimental data Garbarczyk (2001) and the data generated through room studies in BARC. In their study, Garbarczyk (2001) used corona wire discharge and monitored the depletion of aerosol concentration as a function of time. This was modeled here as a time-dependent problem and the results of comparison are shown below.

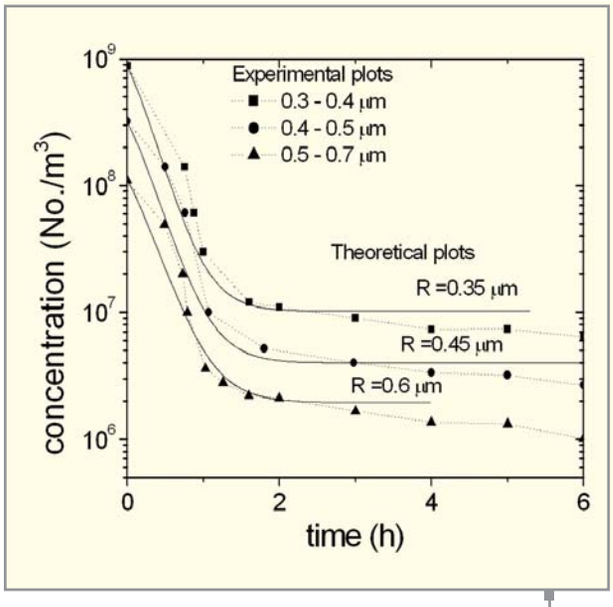

Comparison of the model predicted and the experimental data on the depletion of the particle concentrations with time.

The pattern of fall of concentration observed experimentally at various sizes is fairly well reproduced by the model. One specially notes that the turning point in the concentration decrease occurs between 1 to 2 hours in both. Here, the steady-state concentrations obtained after a long time

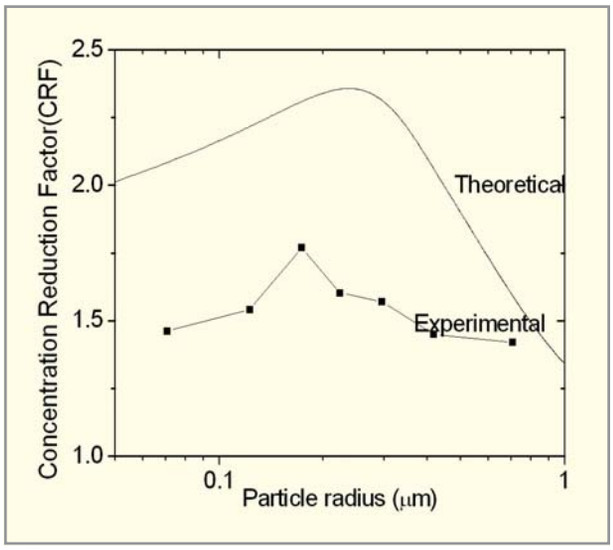

Comparison of the model predicted and the experimentally observed concentration reduction factor (CRF) for a typical room study

of operation of ionizer is compared for various sizes. The theory predicted somewhat higher removal rates as compared to that observed. However, the interesting aspect is that the experimental data showed a peak in the CRF close to that predicted by model. This is an important validation of the overall adequacy of the inherent assumptions of the model.

An important application of ionizers in occupational context is to deploy them for reducing radon and thoron progeny concentrations in breathing zones of workers engaged in uranium mining and thorium handling.

Khan A., Sapra B.K., Sawant V.D., Shaikh A.N. and Mayya Y.S. (2000). **Behaviour of cigarette smoke in a test enclosure,** in: Bulletin of Indian Aerosol Science and Technology Association (13), pp.160-163.

Sapra B.K., Khan A. and Mayya Y.S. (2001) **Theory of aerosol removal By unipolar ionizers in indoor air,** in: Proc. of Asian Aerosol Conf., Pusan, Korea, pp. 353.

YS Mayya, BK Sapra, Arshad Khan and Faby Sunny: **Aerosol removal by unipolar ionization in indoor environments:** J.Aerosol Sci. 923-941 (2004).

2.8 ROLE OF SULFUR-OXY-ANION RADICALS IN THE FORMATION OF ATMOSPHERIC SULFURIC ACID

As a consequence of the industrial revolution, a large number of man-made chemical pollutants have been, and are being released into the atmosphere. The harmful and long lasting impacts, such as ozone depletion, green house effect and perceptible changes in the climate, of a number of these chemicals have been realized only recently. Such effects depend on the atmospheric lifetimes of the species, which, in turn, can be predicted only if all the physico-chemical pathways of removal of the species from the atmosphere are known. Radiation Chemistry and Chemical Dynamics Division, BARC, has been engaged in studies on atmospherically important physico-chemical processes of organic chemicals containing functional groups, such as halogens, sulfur, cyanide, carbonyl, hydroxyl and hydrogen. A spectrophotometric method has been devised for measuring the Henry's law constant, which decides the distribution of a gaseous chemical between air and water. Photodissociation and destruction initiated by OH radical are the key reactions to remove most of the pollutants from the atmosphere. These are being studied, using modern experimental techniques, such as laser flash photolysis, laser induced fluorescence and resonance fluorescence, discharge flow, competition kinetics and pulse radiolysis.

The Henry's law constant of CF_2Br_2 (halon-1202, a fire retardant) has been measured, which suggests that this molecule would be distributed in both aqueous and air phases. Its photochemical dissociation, using UV-C (< 290 nm), has been investigated in both gas phase and aqueous solution. A new reaction producing BrO, an intermediate molecule that catalytically destroys ozone, was observed. The UV spectra of other intermediates were measured and their kinetics was investigated. The results also suggest a hydrolysis reaction in the presence of UV light. In addition, several new homogeneous and heterogeneous photochemical reactions of CF_2Br_2 have been discovered and their atmospheric implications understood.

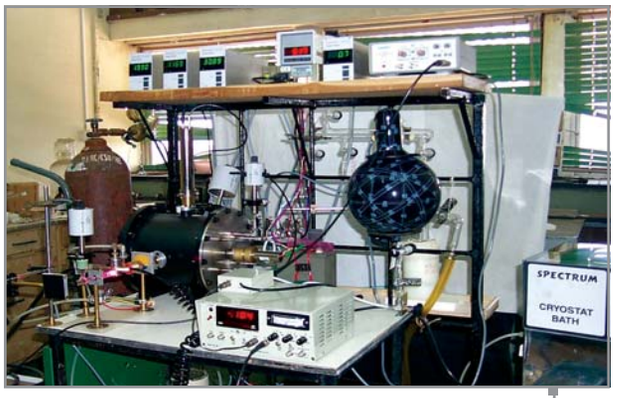

Flash photolysis resonance fluorescence machine

Reactions of OH radicals with unsaturated alcohols and important VOCs (volatile organic compounds), have been studied. The measured rate constants, in combination with *abinitio* calculations, provide a better understanding of the structure-reactivity relationships.

A semi empirical theoretical model has been developed to predict the tropospheric lifetimes and hence the ozone depletion and global warming potentials of new molecules. This would help in the speedy development of CFC-substitutes.

Recently, the measurement of rate constants for the reactions of Cl atoms with hydrocarbons has attracted a lot of attention due to their importance in the marine boundary layer. Investigations of such reactions, using competition kinetics method have been initiated and rate constant of the reaction between Cl atom and ethylene has been evaluated.

■ Role of Sulfur-oxy-anion Radicals in Atmospheric Sulfuric Acid Generation

Although simple gas-phase oxidation of sulfur dioxide to sulfuric acid in the atmosphere was realized a long time ago, recent understanding of various atmospheric physico-chemical processes suggest presence of an alternative route involving various types of liquid-hydrometeors (dispersed aqueous-droplets, diameter 5 μm to 3 mm) as the reaction media, omnipresent in the atmosphere. In these media, ready uptake of sulfur dioxide (good solubility) along with facile *in situ* generation (or presence) of a number of free radical initiators allow the oxidation to occur via a radical induced mechanism. The latter has been shown to be highly efficient and entirely different as compared to the generally familiar, slow gas-phase chemistry. In addition, free mobility of the hydrometeor, which acts both as a reaction medium and a carrier, influences the

global transportation of any locally released SO_2 gas, and thus causes widespread acid rain, affecting larger areas.

In order to have complete understanding of this heterogeneous, gas⇔liquid, oxidation route, we have recently re-evaluated the complete aqueous medium SO_2 oxidation mechanism and updated the important missing links in this auto-chain oxidation process. Employing radiation assisted (desired) free radical generation and starting with the sequential one-electron transfer processes, our studies dealt with (1) the evaluation of mandatory thermodynamic parameters to verify the feasibility of such processes and (2) measurement of all the relevant kinetic rates, which together helped to map each individual step, leading to the complete mechanism. This study is summarized as follows.

After dissolution of SO_2 into the aqueous phase, the resulting oxyanions HSO_3^-/SO_3^{2-} are readily oxidized, either following an electron transfer to a suitable free radical oxidant, like a (multivalent) metal ion (M^{n+}), or other radicals, like $NO_x\bullet$, $\bullet OH$ *etc.*, or as a result of photo-assisted or thermal reaction. Some of these free radical oxidants are common pollutants and dissolve readily in the said medium. The O_2 addition reaction to the resulting $SO_3\bullet^-$ species (sulfite radical) initiate the complex chain process that can be divided mainly into two reaction types:

(1) R*adical to radical* conversion wherein the reactions: $SO_3\bullet^-$ ($+O_2$) → $SO_5\bullet^-$ (peroxymonosulfate radical) →$SO_4\bullet^-$ ($+1/2O_2$) → HSO_4^- occur. The highlight of our study is to unequivocally show the important contribution of the peroxymonosulfate radical in this seemingly complex mechanism, for the first time, by standardizing its generation and chemical evaluation method.

(2) Various *radical + solute* reactions, wherein each of these three oxyanion-radicals reacts separately with the various solutes, either present (HSO_3^-/SO_3^{2-}) or generated from subsequent radical reactions (*e.g.* HSO_5^- ← HSO_3^-/SO_3^{2-} + $SO_5\bullet^-$; $S_2O_6^{2-}$ ← $2SO_3\bullet^-$ and $S_2O_8^{2-}$ ← $2SO_4\bullet^-$) during the course of this oxidation. The dissolved SO_2 gets consumed within a milli-second to generate H_2SO_4 (~ 98%), following a chain reaction, the length of which maybe as long as 10000 under polluted conditions. Subsequently, within the hydrometeor, the product sulfuric acid is retained due to its high solubility and eventually gets transported globally. In our study, employing various types of radical scavengers, it has also been shown that the individual oxy-anion radical chemistry can be separately modified, suggesting the possibility of use of an external influence to break the chain reaction for any desired purpose.

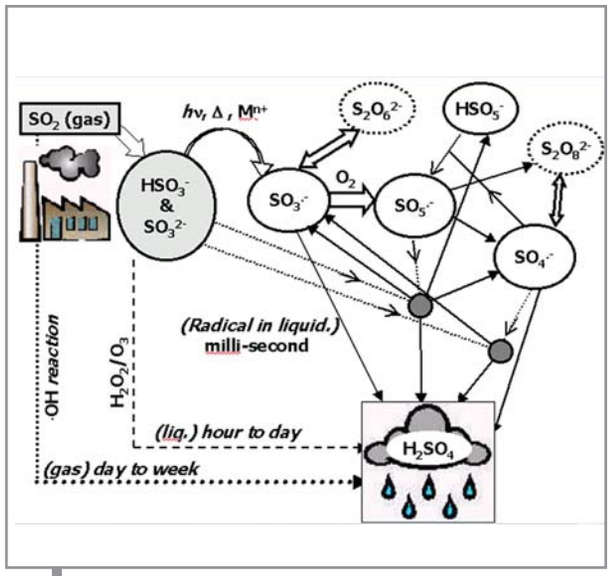

Mechanisms of SO_2 oxidation to H_2SO_4 in an aqueous environment

Dr. P.N. Bajaj, <**pnbajaj@barc.gov.in**>

2.9 RADIOTRACER INVESTIGATION ON DISPERSION OF SEWAGE DISCHARGED THROUGH THE WORLI SUBMARINE OUTFALL, MUMBAI

Wastewater management is a major problem in mega cities. Coastal cities have the unique advantage of disposing the generated municipal and industrial effluents by discharging them into the adjacent coastal waters through long offshore outfalls to reduce any environmental concerns. The island city of Mumbai with a population of about 12 million currently experiences severe coastal pollution problems associated with the disposal of about 2225 million litres of untreated or partially treated sewage into the coastal waters every day. In order to improve the coastal water quality standards by dilution, dispersion and flushing, a few offshore sewage outfalls have been constructed at various locations and a few are underway. One such recently commissioned submarine outfall is located at Worli.

Here, the collected wastewater is screened, degritted and then discharged into the tidal waters by gravity through a 3.4 km long offshore submarine outfall equipped with multi-port diffuser system aligned normal to the direction of tidal currents. Under normal operating conditions, the flow rate of sewage is about 7.2 m^3/s. To assess the functioning of the Worli outfall by studying the sewage dilution and dispersion processes, three radiotracer injections were carried out under various tidal conditions in the post commissioned regime. The data obtained from radiotracer investigations were used for the calibration and validation of various mathematical models.

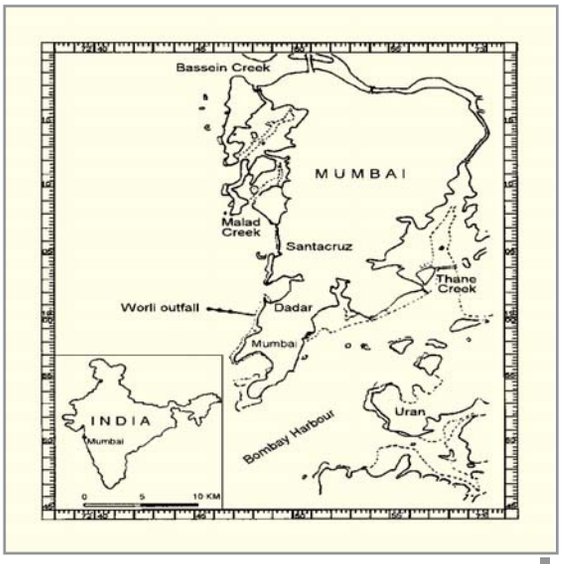

Location map of Worli submarine outfall, Mumbai

Radiotracer injections and monitoring

Radioactive ^{82}Br ($t_{1/2}$ = 36 hrs) in the form of aqueous ammonium bromide was used as the tracer for all the injections in view of its excellent property for tracing the sewage discharge.

The first tracer injection was conducted at the onset of (spring) ebb tide. About 110 GBq of ^{82}Br was diluted in 15 litres of water and continuously injected along with the sewage for 1 hour at the rate of 250 ml/min into the effluent channel leading to the diffusers. As the radioactive plume was established in the coastal waters, the area downstream of the diffuser was tracked using submersible water proof γ-scintillation detector coupled to scaler/ratemeter. Integration of data from the plume monitoring program helped to construct 3D picture of the sewage field in the form of iso-activity contours. It was observed that the sewage movement is predominantly tide drifted and follows the current direction. At the near-field, the sewage comes out from the risers in the form of non-merging and surfacing plume. In the far-field, the plume was found to be confined to the top 1-2 m without mixing over the entire depth. The two observed surfacial plumes suggest that advection processes dominate over lateral mixing. Dilution factors and dispersion co-efficients were also estimated from the radiotracer data.

About 64 GBq of ^{82}Br was used in the second injection which was conducted during an (neap) ebb slack period. Counter clockwise movement of sewage plume was observed during flow reversals and the dispersion during slack periods are mainly controlled by the onshore winds.

Worli sewage pumping station

Radiotracer monitoring

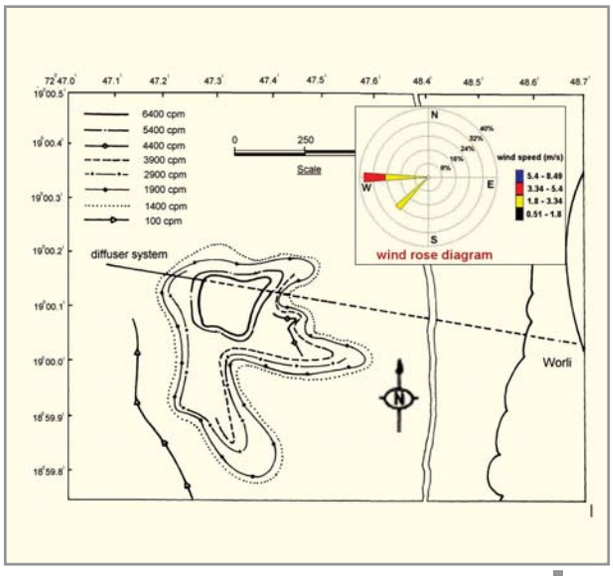

Isocount contour map showing the dispersion pattern of labeled sewage during neap ebb slack period

In the third injection conducted during a flood tide, about 74 GBq of ^{82}Br was used. The obtained radiotracer data was utilized for the validation of commonly used near-and far field models.

Validation of mathematical models

Initial dilution being an outfall design parameter, is normally computed using various mathematical models. Other dispersion characteristics such as plume geometry, dilution factors, dispersion coefficients etc. can also be predicted using empirical models. These models generally developed for highly idealized flow conditions are rarely validated for complex field conditions. In the present study, the data obtained from radiotracer studies was also used for the validation of various empirical and numerical near and far-field models.

Near field models: The validated near field models include Cornel Mixing Zone Expert System (CORMIX), 3D Lagrangian Jet Model (JETLAG) and the empirical model suggested by Roberts and others. It is seen that the model predicted dispersion characteristics matches fairly well with those of radiotracer data. However, the slight variation in dilution factors near the outfall is because of the limitation of those models in representing the complex design of Worli outfall.

Far-field models: Far-field models like the empirical models proposed by Brooks & Gardanov and a depth integrated 2D hydrodynamic and solute transport finite difference model, DIVAST was also validated with radiotracer data. The numerical model (DIVAST), with three open boundaries (two flow and one elevation boundary), was initially calibrated with observed tidal elevations and velocity data. The model was simulated to predict the dispersion of radiotracer discharged through the Worli outfall. The predicted far-field dispersion characteristics were found to match fairly well with radiotracer data.

	Measured with radiotracer	CORMIX	JETLAG	Roberts
Average dilution at the end of near field, S_1	50	68	55	60
Length of initial mixing zone, X_i (m)	11-20	7	14	5
Width of the plume at the end of near field, w_0 (m)	250-300	320		375

Comparison of near-field model predictions with radiotracer data

Distance along the plume axis(m)		Measured with radiotracer	Predicted values with models of		
			Brooks	Gardanov	DIVAST
Far field dilution, S_2	225	63	62	64	64
	625	90	70	81	108
	930	113	87	95	124
Width of the plume, w (m)	225	660	440		400
	625	642	555		600
	930	680	650		400
Lateral dispersion coefficient, D_y (m^2/s)		*1.25	1.5		

* Calculated by method of moments

Comparison of far-field model predictions with radiotracer data

Conclusion

From the study, it is concluded that, even though the outfall operational parameters have not yet been optimized by the operating agency, the sewage discharged through the Worli outfall is found to be adequately diluted by the entrainment caused by the outfall configurations and prevailing hydrodynamic conditions and thereby reducing any adverse impact on coastal waters. Also, the various dispersion characteristics including dilution factors predicted by the mathematical models compared well with those obtained from radiotracer studies.

Noble Jacob, Saravana Kumar U., Kulkarni U.P., Walinjkar P.B., Dhage S.S., Chandorkar A.A., Patil D.A., Rakesh Kumar (2000) **A Radiotracer Study on Near-Field Dispersion of Sewage from a Submarine Outfall off Worli Coast, Mumbai,** Proc. of NARRI annual conf. on Plans and strategies for applications of radioisotopes and radiation technology in the new millennium, Mumbai, p 185-188.

Noble Jacob, Saravana Kumar U., Kulkarni U.P., Navada S.V., Gupta I. & Kumar R. (2004) **Performance evaluation of the recently commissioned Worli submarine outfall, Mumbai, India using radiotracer studies and mathematical modeling** Proc. of Int. Conf. on Isotopes in Environmental Studies - Aquatic Forum, IAEA Marine Laboratory, Monaco.

Lee J.H.W., Cheung V., (1990) **Generalised Lagrangian model for buoyant jets in current**, J. Env. Engg. ASCE, 116 6, 1085.

Brooks, N.H., (1960) **Diffusion of sewage effluent in an ocean current**, (Proc. 1st Int. Conf. on Waste Disposal in the Marine Env.), Pergamon Press, N.Y.

Gardanoc, T.V. (1995) **Determination of the pollutant far-fields dilution using variable turbulent diffusion coefficients**, Wat. Sci. Tech., 32 7 41.

2.10 DATA MINING TECHNIQUES FOR STATISTICAL ANALYSIS OF ENVIRONMENTAL DATA

The growing field of data mining techniques involve machine learning methods in addition to the use of statistical models and mathematical algorithms. Learning methods include algorithms that improve their performance automatically through experience, such as neural networks and decision trees. These tools are applied to discover the unknown characteristics of the system hidden within the data, valid patterns and relationships existing in large data sets. Consequently, data mining involves not just collecting and managing data; it also includes analysis and prediction. Data mining tools use a variety of parameters to examine the data. The Artificial Neural Network (ANN) applications in data mining are used to discover relationships and recognize patterns within data. In this article, the case study for forecasting of dispersion of contaminants in the atmospheric or aquatic environment is considered.

Structure of ANN Models

Prediction or forecasting is the ability of the system to predict future values and outcomes based on current input values. The assessment of impact of atmospheric pollutant that affects

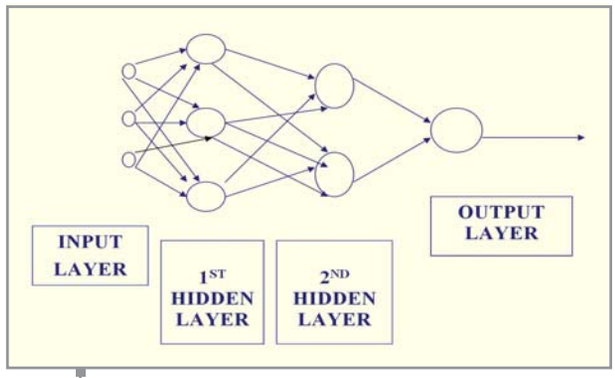

Multilayer perceptron model

a population at a predetermined location requires information on the weather parameters such as wind direction, wind speed and stability. In such a case, point measurement of the weather parameters may not fulfill the actual requirement. To generate the forecasting result of the environmental measurements, NN architecture is designed with available data pertaining to the operational behaviour of the system constrained with various meteorological conditions. The training of a NN is accomplished through the minimization of an index function using an in-house developed software BACKPROP. This contains MultiLayer Perceptron (MLP) model and employs the Radial Basis Function (RBF) as an activation function. Gaussian RBF is commonly used as it capable of approximating nonlinear functions reasonably well. Two problems encountered in training NN to ensure high efficiency in forecasting are (a) overtraining of multilayer perceptrons and (b) data reduction. Overtraining

can be minimized by increasing the hidden layers. Data reduction has been achieved by the Principal Component Analysis (PCA) technique or heuristic technique. An overview of intelligent forecasting applicable to search the wind pattern is worked out by BACKPROP.

The wind pattern is basically required to locate the propagation status of the environment. Multilayer Perceptron model is based on Back Propagation (BP) algorithm. Multilayer perceptrons are networks in which the processing units (neurons) are arranged in layers (e.g.atmospheric layers). The input to the nodes of each layer is taken from the outputs of the previous layers and the activation of the network layers is performed using a non-linear transformation (usually sigmoidal) to produce the desired outputs.

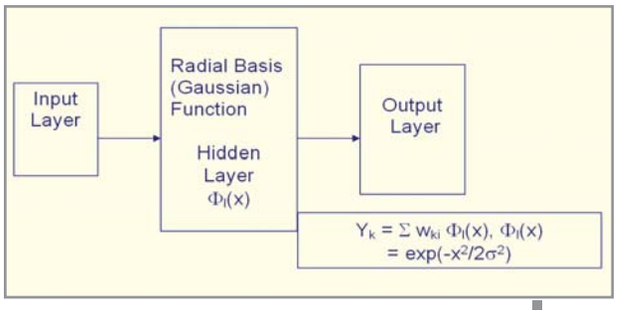

Radial basis network

An RBF network maps an input-output relation using a linear combination of radially symmetric functions. The output is modelled by a Gaussian RBF because of its symmetry about the mean. The training procedure of an RBF network includes several steps such as grouping the training patterns, hill climbing, computation of RBF function and computation of weight vectors.

Case study 1: Forecasting of Wind Direction

The case studied pertains to forecasting of wind direction in and around a typical plant site. Inputs are taken as a seven year historical meteorological data such as wind direction, wind speed measured at three different heights and stability class from a database controlled by specific rules. For the 2 - 3 - 1 NN architecture used, the mean absolute error computed was the smallest for a small data set and with data rejected by KB rules. A control rule in terms of Mean Absolute Error (MAE) has been specified to decide whether results are acceptable or not. Observation reveals further that If the MAE is more than 60% then results are categorized as "*not up to the acceptable mark*" and if the MAE is greater than 20% but less than 30% results are categorized as "*the best data set*". The results obtained with no rejection of data were not up to the acceptable mark. The best data set generated was for the twenty-two neurons.

Item	Winter	Summer	Monsoon
Most Predominant Wind directions	N, NNE, NNW, NE, ENE	WSW, WNW, SW, NNW, W	WSW, SW, W, SSW, WNW
Percentage Occurrence	72.9	55.3	82.8
Max. Abs. Error (MAE)	22 %	20 %	20 %
Training	N=9	N=9	N=9

Results of wind direction simulation using 7-year data

Case study 2: Effluent Releases from Indian NPPs

Data mining techniques are also applicable for carrying out statistical analysis. As an illustration, an extreme value analysis of gaseous and liquid effluent releases from Indian nuclear power plants has been carried out. An extreme value is the largest or smallest number in a data set. Principally, it concerns the limiting distribution of sample extrema (maxima and minima) described by the Generalized Extreme Value (GEV) distribution $G(x) = \exp[-\exp\{(x-L)/d\}]$ (Gumbel's distribution). The parameters L, d and x represent the location, scale and shape parameters respectively.

The variables selected for extreme value analysis are yearly, daily maximum release of Fission Product Noble Gases (FPNG,

Ci/day) and tritium (Ci/day) in the atmospheric environment and the daily maximum release of tritium (Ci/day) and gross beta (mCi/day) in the aquatic environment. The input data pertains to the following periods: TAPS:1969-2000; MAPS:1983-2000, RAPS:1975-2000,NAPS:1989-2000 and KAPS:1994-2000. The probability of exceeding of any given design value of environmental discharge in a given year has been worked out from the extreme value distribution. Typical results for the mean extreme value and other parameters obtained using NAPS data are presented in the table.

Nuclide	Mean value	Moment Method		Regression Method	
	Ci/d	Location (L)	Scale (d)	Location (L)	Scale (d)
FPNG	454.0	174.81	483.6	202.54	499.4
H^3 (air)	376.5	118.32	447.4	151.4	447.3
H^3 (liq.)	24.5	15.31	15.93	15.08	18.87
Gross β	0.003	1.57	2.46	1.6	2.8

Mean Extreme and Parameter Values of Gumbel Distribution

The computed extreme values are particularly useful for arriving at design basis values for effluent discharges to ensure the operational safety of Indian power reactors.

Conclusion

Statistical analysis and machine learning (neural networks) are data mining that encompass a soft computing environment. Validation of inputs in both the cases is inspected by knowledge base. Neural networks along with fuzzy input i.e. neuro-fuzzy computing provides a most powerful decision-making computing environment. Based on these, a software for deciding an effective countermeasure during nuclear or radiological accident situation is under development.

Datta D., Narayanan K.K. and Sharma R.M., **Extreme Value Analysis of Effluent (Gaseous and Liquid) Releases from Indian NPP,** Radiation Protection and Environment, vol. 26, No. 1-2, pp. 381-384, 2003.

Datta D., **Development of a knowledge based system for decision making of protective measures during a radiation emergency,** Bulletin of Radiation Protection, pp. 102-107, 1999.

Datta D. **Application of neural network to forecast the wind direction - A Parameter for controlling the environmental pollutant, Plant Engineering News** -Tarapur, Pen-t, Environmental Management Special - II, vol. 13, pp. 3-7, January 2003.

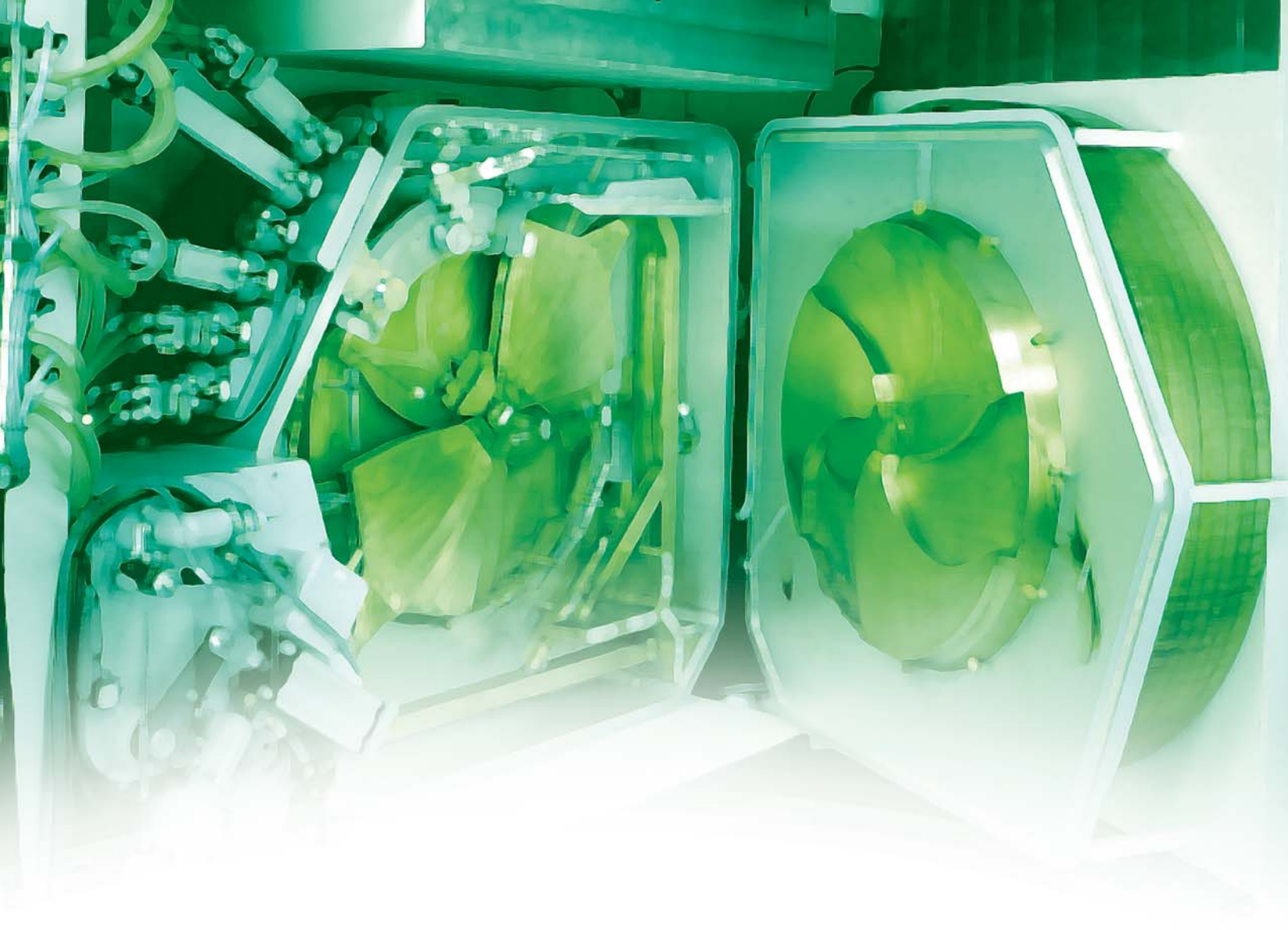

3. SAFETY IN INDUSTRIAL AND MEDICAL APPLICATIONS OF RADIATION

INTRODUCTION

Radiations and radioisotopes find important applications in industrial radiography, cancer treatment and medical diagnostics. In order to minimize unwanted exposures either to patients, their family members or to personnel handling these sources, appropriate shielding designs and dosimetric plans are evolved and implemented. A special case in point is the elaborate shielding arrangement for PET cyclotron. BARC also carries out development and dosimetric evaluation of sources for brachytherapy and industrial applications. This section contains articles dealing with the safety aspects associated with the radiation sources used for these purposes.

3.1 DOSIMETRIC EVALUATION OF ^{137}Cs MANUAL AFTER-LOADING KIT

For the treatment of cancer, several radioisotopes are used, among which ^{137}Cs is most commonly employed for intracavitary therapy. In India, Board of Radiation and Isotope Technology (BRIT), a unit of DAE fabricates ^{137}Cs tube sources for manual after-loading intracavitary applications. The nominal activities of these sources are quoted in terms of mCi or MBq, based on measurements in a re-entrant ionization chamber. The internationally recommended unit for specification of brachytherapy sources is Reference Air Kerma Rate, the air kerma rate at 1m. To correlate the supplier quoted activity to reference air kerma rate, traceable to international standards, measurements have been carried out using a calibrated well-type ionization chamber and a reference ^{137}Cs source.

^{137}Cs intracavitary kit, supplied by BRIT, is in clinical use for almost two decades and is in use in about seventy brachytherapy centres in the country and outside. The indigenously produced ^{137}Cs sources have now replaced the imported sources, used earlier. This replacement calls for a detailed dosimetry analysis of the kit. The Cs- Kit supplied by BRIT is meant for treatment of two patients at a time, one with long uterine tube and the other with medium uterine tube, both combined with two sets of vaginal ovoids. The dose rate at reference points and isodose distributions have been obtained for standard loadings of intracavitary applications. A User's Handbook has been prepared for the guidance of hospital users.

■ Materials and methods

The new ^{137}Cs sources produced by BRIT are of two types, namely, CSA-1 and CSA-2. The CSA-1 type source has an active length of 15 mm and total length of 21 mm and the CSA-2 type source has an active length of 10 mm and total length of 18 mm. The nominal activities of these sources are 120 mCi and 80 mCi, respectively. The sources have a sheathing of 0.1 mm platinum and are encapsulated in a stainless steel capsule of wall thickness 0.6 mm. For establishing traceable calibration, a well type ionization chamber, model HDR-1000 plus and a CDCS-J type ^{137}Cs source have been procured. The HDR-1000 plus model chamber is a versatile brachytherapy chamber for measurement of LDR and HDR sources. The CDCS-J type ^{137}Cs source has an active length of 13.5 mm, total length of 20 mm and filtration of 0.5 mm stainless steel and is one of the two types of ^{137}Cs sources for which IAEA provides calibration.

The HDR 1000 plus chamber was calibrated at the IAEA Dosimetry Laboratory using CDCS-J type ^{137}Cs sources. Prior to sending the chamber to IAEA Dosimetry Laboratory and on receiving back, the response of the chamber was measured using the local ^{137}Cs source, under identical conditions, to monitor the calibration stability during transit.

The reference air kerma rate of locally acquired CDCS-J type reference ^{137}Cs source was measured using the IAEA calibration factor for similar source. The calibration of the chamber at IAEA and subsequent measurement of reference source was carried out using the same source holder, to maintain reproducible conditions of measurement. The source, along with the calibrated well-type chamber, has been subsequently used to establish air kerma rate constant (reference air kerma rate per unit activity) of indigenously produced ^{137}Cs brachytherapy sources.

The intracavitary applicators are made of stainless steel and have external diameter of 6.0 mm with 0.5 mm wall thickness. As linear sources of length 21 mm and diameter 3.0 mm are to be used in this applicator, the radius of curvature of the applicator at any point is such that these sources can negotiate the curvature smoothly. The intrauterine applicators are either straight or bent at angles of 15^0, 30^0 or 40^0. By adjusting the position of the flange, the same applicator can be used for long or medium size uterine canal. For long intra-uterine applicator, the source pencil with three sources will be loaded and for medium size uterine applicator, the pencil with two sources will be loaded. A computational programme generated in Quick Basic was used for computing the dose fall off in the coronal and sagittal planes for different combinations of uterine and vaginal applicators. The attenuation due to 0.5 mm stainless steel applicator was also considered in the dose computations. The dose rates at points A and B, the reference points chosen for dose specification of intracavitary therapy and defined as 2 cm lateral to uterine canal and 2 cm above the lower end of the uterine source and isodose distributions have been computed for different loadings of uterine tubes and vaginal ovoids. The dose fall off in the coronal plane indicate the dose

variation in the parametrium and that in the sagittal plane, the dose to rectum lying posteriorily and bladder lying anteriorily.

Results and discussion

The air kerma rate constants of ^{137}Cs sources supplied by BRIT worked out to be 2.95 ± 0. 02 $\mu Gy.h^{-1}.m^2$. mCi^{-1} for the 15 mm long source and 2.85 ± 0. 03 $\mu Gy.h^{-1}.m^2.mCi^{-1}$ for the 10 mm source. The mean reference air kerma rate of 2.90 $\mu Gy.h^{-1}.m^2$. mCi^{-1} has been recommended for the dosimetry of ^{137}Cs sources produced by BRIT.

Two dimensional dose distributions have been computed for both types of sources, using Sievert Integral (SI) formalism. Monte Carlo (MC) calculations have also been attempted using the well-established MCNP code version 3.1. The dosimetry data obtained by SI formalism was compared with the data obtained by MC simulation. The absorbed dose in water, obtained using the latter was converted to that in muscle tissue using the ratio of energy absorption coefficient of water to tissue. The variation between SI and MC calculated dose rate at different points around CSA-1 type source is less than 1%, except at short distances and in the paraxial regions. The MC simulation accounts for the asymmetric inactive region on either end of the source, which is not accounted for in the SI formalism.

The dose rate constant (Λ) which is the dose rate at 1 cm, in water, on the transverse axis along the centre of the active source, worked out to be 0.934 $cGy.h^{-1}.cm^2.U^{-1}$ (where U is unit air kerma strength), for the CSA-1 type source of active length 1.5 cm. It is in good agreement with published values for other similar active length sources of different core materials and filtration. For comparison, the dose rate constant in water has been converted to that in tissue using the ratio of (μ_{en}/r) of tissue to water, which works out to be 0.99. The dose rate constant for CSA-2 type source of active length 1.0 cm worked out to be 1.012 $cGy.h^{-1}.cm^2.U^{-1}$. This is also in good agreement with the value of 1.002 derived from published data. The dose rate constant evaluated using Monte Carlo simulation agrees within 1%.

Dose computations were carried out to get the dose distributions in the Coronal and Sagittal planes for different combinations of uterine and vaginal applicators. The dose variation at points A and B for different sizes and angulations of uterine applicators and for different positions of vaginal sources has been analysed. It was seen that the dose rate variation at point A is negligible with angulation of uterine tube. The dose reduction due to vaginal sources is significant with increase in distance from vaginal fornices (~ 5 % per mm).

Conclusion

The basic dosimetry data for the new model ^{137}Cs sources has been worked out. Dosimetry data for standard loadings of intracavitary applications has been derived. A Users' Manual incorporating the details of sources, applicators and dosimetry has been prepared to supply to the Hospital users. Users' have been advised to use the data only as guidance and generate data for actual clinical conditions, as the geometry could vary significantly, in clinical applications.

A. Shanta, **International recommendations for establishing traceability of calibration for brachytherapy sources.** Journal of Medical Physics, 25, 2, 53-59, 2000.

A. Shanta, H.A. Sabuwala, V.S. Patki and K.N. Govindarajan. **Correlation of reference air kerma rate and activity for indigenous brachytherapy sources.** Journal of Medical Physics, 27, 4, 297-303, 2002.

A. Shanta, S.Vandana, H.A. Sabuwala, K.N. Govindarajan, U.B. Tripathi and B.C. Bhatt. **Implementation of IAEA recommendations to brachytherapy source calibration in India.** Presented at the International Symposium on Standards and Codes of Practice in Medical Radiation Dosimetry. Vienna, 25-28 Nov, 2002.

A. Shanta, P. Palaniselvam, S. Vandana, M. Banerjee, U.B. Tripathi and B.C. Bhatt. **Dosimetry data for ^{137}Cs Manual Aftertloading Kit - Users' Handbook.** BARC Report, BARC/2004/I/013.

3.2 EXTREMITY DOSE MEASUREMENTS FOR THE STAFF HANDLING UN-SEALED SOURCES

In India, for the past five decades, whole body radiation dose is being monitored by means of film and Thermo-Luminescent Dosimeter (TLD) badges worn on the body. From January 2003, some of the radiation workers in nuclear medicine activities and those involved in despatch and transporting of radioactive material from Board of Radiation and Isotope Technology (BRIT) have been monitored for their extremity doses (fingers) by providing them with finger ring dosimeters.

BRIT is supplying a variety of radioisotope products and equipment to about 2000 institutions in the country as well as abroad. On an average, over 50,000 consignments of radioisotopes are being supplied every year. However, the staff available for the above work being limited; each individual handling the radioactive consignments was monitored once to have an idea of the order of doses received by the extremities of the above staff members.

In nuclear medicine laboratories where 1000 GBq of radioactivity is being handled annually by the technical staff in eluting $^{99m}T_c$ activity from in-house generators, handling ^{131}I, administering large dosages to patients undergoing diagnostic and therapeutic procedures and in scintigraphy, the extremities of the staff are likely to receive radiation dose. These members of staff are also monitored as and when asked to assess the doses received and ensure safe work practices in the department.

Different designs of Finger Ring dosimeters

The dosimeters used for monitoring are $CaSO_4$:Dy discs, cut to size 6 mm diameter and 0.8 mm thick and loaded in finger ring gadget. These have been redesigned from time to time as per the comfort of the workers.

Each worker was provided four dosimeter rings to be worn on index and ring fingers of both right and left hands for a period of 2 months. These rings were worn in such a way that the dosimeters face the dorsal side of palm. The dosimeters were read in conventional TL dosimeter reader.

A palm showing the Finger Rings with dosimeters

■ Results of Monitoring

a) Exposure in nuclear medicine diagnostic procedures

It is found that the annual equivalent dose received during extraction and radio-pharmacy procedures ranges from 7 to 300 mSv. There have been institutions handling low radioactivity but have registered reasonably high doses to extremities. The maximum exposure to extremities is recorded in dispensing, injecting and PET scintigraphy with ^{18}F-FDG.

b) Exposure in nuclear medicine therapy procedures

Exposure received by extremities in the treatment of radiation synovectomy with 6 GBq of ^{153}Sm radionuclide is found to be in the range of 22 - 39 mSv. This study indicates that in order to keep the extremity dose within the prescribed limit of 500 mSv, the number of operations performed by a radiation worker should not be more than 20 in a year.

c) Exposure in packaging and despatching of radioactive materials

Proper containment, safety and security of the radioactive material are the most important requirements of any radioactive material package. Depending upon the nature, form and activity of the radioisotope, different types of packages such as Type-A, Type-B and Excepted packages are used. The maximum dose received by the extremities of a radiation worker was 6.4 mSv whereas the whole body dose received by the same worker was 1.39 mSv.

Conclusion

Thermoluminiscent dosimeters have been established as a valuable and versatile dosimetry system for assessment of point doses and dose distribution in all applications of ionizing radiation. Though, the extremity doses received by the workers are well within the limits prescribed by the national Competent Authority, the monitoring of these doses periodically using finger ring dosimeters may help in optimization of doses during these procedures and adoption of better work practices.

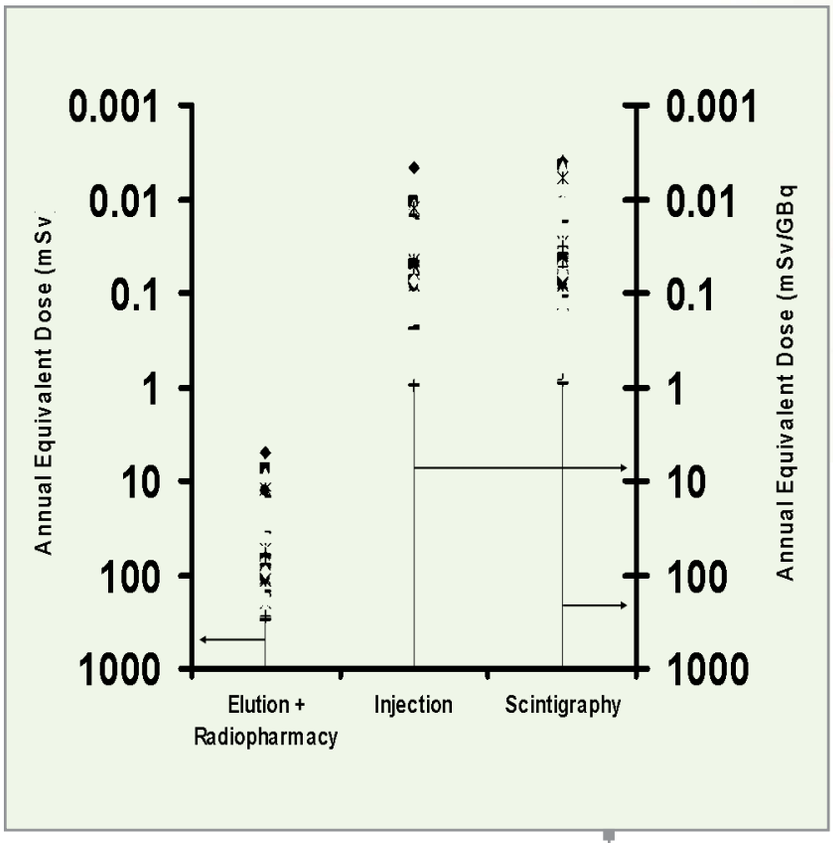

Annual Equivalent Doses received by the workers of the institution during (Extraction+Radiopharmacy), Injection of radiopharmaceuticals scintigraphy

P. Tandon, K.S. Kini, P.K. Gaur, P. Ramanathan & Veeresh Dubey, **"Finger Dosimetry in Nuclear Medicine Activities using TLD Ring Dosimeter"**: Journal of Medical Physics, vol. 20, no. 4, pp. 57-58, Oct-Dec (1995).

P. Tandon, K.S. Kini & B.C. Bhatt, **"Analysis of Finger Dose to the Staff involved in Nuclear Medicine Activities"**: Proceedings of Luminescence & its Applications, 1997, pp. 227-230.

K.S. Kini, P.K. Gaur, P. Tandon, & B.C. Bhatt, **"Development of New Gadgets for Measurements of Radiation Exposure to Occupational Workers and Public from Use of Unsealed Sources in Medicine"**: Journal of Medical Physics, vol. 24, no. 3, pp. 118-119, July-Sept (1999).

P. Tandon, V.G.R Subramanian, **"An Analysis of the Finger Doses received by Occupational Workers Involved in the Packing and Dispatch of Radioactive Material and Equipment"**: Proceedings of NAARRI Annual Conference (NAC-2000), pp. 155-157.

Pankaj Tandon et al. **"Extremity Dosimetry for the Staff involved in Nuclear Medicine procedures using Cyclotron produced Radioisotopes"** published in Vol.29 No. 3, PP. 184-185, July-September, 2004.

Kher, R.K. **"Occupational exposure in the application of radiation in Industry, Health and Research: Indian Scenario"**. Radiation Protection and Environment Vol. 26, No. 1-2, PP. 33-38, (2003).

3.3 DOSIMETRY OF BARC I-125 SEED SOURCE FOR INTERSTITIAL AND OPHTHALMIC BRACHYTHERAPY APPLICATIONS

A new model of ^{125}I seed source, named OcuProsta seed, was designed and fabricated by Radiopharmaceuticals Division of Bhabha Atomic Research Centre for ophthalmic and interstitial applications. Dosimetry parameters of this new seed source were determined experimentally using thermoLuminescent Dosimeter (TLD) and by Monte Carlo (MC) simulation. Dosimetry data required for dose rate calculation from ^{125}I seed loaded eye plaque were also generated using the measured and calculated single seed data.

■ Methodology

The source consists of 0.5 mm diameter and 3.0 mm long silver rod coated with palladium and on which ^{125}I is adsorbed. It is encapsulated in a hollow cylindrical titanium tube of 0.05 mm thick wall. The external dimensions of the seed are 0.8 mm diameter and 4.75 mm length. The maximum air kerma strength per seed is about 4.45 U (≈ apparent activity of 3.5 mCi) where, 1 U = 1 μGym^2h^{-1} = 1 $cGycm^2h^{-1}$. The air kerma strength (AKS) of the OcuProsta seed was estimated using two different well-type ionisation chambers.

Experimental measurements were carried out using TLD-100 cylindrical rods of length 6 mm and diameter 1 mm in a specially fabricated full scatter (30x30x30 cm^3) PMMA phantom. Central slab of this phantom is 6 mm thick and has a circular groove where a circular PMMA disc of diameter 12 cm can be positioned. Three such PMMA discs with different patterns of holes to accommodate TLD rods were fabricated for measurement of dose distribution around the OcuProsta seed. The irradiation time for TLD rods was so adjusted to keep the radiation dose in the linear region of their response. Dose rate to water, $D(r,\theta)$, at radial distance r and polar angle (per unit AKS) was calculated from the TL output using the expression

$$\frac{D(r,\theta)}{S_k} = \frac{1.12\ NTL_{(r,\theta),i}\ C_l}{S_k \varepsilon_i t d(t) E}$$

where, 1.12 is the factor used to convert the dose measured in the PMMA to dose to water; $NTL_{(r,\theta),i}$ is the net TL output (nC) of irradiated i^{th} TLD rod placed at (r, θ); C_l is the correction for finite length of TLD rods (1.10 at 0.5 cm and 1.03 at 1.0 cm); ε_i is the calibration factor for the i^{th} TLD rod (nC/cGy) at ^{60}Co gamma ray energy; t is the time (hours) of irradiation; d(t) is the correction factor for decay of ^{125}I source during irradiation; and E is the relative energy response correction factor for TLD rods (1.40).

The well-established MC simulation code MCNP version 3.1 was used to calculate AKS and absolute dose rates in water around the BARC ^{125}I OcuProsta seed source. Single seed dosimetry parameters such as dose rate constant, L, radial dose function, g(r), anisotropy function, $F(r,\theta)$, and anisotropy factor, $\phi_{an}(r)$, for this new seed source were determined as per their definition using the dose distribution data obtained from TL dosimetry as well as MC calculations. Dose computations were also carried out for eye plaques of diameters 12, 14, 16, 18 and 20 mm.

■ Results

The measured and MC calculated dose rate constants and anisotropy constants, radial dose functions and anisotropy functions of BARC OcuProsta ^{125}I seed source are given in Table 1, 2, and 3, respectively. Variation of central axis depth dose with plaque diameter from plaques of unit air kerma strength is given in Table 4.

■ Conclusions

In-phantom TLD measurements and Monte Carlo calculations were carried out to determine dosimetry parameters of newly produced OcuProsta ^{125}I seed source. Measured and calculated values of these parameters were in good agreement to each other within the uncertainty of measurement. The mean value of calculated and measured DRC and the MC calculated values of radial dose function and anisotropy functions were recommended for dosimetry calculations during clinical use of OcuProsta ^{125}I seed source.

Table 1: Dose rate constant (DRC) and anisotropy constant for BARC OcuProsta ^{125}I and Amersham model 6711 seeds

Seed model	Technique of evaluation	DRC ($cGyh^{-1}U^{-1}$)	Anisotropy constant
BARC OcuProsta	TLD measurements	0.950 ± 0.065	0.880
	MC simulation	0.972 ± 0.005	0.902
Amersham model 6711	MC simulation	0.973 ± 0.005	0.930

Table 2: Radial dose function for OcuProsta ^{125}I and Amersham model 6711 seeds

Radial distance, r (cm)	Radial dose function, g(r)		
	BARC OcuProsta		Amersham 6711
	Measured (TLD)	MC	
0.5	1.100	1.067	1.04
1.0	1.000	1.000	1.00
1.5	0.875	0.915	0.926
2.0	0.815	0.827	0.832
2.5	0.744	0.738	0.731
3.0	0.687	0.655	0.632
4.0	0.529	0.507	0.463
5.0	0.367	0.386	0.344

Table 3: Anisotropy function for BARC OcuProsta ^{125}I seed source

Polar angle, θ (deg.)	Anisotropy function, F(r, θ)							
	r = 0.50	r = 1.00[a]	r = 1.00	R = 1.50	r = 2.00	r = 3.00	r = 4.00	r = 5.00
0	0.146	0.244	0.256	0.302	0.363	0.429	0.471	0.499
10	0.338	0.496	0.466	0.481	0.548	0.580	0.619	0.637
20	0.590	0.664	0.672	0.685	0.721	0.738	0.761	0.778
30	0.746	0.798	0.796	0.805	0.823	0.833	0.849	0.852
40	0.845	0.916	0.874	0.878	0.891	0.895	0.906	0.905
50	0.911	0.907	0.926	0.929	0.936	0.938	0.947	0.945
60	0.954	0.926	0.962	0.962	0.966	0.966	0.972	0.966
70	0.980	0.956	0.983	0.984	0.987	0.986	0.990	0.987
80	0.996	1.029	0.995	0.996	0.997	0.994	1.002	0.998
90	1.000	1.000	1.000	1.000	1.000	1.000	1.000	1.000

[a]TLD measured data

Table 4: Dose rate from unit air kerma strength plaques of different diameters

Depth (mm)	Dose rate (cGy/h) from unit AKS plaques					
	12 mm dia. 8 seeds	14 mm dia. 12 seeds	16 mm dia. 13 seeds	16 mm dia. 16 seeds	18 mm dia. 21 seeds	20 mm dia. 24 seeds
0	3.981	3.358	2.903	2.941	2.663	2.300
1	3.854	3.343	2.926	2.915	2.678	2.296
2	3.538	3.259	2.864	2.795	2.636	2.209
3	3.150	2.939	2.586	2.616	2.441	2.073
4	2.639	2.442	2.216	2.195	2.101	1.874
5	2.071	1.946	1.813	1.805	1.733	1.586
6	1.651	1.572	1.498	1.494	1.445	1.353
7	1.338	1.286	1.248	1.245	1.214	1.161
8	1.098	1.065	1.048	1.046	1.028	0.998
9	0.909	0.887	0.882	0.880	0.871	0.858
10	0.758	0.744	0.746	0.744	0.740	0.739

Sharma, S. D., Mahua Basu, Shanta, A., Palani Selvam, T., Tripathi, U. B. and Bhatt, B. C., **Dosimetry parameters of BARC OcuProsta I-125 seed source. Australas.** Phys. Eng. Sci. Med., 28(1), 1 - 7, 2005.

Sharma, S. D., Shanta, A., Palani Selvam, T., Tripathi, U. B. and Bhatt, B. C., **Medical physics aspects of opthalmic brachytherapy.** BARC report 2004/E036

Nath, R., Anderson, L.L., Luxton, G., Weaver, K.A., Williamson, J. F., and Meigooni, A.S., **Dosimetry of interstitial brachytherapy sources:** Recommendations of the AAPM Radiation Therapy Committee Task Group No. 43. Med. Phys. 22(2): 209 - 234, 1995.

3.4 RADIOLOGICAL SAFETY ASPECTS OF MEDICAL CYCLOTRON AND PET FACILITIES

Positron Emission Tomography (PET) is the latest diagnostic modality in Nuclear Medicine used for obtaining high resolution, 3-D computer reconstructed images of distribution of radionuclides in the specific organs showing their functional status, which needs cyclotron produced radionuclides such as ^{11}C, ^{13}N, ^{15}O and ^{18}F. They have wide applications in the field of oncology, neurology and cardiology.

In medical cyclotrons protons are accelerated to energy ranging from 11 MeV to 18 MeV and deuterons to half of proton energy. When energetic particles are bombarded on suitable target materials, they produce positron emitting radionuclides such as ^{18}F ($T_{1/2}$ =109.8 min), ^{11}C ($T_{1/2}$ =20.3 min), ^{15}O ($T_{1/2}$=2 min) and ^{13}N ($T_{1/2}$=10 min). The positrons interact with a nearby electron and produce two annihilation photons of 0.511 MeV each in opposite direction. The most commonly used radionuclide in PET imaging, is ^{18}F because of its suitable half-life and ease of labeling. It is labelled with glucose to form Fluoro-Deoxy-Glucose (^{18}FDG), which exhibits higher concentration in malignant cells and thus differentiating them with normal cells. ^{18}F as FDG, once taken up inside the cells, is not metabolized in the same manner as glucose, but is trapped for a longer duration. This enables localization of malignant tumors of size 0.5 – 1 cm, with a PET scanner.

As ^{18}F and other positron emitters have short half-life, it is essential to have medical cyclotron in the vicinity of PET facility. First cyclotron in our country was commissioned at RMC in 2002. Later many hospitals have come up with proposals to set up a medical cyclotron unit in their premises. Two unshielded units (one of proton energy 16.5 MeV and another of 18MeV); and another three self-shielded units of proton energy 11 MeV have been approved. Two self-shielded units have been commissioned and other three (two unshielded and one self-shielded) are in the process of installation. The shielding adequacy of installed units has been evaluated from radiological safety point of view.

PET scanner room also needs adequate radiation shielding for annihilation photons of 0.511 MeV energy. This is because the energy of radiation involved and the amount of activity administered is about 2.5 times more than normal diagnostic procedures used in SPECT and conventional gamma camera imaging.

■ Shielding Aspects of Medical Cyclotron

Medical cyclotron facilities include *a cyclotron vault;* where the cyclotron is housed, *a control room*, a *hot laboratory area;* where the labeling of pharmaceuticals are automatically done in chemistry modules and *a cold laboratory area;* where QA of radio-pharmaceuticals is carried out.

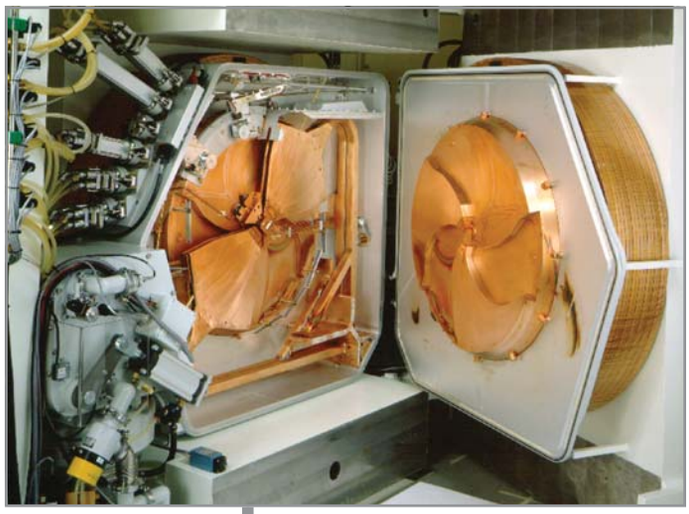

Inside view of the cyclotron

During the production of radionuclides in medical cyclotron, neutrons of energy spectrum 0 - 10 MeV (Avg energy 2.1 MeV) are generated by (p, xn) reaction, where x = 1-3. The neutrons, generated by inelastic scattering of protons from target material produce prompt γ-rays up to 8 MeV energy. The levels of gamma rays and neutron flux varies depending upon energy of the beam, beam current, number of target ports in use, direction of beam, material of target in use and the composition of target container. The cyclotrons installed at RMC (unshielded unit) can run at a maximum current rating of 80 μA for proton and 60 μA for deuteron, whereas the other two self-shielded units (accelerate protons only) can be operated at a maximum current of 60 μA. In this unit, two ports can run at two separate currents of 40 & 60 μA simultaneously. The unit is equipped with target

ports ranging from 6-12 in number. After irradiation of target material the radionuclide is transferred to the chemistry module through pneumatic systems via shielded transfer lines.

Cyclotron machine (unshielded unit)

The shielding for medical cyclotron facility has been evaluated for emitted neutron components. The shielding thickness achieved in this way has been found to be more than adequate for prompt gamma radiations too. The factors used in calculations are a) radiation dose rates provided by the manufacturers of unit as well as the values taken from NCRP-51 in Al target b) occupancy factor and c) tenth value thickness for neutrons in concrete. Using the equations, given in NCRP-51, it was found that in case of unshielded units (other than RMC), a vault of 150-200 cm thick concrete of density 2.35 gm/cc is adequate to keep the radiation exposure within the permissible limit The TVT value in concrete for neutron, considered in evaluation comes out to 35 cm.

Measurements were carried out to evaluate gamma and neutron levels inside outside the cyclotron vault of unshielded unit at RMC, Mumbai and the two self-shielded units installed in the country. Gamma radiation levels were measured using

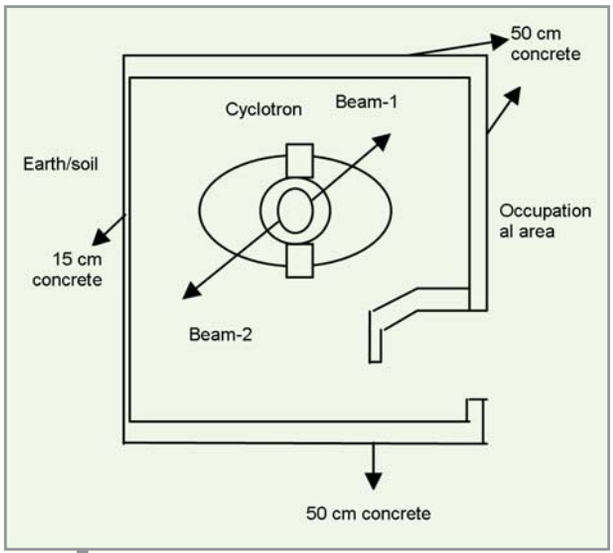

Block diagram of self-shielded cyclotron facility showing dual beam direction

LiF:Mg,Cu,P ThermoLuminescent Dosimeter (TLD) in powder form, loaded in plastic capsules. Fast neutron doses were measured using CR-39 foils. The capsules were placed at different locations inside the vaults and foils were placed at the maze and the entrance doors of unshielded unit. They were kept for a period of 24 hours, which includes exposure time of 1 hour irradiation time at 40 μA, the operational current.

In case of self-shielded units the shields are made up of high density mixture of lead, epoxy, boron carbide and concrete which brings the level to 30 mSv /hr inside the vault. In this case a concrete vault of 50 cm thick is required to bring down the exposure rate within permissible limits. Monte Carlo computations carried out, to evaluate shielding around the unshielded cyclotron units were compared with the analytical results. They were found to be in agreement with good approximation.

The radiation doses range from 2 Gy (near the target) to 0.04 Gy (at a distance of 5 m from the target). The neutron levels are in the range of 22 – 825.0 μSv/hr at the door outside the vault and inside the maze. The gamma and neutron radiation levels found outside the shield and inside cyclotron vault/room were found in the range of 10.8 – 14.5 μSv/hr and 0 – 16.8 μSv/hr respectively.

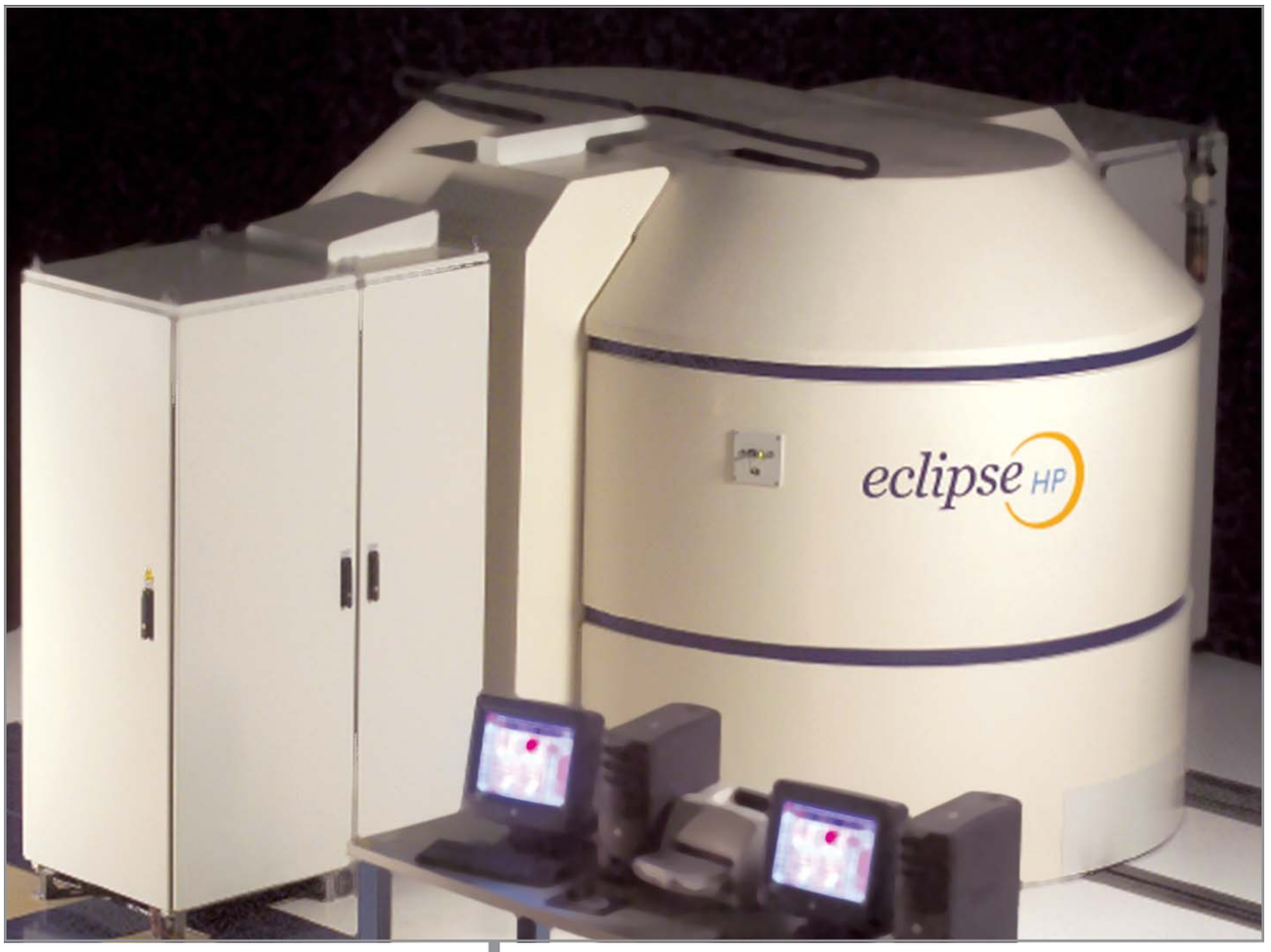

Self Shielded Cyclotron Unit

Shielding Aspect Of PET Facility

PET facility requires shielding for annihilation photons of 0.511 MeV from the radio-isotope administered in the patient for scanning. Here, the patient acts as the source of radiation as the activity administered is high. Hence, the dose administration room, post-administration patient-waiting area and the scanner room require sufficient shielding. The thickness of shielding is evaluated from patient load per week, activity administered per patient, room dimension and the duration of scan per patient. As per our calculations a PET facility should have 9" (15cm) of concrete wall, 2.5 mm lead lining on door and 2.5 mm lead equivalent viewing glass window in a 7 x 5 m^2 room dimension. The measurements carried out at 4 NM centers show radiation levels in the range of 0.02 – 1.5 μSv/hr around the scanner room.

P.Sethulakshmi, R.Rohatgi K.Biju, S.S.Sanaye and M.P.Dhairyawan, **"Radiological safety aspects of Cyclotron and PET facilities"**. Published in the proceedings of conference on Accelerators and radiation Physics (April 2005)

"Radiation shielding Guidelines for Eclipse Cyclotrons", CTI Siemens Technical Guide, (2003),

"Radiation protection design guidelines for 0.1-100 MeV particle accelerator facilities", NCRP, Report No-51; (1977),

M.Basu, P.K.Gaur, and P.Tandon, **"Radiological Safety consideration during installation of PET facility".** Proceedings of Indian Journal of Nuclear Medicine, Vol. No.18(4),27-28,2003.

3.5 NEUTRON SHIELDING ARRANGEMENT FOR MEDICAL CYCLOTRON AT RADIATION MEDICINE CENTRE, MUMBAI

Medical cyclotron is used for production of radio-isotopes. These are used for the formulation of radio-medicines for early detection of cancerous cells. Recently, "PET Trace" cyclotron machine has been procured and installed in the basement of Radiation Medicine Centre, BARC, located in the Annexe Building of Tata Memorial Centre, Mumbai. Neutrons and gamma radiations emitted during the operation of cyclotron have to be shielded from coming out to the occupied area such as control room, air conditioning plant, the patient waiting lounge, etc. located nearby which otherwise can become a potential health hazard. It was, therefore, necessary to provide shielding by designing and fabricating it locally to suit the vault requirement. This task of providing an improved local shielding has been successfully completed through a unique design and the adequacy of the shielding was certified by the Health Physicists.

■ Maze passage of medical cyclotron

The shielding arrangement for the radiation coming out of the maze passage of the cyclotron vault essentially consists of two parts namely the fixed part and the hinged type mobile part which are provided at the entrance and at the exit of the maze passage. While the mobile part provides an entry and exit of the personnel/equipment to the main vault, the fixed part located above the mobile part prevents the leakage of radiation from the ceiling area. The fixed part also provides necessary space for mounting various monitors and safety interlocks.

Following were the design features:

1. The size of mobile part was 1015 mm wide x 2020 mm high and the fixed part 1015 mm x 965/1715 mm.

2. The assembly of the mobile part weighed around 2500 kg.

3. The possibility of dismantling the shields in future if required was considered in the design.

4. The operation of the mobile part was assumed to be manual and hence had to be very smooth and easy.

5. Minimum ground and side clearance of 5mm was provided to restrict streaming of neutron radiation less than 0.1 mR/h as stipulated by AERB. The design had to accommodate variation in the floor level and slope and the possible leaning of the mobile shield at the outer edge which should be well within 5 mm.

There were several limitations posed by the site during the installation of the massive shields. These were:

(i) Limited space for free movement and handling of the shields during their erection,

(ii) Limited (75 mm) allowable working depth of the foundation for the hinged parts, and

(iii) The curved column of the maze passage towards the cyclotron was not square to the floor thus leaving a large crevice near the top edge of the mobile shield which required scraping of the column plaster varying in depth up to 30 mm.

■ Design of shielding structure

The shielding structure was designed in the form of a framework fabricated in channels. The thickness of this structure worked out to be 175 mm. Four 40 mm thick sheets of High Density Polythene (HDPE) were inserted in the channel framework and were covered by 8 mm thick mild steel plates facing outside to offer the required strength to the structure and absorb stray gamma radiation. The mobile shield was supported vertically by a mild steel pipe which also filled with HDPE granules. The pipe further provided the pivot arrangement through a pair of thrust bearings for the mobile shield and fixing arrangement for the fixed shields.

■ Installation

The foundation was made by digging the floor up to allowable limit i.e. 75 mm. Then, the base plate was fixed with concrete and left 72 hrs for gaining full strength. Lowest part of the

door was erected. Then middle portion, around 500 kg weight, was kept above lowest portion and its spindle was inserted. This lifting and erecting activity took place at the height of 2000 mm with space constraint which prevented the use of any short weight lifting machine. The major task was erecting the third part, around 500 kg weight and fixing it on the ceiling at the height of around 3500 mm.

■ Evaluation of the shields

In order to assess the neutron shielding arrangement for the maze passage of medical cyclotron at RMC, Parel, a radiometry test was carried out.

The measured dose rate on the outside of the maze door when the ^{60}Co source was located in the front of the first door inside the cell was 0.2 mR/h. Although this dose rate is greater than the background rate, it may be noted that, the field situation during actual operation will be quite different from the condition during measured value at the time of radiometry. This can be explained as follows: The estimated dose rate from gamma and neutron radiations during the operation of the cyclotron using a proton beam at full current of 80 μA and energy of 16.5 MeV gives 32 R/h (γ-rays) and 3378 rem/h (neutrons) respectively at 1 m away from the target in 0° direction which is towards the wall. These radiations have to pass through local shields surrounding the target, undergo multiple reflections at the walls with consequent degradation in energies and travel considerable distances before they reach the inner door of the maze.

Fabrication, Testing and Installation of Local Shield Assembly and extension of Instrument Panel

One important part of the "TAILORING" work is use of 'Local Shield' around the six target ports, which are the sources of the neutron and Gamma radiation. This local shield along with the self shielding effect of the thick magnet iron yoke of the cyclotron, 1.4 m thick partition of the vault walls, 1.2 m thick hematite ceiling and maze doors have provided adequate shielding to replace the shielded version of the cyclotron. This arrangement has enabled the use of the existing building and resulted in considerable amount of saving in cost.

The assembly consists of Local Shield, its handling arrangement and adjustable leg supports. The local shield is a modular shielding arrangement to supplement the radiation shielding in horizontal (horizontal shield) as well as in vertical (vertical shield) direction. It is made of a S.S. box enclosing steel plates for gamma radiation shielding and HDPE sheets for neutron radiation shielding. They are arranged in six layers and stacked alternately. The steel plates are non-magnetic S.S. to prevent interference to the functioning of the cyclotron. The thickness of SS as well as HDFE sheets in horizontal and vertical shields are provided based on the report of radiation shielding analysis.

The horizontal shield (820 mm x 1075 mm x 300 mm) is supported at the ceiling with the help of channels and beams. The vertical shield (770 mm x 1375 mm x 230 mm) is attached to a trolley, supported on horizontal shield and ceiling. The trolley provides horizontal movement of 500 mm (max.) to the vertical shield. Adjustable leg supports are provided to the horizontal as well as to the vertical shields to have redundancy from safety point of view. The shielding assembly is covered with the help of 3 mm thick aluminium sheets.

The extension of instrument panel consists of SS304 box (200 mm x 170 mm x 1900 mm height) filled with lead sheets for gamma radiation shielding and HDPE sheets for neutron radiation shielding. They are divided into layers and stacked alternately. The steel plates are non-magnetic to prevent interference to the functioning of the cyclotron. This extension lies in line with instrument panel and rests on structural support.

Various sleeves have been provided on the medical cyclotron room wall for the facilities required inside the cyclotron room (e.g. electrical, power and signal, cool and hot gases, AC, water drain, cooling water, RF cables etc.). Proper arrangement for sealing the sleeves with steel wool, HDPE granulated powder and split flanges was worked out. Radiation mapping with Cu-Cobalt source was carried out to ascertain the adequacy of various shielding.

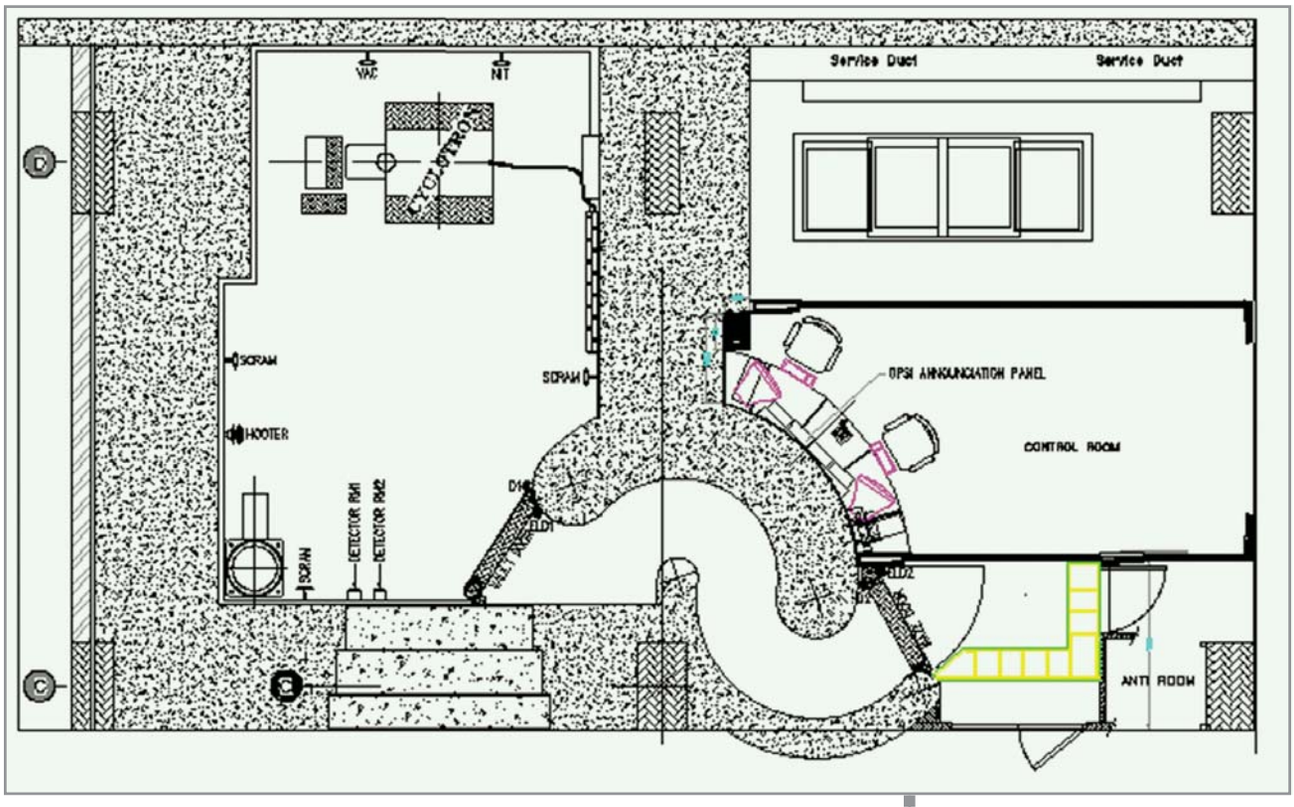

Medical cyclotron facility

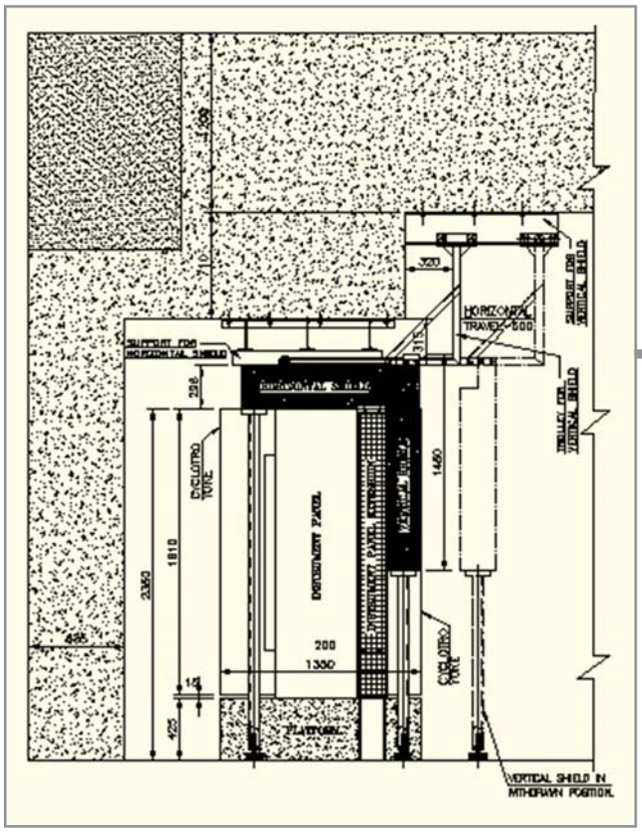

Local shield with handling arrangement &
Instrumentation panel extension

A. W. Matkar <amatkar@barc.gov.in>

3.6 SETTING UP OF NATIONAL STANDARDS FOR TESTING OF MEDICAL X-RAY FILMS

Bureau of Indian Standards (BIS) has recognized RPAD, BARC as the National Laboratory in the country to standardize quality of Imaging devices like Medical X-ray Films (~100 lakh square meters used per year in India), cassettes, screens etc. BIS requires that the film samples from the five major suppliers of medical X-ray films in India who import jumbo rolls and from one indigenous manufacturer, are tested for their quality at our laboratory. This is needed in view of a major problem being faced by the X-ray Departments i.e., inconsistent image quality of X-ray films leading to (1) Repeat exposures (2) Spoilt films (3) missed/wrong diagnosis, leading to increased radiation dosage to the patient.

The existing laboratory has been set up to meet the ISO standard (ISO-9236-1), which is accepted as Indian Standard. For this purpose, presently we have an X-ray machine POLYDOROS LX/KLINOSKOP-H with two BEL tubes, entirely microprocessor controlled high frequency X-ray generator and with interface facility. In addition to this, the laboratory is equipped with radiation measuring instruments and medical imaging devices such as cassettes and image intensifying screens.

As part of BIS project RPAD, BARC has provided Technical support to set up the National Standards on medical X-ray films. The setting up of National standards involves several aspects which are highlighted below:

■ Fabrication of phantom for X-ray sensitometry

The test phantom consists of six PolyMethylMethAcrylate (PMMA) slabs, each 25 mm thick by 300 mm square. The six slabs are arranged in 3 pairs. Between the upper and the middle pair of slabs, a 1 mm thick and 300 mm square aluminium sheet is sandwiched.

On the other hand, between the lower pair of slabs, a similar 2 mm thick aluminium sheet is sandwiched. The system consisting of the upper and lower pairs of slabs separated by a gap of 54 mm is used as a Phantom for obtaining the beam

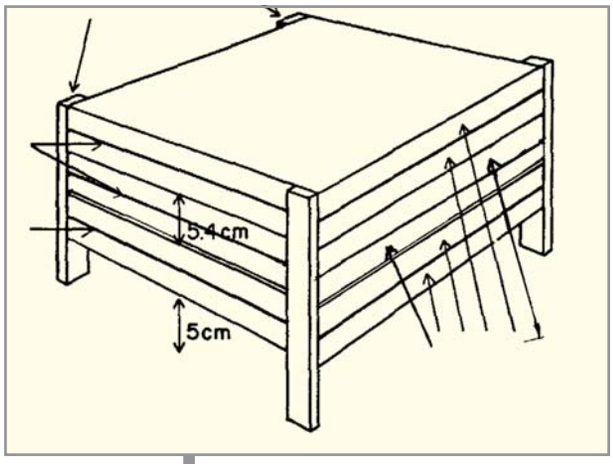

ISO specified Test Phantom

■ Exposure conditions and geometry

A typical geometric set up of measuring arrangement represents high scatter exposure conditions (without grid). The Focus to Film distance indicated as 'x' is 1.8 m for the chest exposure and 1m for all other exposure techniques. The exposure times used for determination of sensitometric curve is 200±10 ms, non-intermittent, intensity scale and kept constant for all exposures.

The X-ray beam is collimated so as to fully irradiate the test object placed in front of the cassette. The intensity is modified by change in the tube current (mA). For plotting sensitometric curve, the film is subjected to at least 20 different exposures equally distributed on a logarithmic scale, which produces net densities 0.1 –2.1. The intensity in terms of air-kerma (Gy) that the film is subjected to is measured using a measuring chamber placed at the film plane (without the film). In order to find D_{max} one may have to increase tube current; in which case it shall be verified that the higher tube current does not change the beam quality. The details of the exposure technique and the beam quality are presented in the table below.

Technique	kVp	HVL (mm Al)	Exp. Time (ms)	Exposure conditions
Chest (low kVp)	80	2.7	100	No grid

The different exposures that the film is subjected to, is measured using an Ionization chamber - neromax™ placed at the same location as the cassette.

Quality Control for processing of exposed films

The exposed films were processed in a manual processor. To eliminate dark room fog, all films were processed under Red coloured safe light and in order to avoid effects due to latent image fading all film samples are processed not less than 30 minutes but not more than 4 hours after exposure. Between exposure and processing the films are maintained at a temperature of 23° C ± 2° C and 50 ±20% relative humidity. The processor quality control is carried out using a light sensitometer (single flash or dual colour) with blue and green emitting light source.

Measurement of Diffused transmission Density and Basic fog

Density of the processed and dried films was measured by a standard diffuse transmission densitometer with an accuracy of $\Delta D/D = \pm 0.01$ or $\Delta D = \pm 0.01$, which ever is greater. White light source was used to measure the density of developed films. An unexposed sample of film from the same sample box as that tested for thickness of base shall be processed under standard condition simultaneously with those samples taken to plot sensitometric curves. The density measured shall be the base + fog density.

Plotting the sensitometric curve

The Diffused transmission density (D) as ordinates shall be plotted against their corresponding log exposure level (log K) values as abscissa and a smooth curve shall be drawn through the plotted points, K shall be expressed in gray (Gy). The scale units on the graph paper for the abscissa and the ordinate shall have equal spacing. For brevity, the diffused transmission density will be referred to as Density and symbol D is used in the standard. Parameters such as Average gradient G, Relative Speed of the screen film combination, and the D_{max} are extracted from the sensitometric curve. A sample film taken from each box is also tested for artifacts.

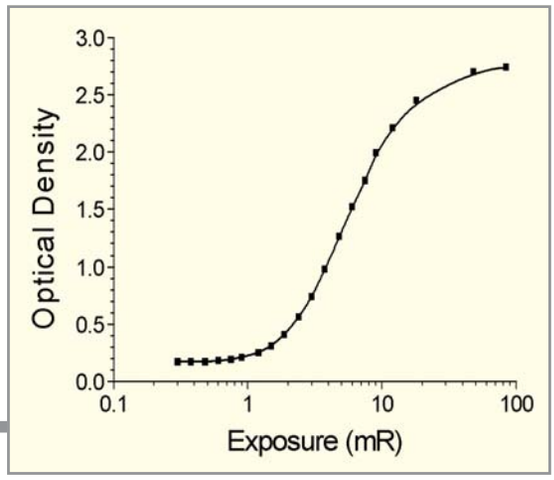

X-Ray sensitometric curve of Medical X-ray film

Conclusions

Presently, the film samples from all suppliers in India (four importers of jumbo rolls and one indigenous manufacturer) are being tested. The film is recommended for use in medical radiography if the characteristics of the film conform to the stipulated limits.

Reena Bohra, v. Jayalakshmi, CPR.Nair, U.B.Tripathi and B.C.Bhatt, **Selection of proper screen film combination for optimum image quality in chest Radiography,** J. of Medical Physics, vol 29, no3, pp 232-233, 2004.

C.P.R.Nair, V. Jayalakshmi, Reena Bohra and K.N.Govindarajan, **Need for National standard for medical x-ray films in India.** J. of medical physics, vol 28, no3, pp123-124, 2003

Reena Bohra, C.P.R.Nair, V. Jayalakshmi, K.N.Govindarajan and B.C.Bhatt. **Effect of basic fog of medical x-ray filmon imaage quality and patient dose- method of evaluation and steps to control.** J of medical physics, vol 28, no3, pp112-113, 2003

Shoba jayapraksh, C.P.R.Nair, V. Jayalakshmi, Reena Bohra, and B.S Rao, **View box and viewing conditions for a mammographic facility.** J of medical physics, vol 28, no3, pp128-129, 2003

V.Jayalakshmi, Reena Bohra, Vandana S, CPR Nair, Neeraj Dixit and K.N.Govindarajan, **Repeat Analysis- A first step in quality audit in diagnostic radiology.,** J of medical physics, vol 27, no3, pp208-209, 2002.

Derrick P Roberts, Nigel &mith, Churchill Livingstone, **Radiographic imaging, a practical approach** ... 200 pages, (1988)

American National Standards Method for the sensitometry of medical x-ray screen film processing systems, ANSI PH2-43, 1982.

3.7 RADIOLOGICAL SAFETY OF SELENIUM-75 SOURCE USED FOR INDUSTRIAL RADIOGRAPHY

Selenium-75, a new radiography source being used in advanced countries has been recently received in India. It is suitable for radiography of steel thickness between 4 mm-35 mm and is an ideal source for low thickness pipes and jobs where Ir-192 and X-ray sources have limitations for use. Theoretical as well as experimental studies have been carried out to find the specific gamma ray constant (RHM) of the source and half value thickness for the different materials such as steel, aluminum, copper and lead.

For radiography of different types of materials, it is essential to have an idea about the exposure time. Exposure charts using Se-75 source for radiography of different types of materials viz. steel, aluminium, titanium and copper for fast and slow film combinations have been prepared. Comparison of radiographic image quality using Selenium-75 source for radiography of steel was also done with Iridium-192 and X-ray source. These studies will serve as guidelines to the user institutions.

■ Characterization Studies

(i) Exposure Rate Constant

The exposure Rate (R/hr/Ci) of the source (both bare and encapsulated with 2 mm steel plus 2 mm titanium) in air at 1 m distance is determined both from a numerical formula as well as with MCNP code. The exposure rate constant was also determined experimentally using a 30 cc ionization chamber and electrometer. The necessary correction factors for calibration, temperature and pressure were applied to get the absolute value. The values of the output obtained from the numerical formula was slightly higher than that obtained using MCNP code. For encapsulated case, the code values agreed well with the experimental results.

	Bare Source	With Encapsulation (2 mm Ti + 2mm SS)
Numerical	0.65	0.2
MCNP	0.61	0.187
Experimental Value	-	**0.1855**

Exposure Rate at 1m (R/hr/Ci) from Se-75 Source

(ii) Half value thickness (HVT)

Transmission through steel, aluminum, lead and copper was measured experimentally using a 30 cc ionization chamber and electrometer. From the plotted transmission graphs, HVT & TVT value in respective materials was determined.

Experimental Value of HVT & TVT

	Aluminium (2.7 gm/cc)	Steel (7.8 gm /cc)	Copper (8.9 gm/cc)	Lead (11.3 gm/cc)
HVT_1 (mm)	34	9.0	6.8	0.9
HVT_2 (mm)	33	10.5	9.4	1.2
HVT_3 (mm)	33	10.5	9.4	1.65
TVT_1 (mm)	105	34	28.5	4.3

(iii) Exposure Chart

For the radiography of different types of materials, it is essential to have an idea about the exposure time. Radiography exposure chart was prepared for a Source to Film Distance (SFD) of 60 cm using different material step wedge blocks viz. steel, aluminum, copper and titanium. Radiography of step blocks was taken using a fast film (Laser NDT-7/Kodak AA) and also using slow film (Laser NDT-4/Kodak MX) with 0.02 mm lead intensifying screen. The amount of exposure required for the above materials with a SFD of 60 cm is presented as 'Curie-Minute' plots of varying thicknesses.

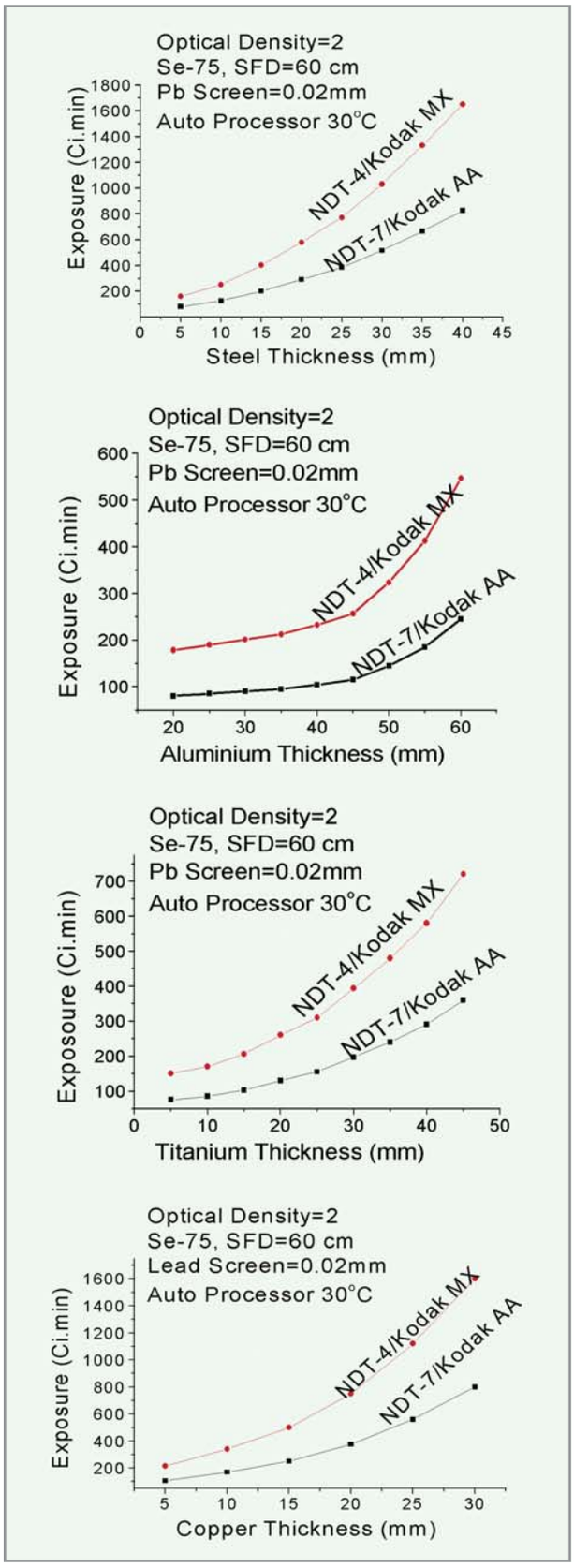

(iv) Image Quality Comparison

As part of our study, comparison of image quality was done for X-rays, Se-75 and Ir-192 source for radiography of steel. For this SFD was chosen such that geometrical un-sharpness (U_g) is maintained the same for each source. Radiography of steel step wedge was taken with ASTM hole type pentameter. Density profile of steel was studied in 5 mm steps variation. It is noticed that the density gradient is better in

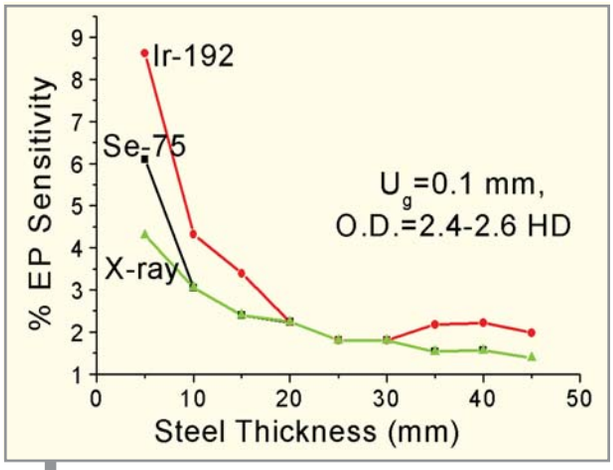

Comparison of Sensitivity Achieved For Radiography of Steel Using Different Sources

Se-75 compared to Ir-192 source in the lower thickness region. Thus the contrast due to Se-75 is also found to be superior to Ir-192 source.

Conclusion

The experimental data provided would be a guideline to new users of Se-75 source. The output and the HVT value obtained experimentally will help user institutions in their fieldwork. Exposure chart will be the guideline for taking radiography of steel, aluminum, copper and titanium using Se-75 source to avoid any retake. As far as the image quality of radiography of steel thickness in the range below 19 mm is concerned, Se-75 can replace Ir-192 source and X-ray source where they have limitations for use. Although Se-75 is costlier it can be a good asset to the field of radiography.

R.K.Yadav, R. Rama and A. Sharma <kannans@barc.gov.in>

4.1 INDIAN ENVIRONMENTAL RADIATION MONITORING NETWORK (IERMON)

The history of environmental radioactivity measurement started with the onset of the nuclear age, in particular with the atmospheric nuclear weapon tests. It was driven by concern of global radioactive pollution and of the resulting radiation exposure to human beings. In the late fifties and up to the end of 1962 nuclear weapon powers conducted a number of nuclear explosions in the atmosphere. By 1960 a large number of countries were reporting data on radioactivity fallout from their respective network of monitoring stations. A number of techniques for sampling and measurement of various fallout radionuclides in a variety of matrices were developed.

The erstwhile Air Monitoring Section (presently known as Environmental Assessment Division) of BARC had carried out extensive measurements on environmental radioactivity across the country using a network of 18 stations. The first station was setup in Bombay in 1956 and by 1969 the network was extended to 18 stations. Regular measurements of radioactivity in airborne particulates, surface deposition and milk were carried out at these stations. Later on the number of operational stations started decreasing on account of the declining levels of fallout subsequent to the banning of atmospheric weapon tests from 1962. During the time of Chernobyl reactor accident on April 26, 1986, only two monitoring stations were operational in India.

The need was felt the world over for permanent monitoring networks and thus WHO and UNEP jointly promoted the Global Environmental Radiation Monitoring Network (GERMON) Programme. India was a member country and a member of the scientific advisory committee of GERMON. With effect from April 2002, the Indian GERMON Programme was renamed as Indian Environmental Radiation Monitoring Network (IERMON) without any affiliation to GERMON.

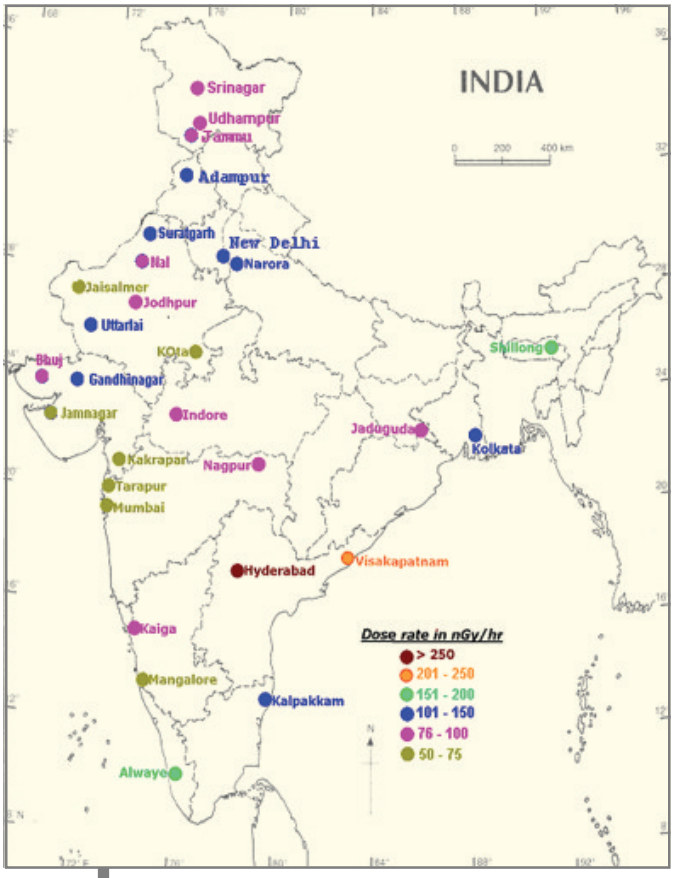

IERMON Stations across the country, with on-line data communication

Objectives of IERMON

The objectives of the IERMON network are:

- To provide on-line information about radiation levels at various stations to the Emergency Control Rooms of DAE
- To facilitate environmental impact assessment of nuclear emergencies
- To study diurnal and seasonal variations of radon across the country and to explore various applications of radon research
- To monitor the long term shift in the background radiation levels
- To provide knowledge-based environmental awareness to the public through participation of Universities and other educational institutions
- To facilitate R&D on new techniques and methods for environmental monitoring
- To develop and validate mathematical models for atmospheric dispersion of radioactive pollutants for short, medium and long ranges.

The IERMON network presently consists of 29 monitoring stations, connected by telephone lines with the Central Station located at the Environmental Assessment Division, Bhabha Atomic Research Centre, Mumbai, where hourly data from all the stations is received, assimilated and sent to the Emergency Control Room of Department of Atomic Energy using the Department's VSAT network called ANUNET. The Central Station is also linked to the Emergency Response Centre at Modular Laboratories, BARC, Mumbai using Local Area Network.

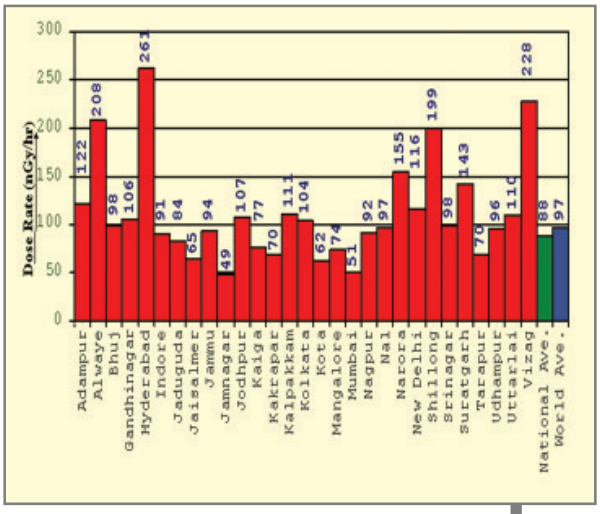

Environmental radiation dose rate recorded at IERMON stations

■ Systems deployed at IERMON Stations

Each IERMON station records the ambient gamma radiation levels of that location at intervals which can be suitably selected from 5 minutes to 1 hour. The station consists of the following equipment:

a) Data Acquisition and Communication System (DACS)

This system is developed at Environmental Assessment Division, BARC. The system consists of a single PCB, having all the components required for the data acquisition and data transmission. It has four RS-232C interfaces for connecting to different monitoring systems having RS-232C interface. A modem is built-in for data communication with dial-up telephone lines. PC interface is provided for user interaction with the system. A serial printer is supported for local printout.

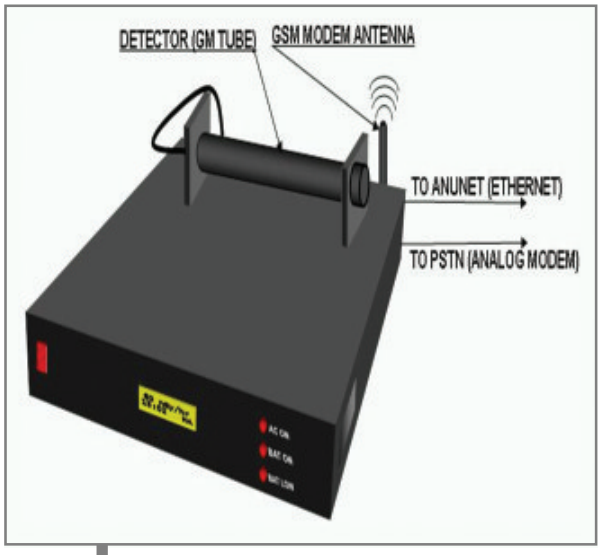

IEROMN DACS with built-in GM Detector

The system is provided with battery backup for uninterrupted power supply. On-line data communication facilities play an important role in emergency response. The data from different locations are required for decision making and coordinating different responses. Hence adequate redundancy must be provided in communication facilities. In IERMON network, the following data communication options are available:

- Fixed Land Line Public Switched Telephone Network (PSTN)
- Mobile Telephone Network using GSM Connectivity Terminals
- ANUNET (DAE's VSAT network)
- Internet

The IERMON DACS is also provided with a large volume GM Detector for recording environmental gamma radiation. The printed circuit board of the DACS has the necessary circuitry including high voltage supply for using the GM detector. The microcontroller is programmed to count the pulses from GM circuit and compute the dose rate at programmed intervals. The dose rates are stored in battery-backed RAM.

With the built-in radiation detector, the DACS checks for any emergency at periodic intervals (every 5 minutes) by comparing the latest recorded counts with the programmed normal background count of the location. If the recorded counts

exceed the normal background by a programmed factor, it signals an emergency and the DACS starts communicating the data to the central station at 5 minutes intervals until the emergency condition disappears or instructed by the central station to stop communication. The normal background and "emergency factor" are programmed in to the system after studying the radiation data of the particular place.

To minimize the cost of communication, the DACS is programmed to communicate the stored data in response to the command from the central station under normal condition. In other words, the remote station is not initiating the communication under normal conditions and the central station is programmed to dial each remote station to get the data transferred to the central station. By default the central station carries out this operation at midnight every day.

b) Solar Powered Environmental Radiation Monitor with GSM-based Data Communication

A solar powered Environmental Radiation Monitor (ERM) for open field installation with wireless data communication using Short Message Service (SMS) of GSM Cellular Network has been developed for deployment at various stations of the Indian Environmental Radiation Monitoring Network (IERMON). The ERM module is based on an energy compensated GM counter (LND 7807) as detector. The power for the system is derived from a solar panel (PV array). The solar panel charges an SMF battery (12 V/40Ah). The battery and the ERM module are mounted in a box which is fixed to the pole of the solar panel.

Solar-powered ERM

The ERM module is designed around a microcontroller (89C51RD+). It is programmed to compute dose rate every five minutes and hourly dose rate is computed every hour which is transmitted as an SMS message. In case of an emergency (dose rate exceeds programmed factor of normal background level), data will be transmitted every five minutes until the dose rate falls below alarm level. The ERM module can also receive SMS message from the Central Station to carry out required operation.

Inside view of the Solar-powered ERM

The Nokia30 GSM modem is mounted on the printed circuit board of the ERM. The modem is connected to the microcontroller using RS232C interface. Nokia30 has internal antenna in addition to the provision for external antenna.

c) IERMON for Uranium Mines

IERMON is being extended to uranium mining environment. As a first step, four locations are identified at Jaduguda for installing IERMON system. The data from these locations will be transmitted to the central monitoring station at UCIL, Jaduguda using GSM modem. From this central monitoring station, data will be transmitted to a public display board as part of public awareness programme. The data will be available to IERMON Central Station, Trombay through ANUNET.

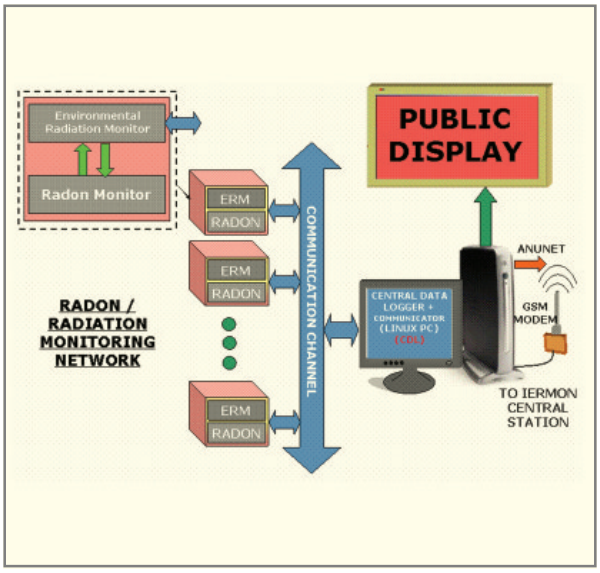

d) IERMON for Emergency Detection at Nuclear Power Plants

Indian Real Time On-line Decision Support System (IRODOS) is the emergency response system for nuclear power plants. This system is being executed jointly by members from BARC, IGCAR, NCMRWF, IMD, ISRO, NPCIL, AERB and CMG. It is proposed to deploy IERMON systems along two rings around the NPP.

e) IERMON Central Station for dial-up network

The Central Station located at Modular Laboratories, Trombay, consists of the following facilities:

1. One PC with password protection is used for data downloaded from various stations. A Modem with telephone having STD facility is connected to this PC, access to which is restricted only to the designated System Administrator who is responsible for safe operation of the telephone facility.

2. Another PC, referred to as 'DataBase PC', will hold the data from various stations in MS Access Data Base. This PC is connected to the Local Area Network (LAN) of Health, Safety & Environment Group. It is linked to the Emergency Response Centre, BARC using the LAN and to the Emergency Control Room of DAE using ANUNET.

3. A large Plasma Display Monitor is used for displaying data from various stations in graphical formats.

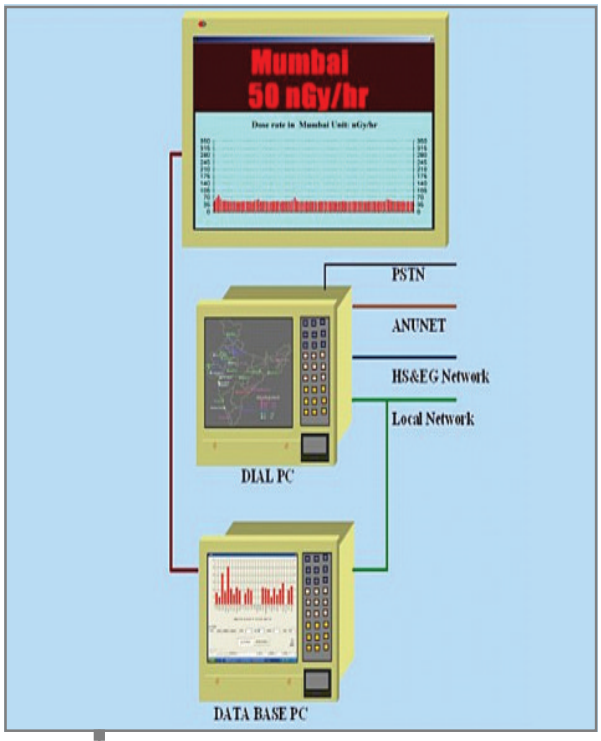

IERMON Central Station

■ Future Plans

It is proposed to divide the countrywide network in to five regions and allocate a separate PC for each region for data collection. Data is normally transmitted from each remote station as an SMS message at pre-determined intervals. In case of an emergency, data will be transmitted every minute until radiation level falls below alarm level. The remote station can be connected online to the central station by using GPRS facility or by making data calls. However, SMS will be the usual communication option under normal conditions.

About 500 IERMON stations are proposed to be installed to satisfy the requirements of monitoring at the existing and upcoming uranium mines and for the IRODOS programme at 7 nuclear power plants.

C.K.G. Nair, <ckgn@barc.gov.in>

4.2 INDIAN REAL TIME ONLINE DECISION SUPPORT SYSTEM (IRODOS)

In keeping with its traditional emphasis on safety, nuclear technology was prompted by the Chernobyl accident (1986) to consider the consequences of accidents Beyond Design Basis Accident (BDBA) scenarios, despite the fact that the probability of such an occurrence was considered extremely low. These consequences, though highly unlikely, necessitate additional measures to protect the public from possible adverse radiological impact and it is in this context that there is need for drawing up Emergency Preparedness Plan for such contingencies.

The two main objectives of a nuclear emergency planning are (i) the early prediction or assessment of the extent and significance of any accidental release of radioactivity to the environment and (ii) rapid and continuous assessment of the accident as it proceeds.

The current emergency plans prepared and approved for practice in Indian Nuclear Power Plants (NPPs) fully depend on environmental radiation monitoring. This along with the prevailing site specific meteorological conditions are used at deciding the areas/sectors affected for implementing the counter measures like iodine prophylaxis, sheltering, temporary relocation, evacuation etc.

This approach may have limited application in case of a BDBA scenario, wherein a long term release of the activity is anticipated, leading to change in affected sectors with time due to change in meteorological conditions (specially the wind direction). Additionally any counter-measures can be implemented only after a certain time duration. Also, in case of a temporary relocation, it is important that during the transit period the public should not be crossing the sectors with high radioactivity during their movement / transport, thereby requiring a best escape route prediction leading to minimum exposure to public, during such type of eventualities.

Keeping in view these limitations / requirements a real time online nuclear emergency response system with 72 hours meteorological and radiological forecasts, for off-site nuclear emergency under the frame work of "Indian Real time Online Decision Support System "IRODOS", for NPPs has been designed and developed, which takes care of the predictive requirement of an emergency planning. This is an inter-divisional programme of the Health, Safety and Environment Group, BARC.

Salient features of IRODOS

- It provides a comprehensive integrated decision support system pertaining to nuclear and radiological emergency in public domain (covering sufficiently long distances around NPP).
- It provides a common framework for incorporating state-of-the-art weather prediction, dispersion and radiological dose models to support the decision makers in initiating counter measures, well in advance, during a nuclear emergency.
- It provides 72 hours meteorological and radiological forecasts at hourly intervals and updates every 24 hours.
- It incorporates state-of-the-art communication between various environmental monitoring stations and reactor status data for the identification / sensing of an event / accident.
- It estimates the likely quantity of radionuclides released and predicts optimum counter measures to minimise radiological exposure to public.
- It displays the results on a Geographical Information System (GIS) with various visual and text outputs to support the emergency response team and district authorities in decision making.

Numerical weather prediction

The system in its present form gets 72 hours forecasted meteorological data [Numerical Weather Prediction (NWP)] from mesoscale weather forecast model MM5, operational at National Centre for Medium Range Weather Forecasting (NCMRWF), Noida, India. The NWP is available in two spatial and temporal resolutions. One is in a grid size of about 30 km x 30 km over the Indian domain covering about

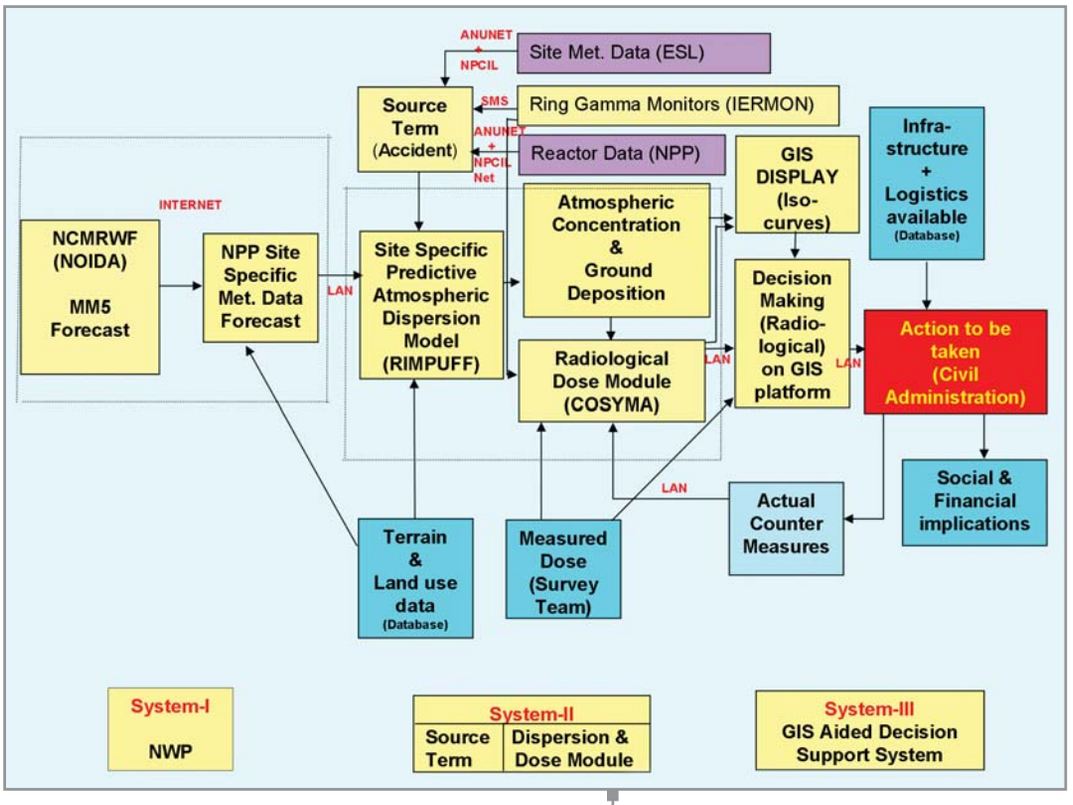

Flow sheet of the IRODOS system

4000 km x 4000 km and a vertical height of about 15 km with a temporal resolution of 12 hours. The second one is in a grid size of 10 km x 10 km covering a horizontal region of 150 km x 150 km over each of the Indian NPP sites with a temporal resolution of one hour. The file size is about 132 MB in first case and 18 MB for each site in 2nd case. This data is received at IRODOS, Emergency Response Centre, BARC, Trombay via Computer Division's (BARC) download server using 2 Mbps internet data transmission line.

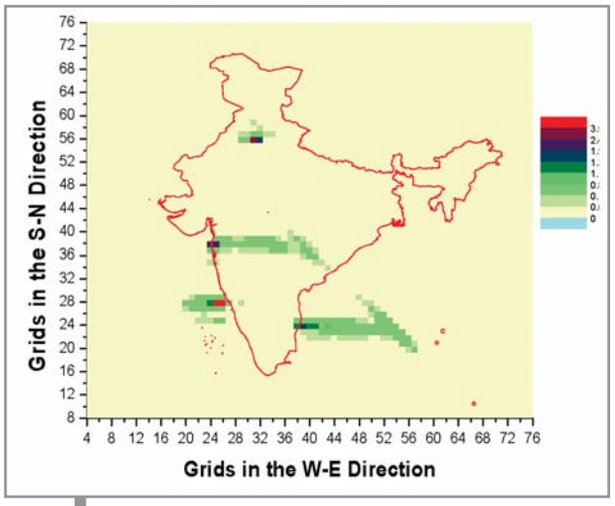

Concentration distribution due to release at NPPs over the Indian region.

Atmospheric transport modelling

The coarser resolution NWP data is used in driving regional scale atmospheric dispersion model to simulate the transport and deposition of various radionuclides in case of a large scale nuclear disaster in a grid size of 30 km x 30 km in the Indian domain.

The finer resolution NWP data is used in driving atmospheric contaminant dispersion model RIMPUFF to simulate the transport and deposition of various radionuclides in case of an accident at NPP in a grid size of 1 km x 1 km with a time resolution of 1 hour upto a radial distance of 75 km from the reactor centre.

Radiological dose modelling

The dispersion model results are utilised in calculating the radiological doses received by the population through various intake pathways using COSYMA code. Optimum counter-measures, based on avertable dose concept is also predicted using this code.

Normal and emergency operation

The system in its normal operation runs with a high release term (possibilistic source term) to simulate a Beyond Design Basis Accident (BDBA) scenario with all counter-measure options activated. An accident/event is sensed by IRODOS system using the reactor (NPP) status sensors and/or from the field environmental radiation monitors located around each NPP. The environmental radiation monitoring network planned in the form of two rings (one at ~ 500 m and another at ~ 1600 m) around each NPP to sense an accident is shown

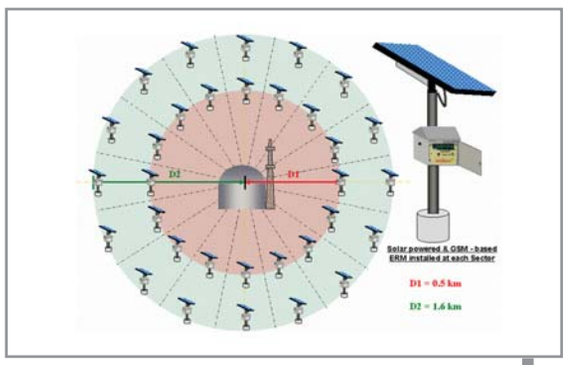

Environmental radiation monitoring network along with the solar powered radiation monitors

The indigenously developed solar powered environmental radiation monitors is to be used in this network. Data from these monitors are continuously received and updated at the IRODOS centre using GSM-based wireless data communication devices, inbuilt in the system.

Once an event/accident is sensed, IRODOS system switches over to an emergency mode. It calculates the likely source term based on the ring monitors (inverse calculations) or from the NPP status data. The atmospheric concentration and dose contours are updated based on this source term for early phase action. The entire dispersion and dose calculation with the new source term is activated along with the estimation of optimum counter measures, for later phase decisions.

Source term calculation

In IRODOS, there are two approaches for estimating source term:

(i) By using pre-release estimates (anticipated from Nuclear Power Corporation's Centralised Operating Plant Information System; COPIS), which are based on actual NPP process status (if available) and based on postulated accident scenarios.

(ii) By using post-release estimates based on the gamma dose rate measurements of the installed online radiation monitors.

The main assumptions used in estimating source term using second approach is that the integrity of the containment would remain intact, however, the release may occur through stack or through leakages at the ground level or both.

Measured dose rate D_{ik}, recorded at receptor (500 m or 1600 m) can be represented by

$$D_{ik} = \sum_{j} Q_j \times DRF_{ijk}$$

where 'i' is the index for weather category, 'j' is the index for height of release, 'k' is the index for receptor location, Q_j is the quantity of radionuclide released at height j and 'DRF' represents dose response function for respective i, j and k for unit activity (from a possibilistic mixture of radionuclides). Using the above relation and an iterative inverse approach a time-dependent source term (Q_j) along with likely radionuclide spectrum is estimated.

■ Geographical information system (GIS)

The atmospheric concentration, deposition and radiological doses are displayed on a GIS platform. The various data bases (layers) available in GIS include city and village boundaries, hospitals, schools, police and fire stations, sheltering and rallying points, vegetation cover and live stocks, transportation, logistics available, road network etc.

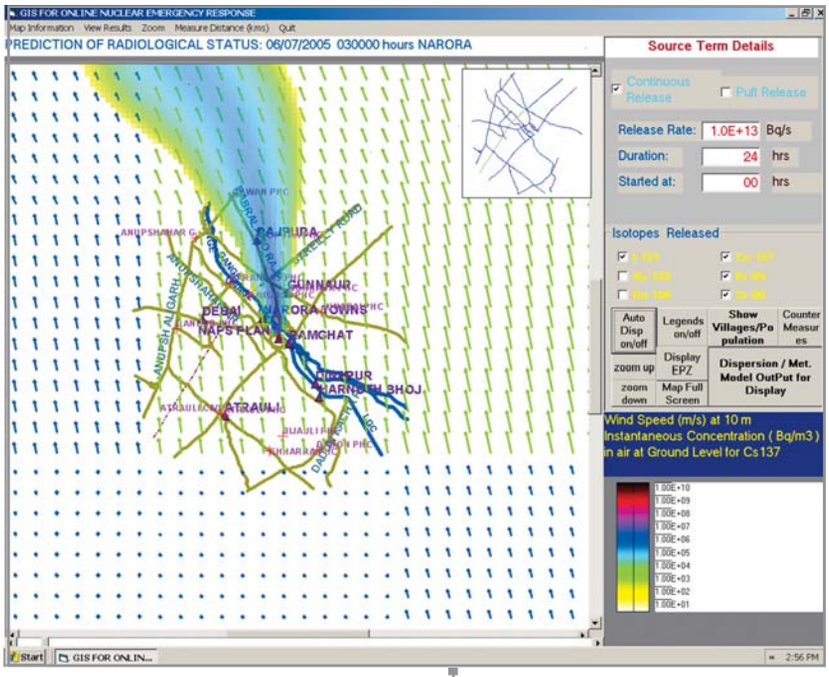

Typical ^{137}Cs concentration predicted for a hypothetical release at NAPS.

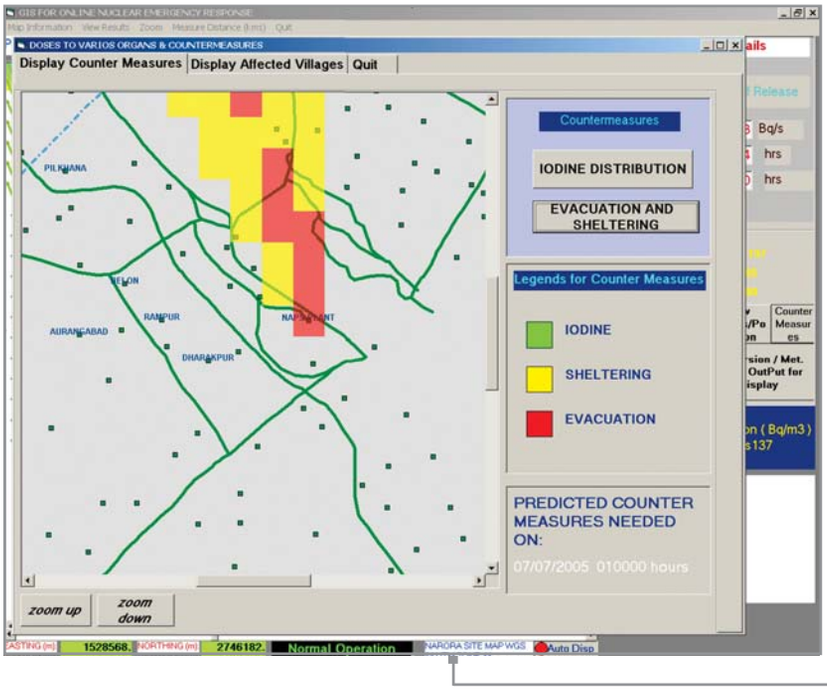

Countermeasures showing sheltering and evacuation areas for a hypothetical release at NAPS

Implementation of IRODOS

A prototype IRODOS system developed under this programme is operational for Narora Atomic Power Station, at BARC, Mumbai. The system after its initial laboratory scale testing is now ready to be installed at NPPs. It is planned to deploy these systems in a phased manner starting with NAPS, Narora, KGS, Kaiga and so on.

H.S. Kushwaha, <kushwaha@barc.gov.in>

4.3 MOBILE RADIOLOGICAL LABORATORY

Mobile Radiological Laboratory (MRL) has been developed by Internal Dosimetry Division of Bhabha Atomic Research Centre (BARC) for quick deployment to assess the radiological impact on the environment in the event of an accident involving radioactive material.

Mobile Radiological Laboratory

Such a situation can arise due to (a) accident involving transport of radioactive materials, (b) accident in a nuclear power plant, (c) loss of control over radiation sources in teletherapy units in hospitals and radiography units in industry, (d) use of Radioactive Dispersal Devices (RDD) by terrorists etc. If there is a nuclear accident with the release of large amount of radioactive substances into the environment, there will be a need to measure both the external and the internal exposure of the population. Quick information on radiological conditions is important to decision-making authorities and also to individuals and families. MRL has been equipped with necessary radiation measuring devices to carry out the required radiological monitoring and for speedy compilation of data in order to evolve and implement a suitable remediation strategy. It includes gamma ray dose rate monitor, gamma spectrometers, gross alpha / beta counters, whole body monitor, thyroid monitor, air sampling unit, self contained power supply unit, weather station, portable gamma spectrometric system for in-situ measurements, various radiation survey instruments etc. MRL is also useful for generating baseline data of radiological importance at sites such as proposed sites for nuclear plants and other nuclear facilities. MRL can also play an important role in the education of public regarding radiation safety.

■ Functions of MRL

MRL is used for training emergency personnel and for conducting public awareness programmes. In addition to the above, during a radiological emergency it serves the following purposes:

1. Quick identification of the affected areas following a radiological emergency and compilation of environmental gamma dose rates.

2. In-situ measurements for identification of radioactive contaminants and assessment of ground deposition of radioactivity and evaluation of dose rate due to ground deposition.

3. Collection of air samples to evaluate alpha and beta activity concentration in air and radionuclide identification.

4. Measurement of radioactive contamination in foodstuffs like milk, vegetables, drinking water etc. to decide about their use or rejection.

5. Measurement of external radiation doses received by members of the public.

6. Assessment of internal contamination (if any) of any person and/or representative groups of population using whole body counter.

7. Generation of meteorological data such as, wind speed, wind direction, temperature, solar radiation and relative humidity which are required for predicting radioactive fallout at other places.

8. Co-ordination with the aerial survey team by collection of ground level monitoring data of the region.

■ Description of MRL

MRL is built on a 10.70 m long and 2.55 m wide air-suspension Bus-Chassis to minimise the impact of jerks and vibrations on the installed instruments/ equipment. MRL is partitioned into four sections:

a) Driver Cabin (Length-1.80 m)

The main entr / exit door to MRL is on the left side in this cabin. Besides the standard vehicle controls, the controls for the diesel-based air-conditioner and a display indicating locked/ unlocked status of adjustable heavy equipment are located on the dashboard. A sleeper berth is provided behind the driver's seat. The entry from driver's cabin to the counting laboratory cabin is only by a number code.

b) Counting Laboratory (CL) Cabin (Length-5.0 m)

Most of the instruments /equipment associated with the functioning of the MRL are located in this cabin. These have been installed on and under an Equipment Table (ET) of cabin length. The computer for centralized data storage and analysis is housed in the projected central-section of the ET. Magnetic compass is located on the glass cover of ET. Alpha beta counting systems, weather station data logger and the control unit for operating the High Volume Air Sampler (HVAS) are fixed on the top of the ET and a 3 KVA on-line UPS is held below the rear section of the ET. The HPGe and NaI(Tl) detector systems housed in appropriate shields are located in the front and rear sides of the cabin, respectively. These detectors are used for measurement of radioactive contamination in environmental samples (soil, vegetation, drinking water etc). A Gamma Tracer unit is inserted in the roof and its data (ambient gamma dose rate) can be downloaded into the computer by aligning the IR remote sensor. There are two operator chairs (fixed) and a sofa-cum-bed, which converts into sleeper berths for two persons in this cabin. The hat-racks above the ET and space below the sofa provides storage place for other monitoring instruments such as survey meters, coveralls, nose mask filters, pocket dosimeters, other tools etc. Two Personal Computers (PCs) and a laptop have been networked to provide a centralised facility for the management of data obtained from the various monitoring systems. The gamma spectrometry data from the HPGe, NaI(Tl) and Whole Body Monitor systems are acquired by PC-MCA Add-on Cards. However, the data from gamma tracer, high volume air sampler, automatic weather station, alpha beta counting systems, Fieldspec and most of the survey meters, are transferred through a RS232 interface to a PC. The processing, analysis and evaluation of the entire data are performed in the MRL and the results can be transmitted to the desired station.

Counting Laboratory Cabin

c) Whole Body Monitor (WBM) Cabin (Length-1.80 m)

Whole Body Monitor, telescopic mast and its air compressor are located in this cabin. This cabin is approachable from the counting laboratory as well as from the utility cabin through the doors in the partition walls. A specially designed chair type whole body monitor has been installed for the assessment of internal radioactive contamination of the human body, in particular, thyroidal uptake of radioiodine. The chair shield is designed for equivalent lead thickness of 90 mm for back and

70 mm for sides. The chair is tilted backward by 15° to provide ease (in getting in and out of the chair) and comfort to the subject. The 300 kg detector shield, housing a 102 mm dia x 76 mm thick NaI(Tl) detector, is fixed to a horizontal arm which can be revolved to allow the subject in and out of the counting position and rotated to facilitate monitoring of specific body section.

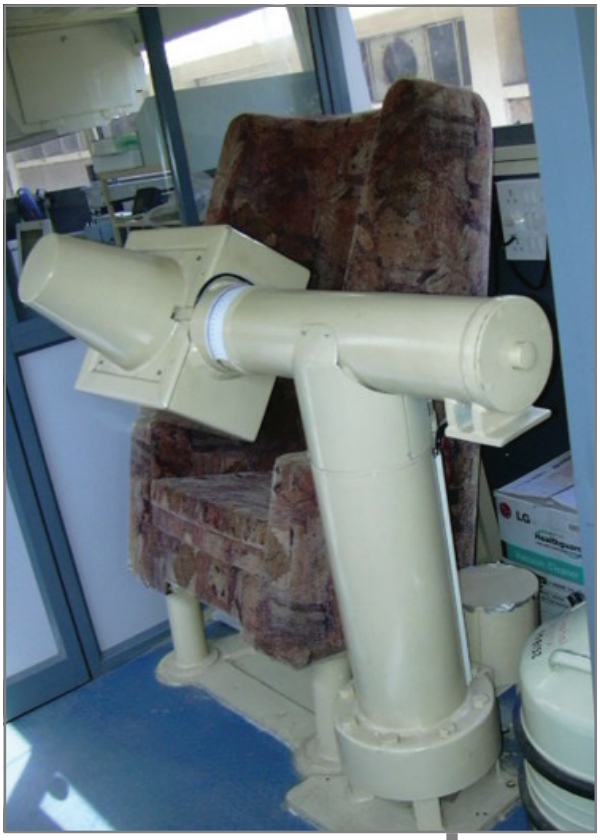

Whole Body Counter

d) Utility Cabin (Length-2.10 m)

It has two folding sleeper berths, a chemical toilet, a microwave oven, a 50 litre fridge, a mixer grinder and a water purifier. A CCD camera has been fitted in the rear to provide a continuous rear view to the operator on a 35.6 cm color TV in the CL cabin. The TV can also be turned towards the driver cabin for providing rear view to the driver through the mirror in front. There is a rear door with a folding ramp for carrying equipment in and out of the MRL.

Conclusion

A Mobile Radiological Laboratory has been developed to cater to a wide range of environmental monitoring requirements during routine and emergency conditions. If there is a nuclear emergency in public domain it will also be useful for carrying out whole body monitoring of the members of the public. In addition to this, the MRL can play an important role in training programmes and public awareness about the facts of radiation.

Katoch. D.S, Sharma. R.C, Mehta. D.J, and Venkatraj. V, **'A Mobile Radiological Laboratory for rapid response to radiation emergencies'**. BARC Newsletter No. 231, (2003).

Vijayagopal. P, Garg. S.P, Vidhani. J.M, and Pradhan. A.S, **'Rapid estimation of radioactivity in the soil of large areas using in-situ gamma-ray spectrometry'**. Paper presented at Thirteenth National Symposium on Environment (NSE-13), Shillong, June 5-7, (2004).

Vijayagopal. P, Singh. I.S, Garg. S.P, Vidhani. J.M, and Pradhan. A.S, **'Calibration of whole body counter in Mobile Radiological Laboratory for measurement of thyroid and whole body activity'**. Paper presented at International Conference on Medical physics (25th AMPI conference), Delhi, Oct 28-31, (2004).

Pradhan. A.S, Garg. S.P, Vidhani. J.M, and Vijayagopal. P, **'A Mobile Radiological Laboratory for Radiation Emergency in Public Domain'**. Paper presented at International Conference on Medical physics (25th AMPI conference), Delhi, Oct 28-31, (2004).

'Mobile Radiological Laboratory', A Sixteen page Brochure published by Scientific Information Resource Division, BARC, (2004).

Vijayagopal. P, Garg. S.P, Vidhani. J.M, Pandit. G.G, Shukla. V.K, and Pradhan. A.S, **'Study of the natural radioactivity in the sol and vegetation near Dahanu thermal power station'**. Paper presented at Fourteenth National Symposium on Environment (NSE-14), Hydrabad, June 5-7, (2005).

4.4 NUCLEAR AEROSOL TEST FACILITY (NATF) FOR REACTOR CONTAINMENT AEROSOL SIMULATION STUDIES

Identification of the accident scenarios and a detailed study of their environmental consequences are important in the area of research on the safety of nuclear reactors. In a scenario involving low probability, severe accident in a reactor, a large part of the radioactivity is expected to be released from the core and transported into the containment through the primary heat transport system. In the further event of the breach in the containment integrity, this radioactivity would be released into the atmosphere in the form of aerosols. Considerable efforts have been made towards a realistic assessment of the magnitude and nature of this release by using several computer codes. The crucial part of these codes involves the estimation of the source term into the containment and modeling subsequent behaviour by considering a host of interacting complex processes such as removal, coagulation, vapor condensation etc. To help the validation of these computer codes an experimental facility, termed as the Nuclear Aerosol Test Facility (NATF) has been set up at BARC. This article describes this facility and highlights the studies carried out.

■ Main components of NATF

Test vessel: The facility consists of a 12 mm thick stainless steel cylindrical test vessel with conical end fittings, having an air space volume of about 10 m^3 housed in a building. The height of the vessel is about 3 m and a total inner surface area is about 22 m^2.

The vessel is fitted with tubes at varying heights for sampling aerosols from the air space, thermocouples for sensing the gas and surface temperatures and a pressure gauge for monitoring the gas pressure. The temperature and pressure data are monitored online through a multi-channel scanner. Assemblies have been placed in the vessel for inserting deposition coupons at various locations. Provisions have been made for injecting steam into the vessel for wet aerosol studies and for passing aerosols through a water column for simulating particle decontamination in suppression pools.

Plasma Torch Aerosol Generator (PTAG): The main criterion for the selecting PTAG as an aerosol source for nuclear simulation studies is its capability to generate an intense source of aerosols of various materials. The concentrations required are of the order of few g/m^3 or, a generation rate in g/sec, which are met by PTAG system.

External view of Test vessel

Plasma Torch Aerosol Generator

This system consists of a Plasma torch and associated power supply capable of generating a sustained argon-nitrogen plasma flame of high temperature (~15000°C). Material to be aerosolized is injected in the form of a powder into the flame where it is vaporised. The vapours pass through a double-walled, water-cooled plenum chamber wherein they are quenched to form particulates. The flow rate in the chamber can be adjusted in the range 5-100 lpm as required. The level of dilution has considerable effect on the onward transport and settling of the aerosols. The generated aerosols are transported forward into the test vessel through tube, having several sampling ports.

Aerosol instrumentation: The type of aerosol instruments used depends on the aerosol characteristics to be examined as well as their size and concentration range. The aerosol gross mass concentrations are monitored with grab samplers in which samples are collected on high efficiency millipore membrane filters. Mass-size distribution of the particles have been measured by Cascade Impactors (CIs) (both 8-stage and 14-stage low pressure impactor). The masses collected on the stages are measured gravimetrically and by Atomic Absorption Spectrometry. Near real time mass concentrations may be estimated using the 10-stage Quartz Crystal Microbalance Cascade Impactor (QCMCI), which uses piezo electric crystals as mass monitors. Similarly, real time, number distribution may be estimated with laser particle counter, which operates on the principle of light scattering by particles. However, the real time instruments cannot be used directly at high concentrations and require diluters.

Andersen Cascade impactor

Experimental Studies in NATF

Several experiments with metallic powders (such as Tin, Zinc and Manganese) have been carried out in the test facility with the aim of validating the physical models used in aerosol behaviour codes. These models involve assumptions of spatial homogeneity of aerosols and processes such as diffusion, gravitational settling etc. for describing the coagulational and depositional rates.

The general protocols followed in the experiments were as follows. The powder to be aerosolised is sieved so that it falls in the size range of 30-70 μm and fed into the powder feeder at a feed rate of 2-5 g/min, through which it flows into the plasma torch. The aerosolised powder emerging from the torch is carried through the plenum chamber into the test vessel by the argon carrier gas and an additional flow of air (for oxide aerosols) or high purity argon (for metal aerosols) has been used for dilution.

The aerosol generation was continued for a period of about 15-20 minutes. During this period, grab samples were taken at the point of aerosol entry into the vessel every 2 min for estimating injection rates. The airborne mass concentrations were measured at two different depths in the vessel (Port 11 and Port 6 at 50 cms and 227 cms from the top respectively) to ascertain spatial uniformity of aerosols. After the generation was stopped, the mass measurements in the vessel at the two ports were continued at regular intervals until the concentrations reached near background levels. The total time of measurements varied from 200 - 4000 min. depending upon the experimental conditions. Measurements of mass-size distribution were also carried out at regular intervals using the cascade impactors. These samples were analysed either gravimetrically or using the Atomic Absorption Spectrometry (AAS) techniques later in the laboratory.

The experiments performed may be classified into two main categories namely, (I) under queiscent conditions and (ii) under turbulent conditions (achieved by running a fan placed at the bottom of the vessel). The data obtained under these conditions provide information on the homogeneity status of aerosols and then physical processes governing their depletion characteristics.

Results and discussions

Mass balancing Exercise: At the end of the experiments, mass balancing exercises were carried out to ensure that the masses deposited at every stage of the facility are accounted for. Masses in various parts of the aerosol generator, the plenum chamber and the test vessel could be accounted for within an uncertainty of about 25%.

Size Distribution Measurements: Bimodal size distributions, with one peak below 1 μm and the other greater than 2 μm were generally observed in most of the experiments. As time progressed, the peaks tended to merge. This is expected due to the interplay between the growth by coagulation and removal by wall losses.

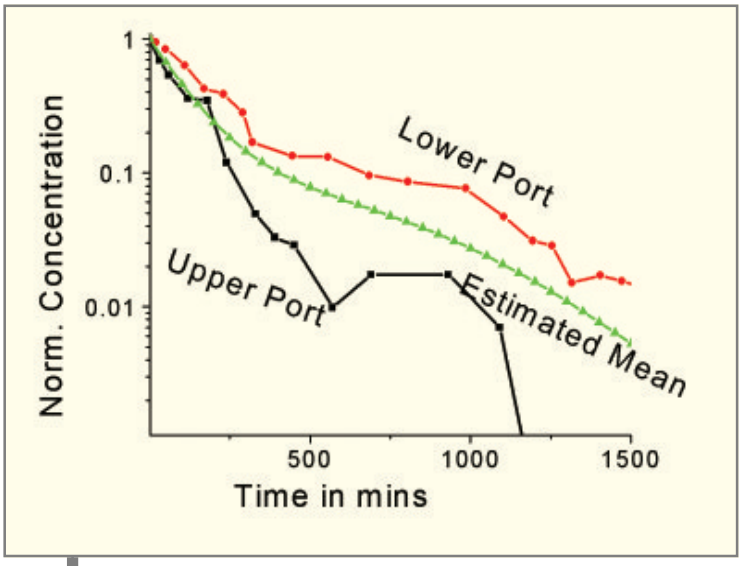

Concentration variation at two heights: aerosol stratification

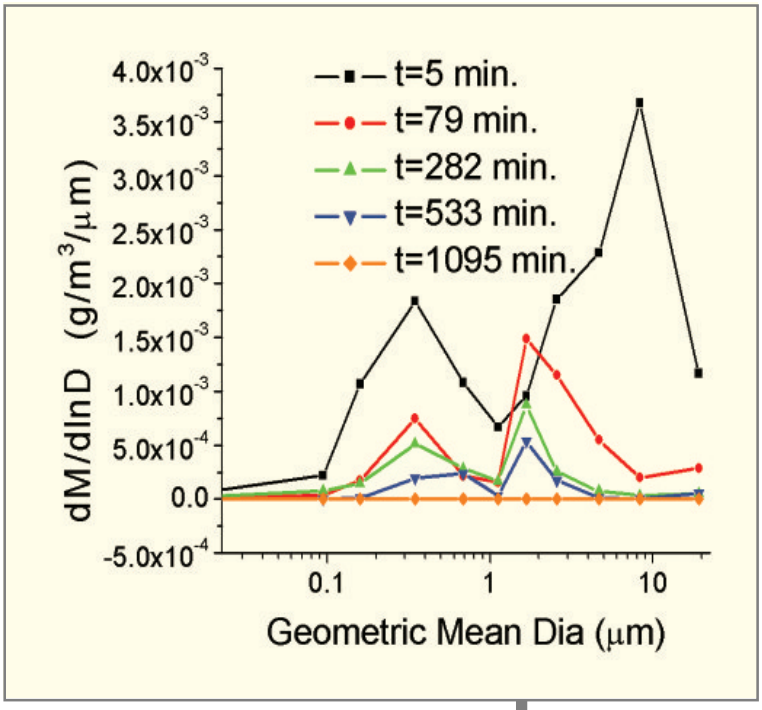

Observed size distributions at various times

Depletion of gross mass

In the experiments conducted under *quiescent conditions,* the upper level concentration decreased far more rapidly with time as compared to that at the lower level of the vessel. This behaviour clearly hinted at the effect of gravity induced stratification. This was modelled theoretically by including a bulk drift term into the aerosol dynamics equation. The theoretical results fitted fairly well with experimental data.

Also, the mean concentration generated from this theory showed a good fit to the predictions of NAUA-MOD5 code, thereby suggesting that although the code is unable to predict stratification, it is capable of correctly describing the time variation of mean airborne mass.

In contrast to the above, the experiments performed under conditions of persistent turbulence (due to fan) showed that the mass concentrations at the two levels were close to each other at all times. However, aerosol depletion rate was far more rapid. Besides, the mean aerosol lifetimes in the vessel was lower (76 mins) when the initial concentration was higher (0.9 g/m^3) as compared to the case of mean lifetime (111 mins) when the aerosol concentration was lower (0.3 g/m^3). This data is valuable for validating computer codes such as NAUA-Mod.5 and ASTEC. In fact, it is seen that the NAUA code predicted far slower depletion rates than the experiments

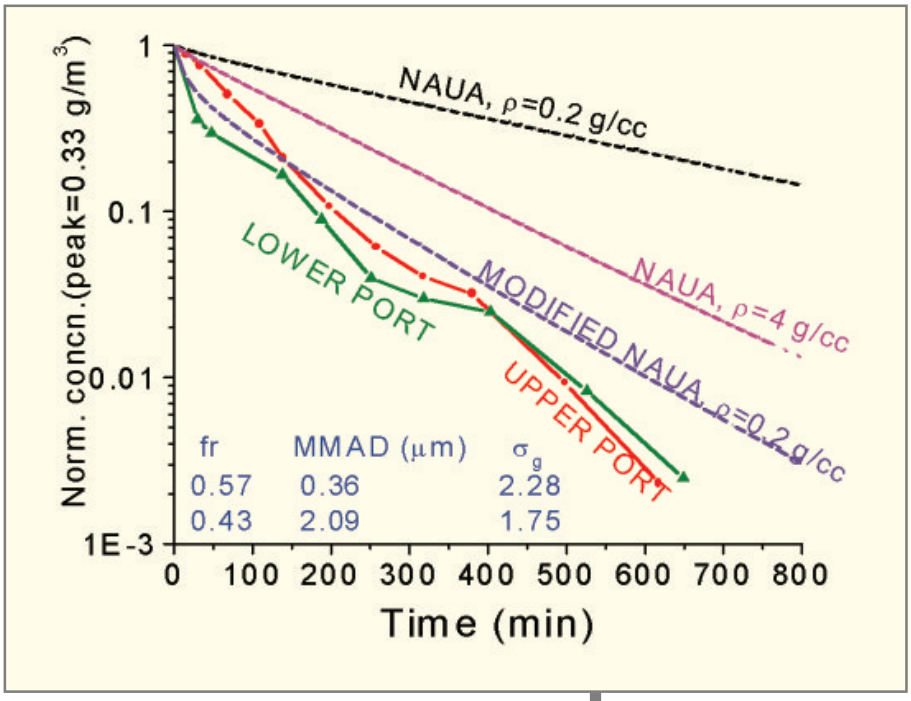

Comparison of mass depletion data under turbulent conditions with aerosol computer codes

indicate. This is attributable to the neglect of the inertial deposition effects by the NAUA code.

This observation led to the development of new formulae for deposition rate estimates that includes inertial effects in addition to turbulent and gravitational removal mechanisms.

Particle fractal dimensions

Gross measurements of aerosolized powder collected on petri-dishes hinted at the possibility of ultra low densities of the particles formed from PTAG. This suggested fractality of aggregates. A new method was evolved in order to determine the fractal dimension by simultaneously carrying out *in situ* measurements of mass and number size distributions using inertial impactors and optical particle counters. The fractal dimension is estimated through an analysis based on correlating it to the parameters of the observed size distributions. With this, the metal aggregates showed low fractal dimension (1.6) and hence a rapid decrease of densities with size. At about 1 μm the density of aggregates were found to be about 0.2 g/cc, far lower than the bulk metal densities of 7 g/cc. This is as expected from the cluster-cluster aggregation models generally employed to describe metal aerosol coagulation. These density estimates were used as input parameters in computer codes.

Conclusions

An aerosol test facility has been built and operated at the Bhabha Atomic Research Centre for carrying out nuclear aerosol behaviour studies from the point of view of validating the aerosol codes used in the context of nuclear reactor accidents. The results of several experiments carried out have been used to validate the aerosol deposition models used in the computer codes. The focus of the future experiments in the facility includes the validation of the codes that account for aerosol removal by condensation (i.e., in the presence of steam) and by bubbling through suppression pools. Also, it is intended that the facility be made available for studying several basic aspects connected with the evolution of high concentration aerosols, chief among them being the effect of the structure of the particles and the effect of electrical processes on the removal characteristics. These studies have the potential of making important contribution to our understanding of how nuclear aerosols behave in confined environments.

Y.S. Mayya, B.K. Sapra, Arshad Khan, Faby Sunny, R.N. Nair, Radha Raghunath, R.M. Tripathi, S. Ganju, S.G. Markandeya, V.D. Puranik, A.K. Ghosh, H.S. Kushwaha, K.P. Shreekumar, P.V.A. Padmanabhan, P.S.S. Murthy and N. Venkataramani (2005): **Containment aerosol behaviour simulation studies in the BARC nuclear aerosol test facility,** BARC/2005/E-03.

Sapra B.K., Arshad Khan, Faby Sunny, Mayya Y.S., Tripathi R.M., Raghunath R., Ganju S., Markandeya S.G. and Venkat Raj V. (2002) **"Aerosol behaviour in BARC-Nuclear Aerosol Test Facility: Objectives and experimental results"** Indian Aerosol Science and Technology Association (IASTA) Bulletin, 14(1), 199-201.

4.5 INSTRUMENTAL TECHNIQUE FOR ESTIMATING DENSITIES AND FRACTAL DIMENSIONS OF AEROSOL PARTICLES

For understanding the behaviour of an evolving aerosol system, it is necessary to have information on the structure and densities of aerosol particles, in addition to their size distribution. In the context of predicting the behaviour of nuclear aerosols released into containments following reactor accidents, the computer codes require density as an input parameter. Since a good part of the nuclear aerosols are formed from condensation from vapour phase, they are quite likely to lead to well-known fractal-like structures. The densities of these structures will be quite different from material densities in view of large voids present in the particles. While one can collect these particles on substrates and then estimate the densities of deposits by gravimetry and electron-microscopy, there is a possibility of an error in estimation as the densities post-deposition will be different from the densities when they were airborne due to restructuring. Hence it is essential that one estimates densities in-situ, i.e. in the air-borne phase itself. Several methods have been proposed in literature for determining the fractal dimension (and hence densities) by the tandem use of Differential Mobility Analysers (DMAs) and impactors. However, DMAs are expensive instruments not readily available in most situations. An alternative technique of obtaining fractal dimension and particle density by simultaneous *in situ* measurements of mass and number size distributions of polydisperse aerosols using inertial impactors and optical particle counters has been devised. These instruments are relatively inexpensive and are available in most aerosol laboratories. The fractal dimension is estimated through an analysis based on correlating it to the parameters of the observed size distributions.

■ Theoretical analysis

The density of a porous object is defined as the mass of the object contained in a sphere of radius equal to the geometrical radius (size) of the object. Unlike normal porous materials, in fractal objects, the density decreases monotonically with size. This is mathematically written as

$$\rho(d) = \rho_0 \left(\frac{d}{d_0} \right)^{f-3} , d > d_0 \qquad (1)$$

where, ρ is the density for a particle of geometrical diameter d, d_0 is the diameter of the primary particle which is supposed to be compact with material density ρ_0 and f is called the fractal dimension. This may be expressed alternatively as

$$\rho(d) = \frac{6}{\pi} B d^{f-3} \quad \text{where} \quad B = \frac{\pi}{6} \rho_0 d_0^{3-f} \qquad (2).$$

Thus the density of a fractal particle of size d may be estimated once the constants f and B are known. When aerosol particles of solid materials are formed by condensation of their vapours, they grow into approximately fractal structures by leaving large voids in the interiors. Their densities would decrease with size according to Eq.(1) or (2). As a result, they are far lighter than their parent materials and hence settle very slowly in air. For aerosols, the aerodynamic diameter d_a is the measure of the settling velocity. This is defined as

$$d_a = d\sqrt{\rho(d)} \qquad (3)$$

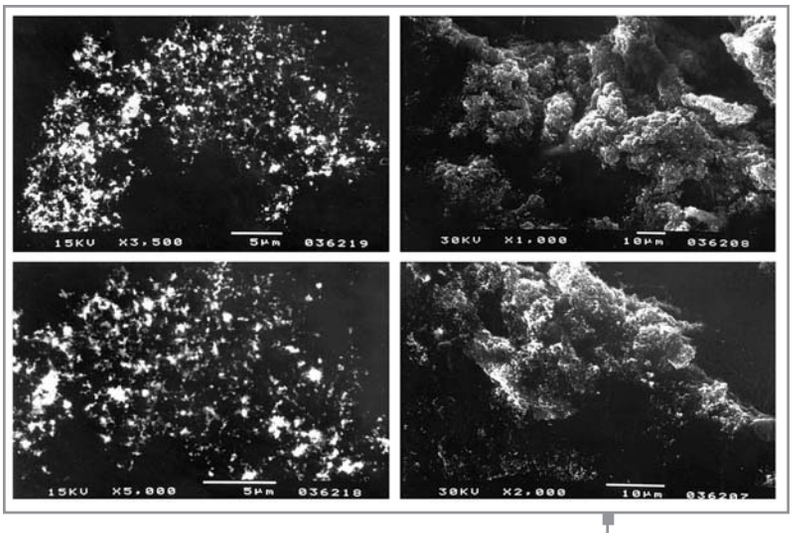

SEM micrographs of Zn aerosols produced using PTAG

Aerosol particles are generally polydisperse and the distribution of masses in different d_a categories is usually determined by sampling aerosol through cascade impactors. The Quartz Crystal Microbalance Cascade Impactor (QCM) accomplishes this by segregating particles in different d_a's and automatically weighing the masses deposited in each stage through a quartz crystal based sensing system. In brief, it provides the mass distribution function $\partial M/\partial d_a$.

Photograph showing: (a) Quartz-crystal microbalance cascade impactor (b) Optical particle counter

$$\frac{\partial M}{\partial d_a} = \frac{\pi d^3}{6}\rho(d)\frac{\partial d}{\partial d_a}$$

The geometrical diameter (d) of fractal particles is not unique, but would depend upon the method employed to determine it. In the present, we assume it to be the light scattering diameter of the particles. The determination of the number distribution of particles with respect to d (i.e. $\partial N/\partial d$) is accomplished by sampling the aerosol with an Optical Particle Counter (OPC). This instrument classifies particles according to the intensity of the light scattered by them as they enter a narrow zone of the laser beam.

It may easily be shown by deductive reasoning that the mass and the number distributions should satisfy the relationship

(4)

From the experimental data, the size distributions may be fitted to power-law of the form,

$$\frac{\partial N}{\partial d} = Ad^{-\beta} \quad \text{and} \quad \frac{\partial N}{\partial d_a} = Cd_a^{-\nu} \qquad (5)$$

where A , C, β and ν are the parameters obtained through the experimental fits. Upon manipulating Eq.(4) using Eqs. (1)-(3) and Eq.(5) , we can obtain an explicit expression for fractal dimension as

$$f = \frac{2\beta + \nu - 3}{\nu + 1} \qquad (6)$$

Correspondingly, the unknown prefactor B may be estimated by the implicit relation

$$C = \left[2AB/(f-1)\right](\pi\rho_s/6B)^{(f+1-\beta)/(f-1)} \qquad (7)$$

where ρ_s is the standard density with respect to which the impactor is calibrated.

Experiments and results

Experiments were conducted in the laboratory using three types of aerosols, viz., (i) ambient room aerosols, (ii) incense stick smoke aerosols and (iii) metal (Tin) aggregate aerosols produced using a Plasma Torch Aerosol Generator system. Number concentrations were monitored using the optical counter (PMS, LASAIR 1001) having 8 size intervals ranging from 0.1 -2.0 μm. Mass measurements were carried out using QCM having 10 aerodynamic size intervals ranging from 0.05-25 μm. The data was fitted to power-laws and the coefficients A, C, ν, β were extracted for number and mass concentrations respectively.

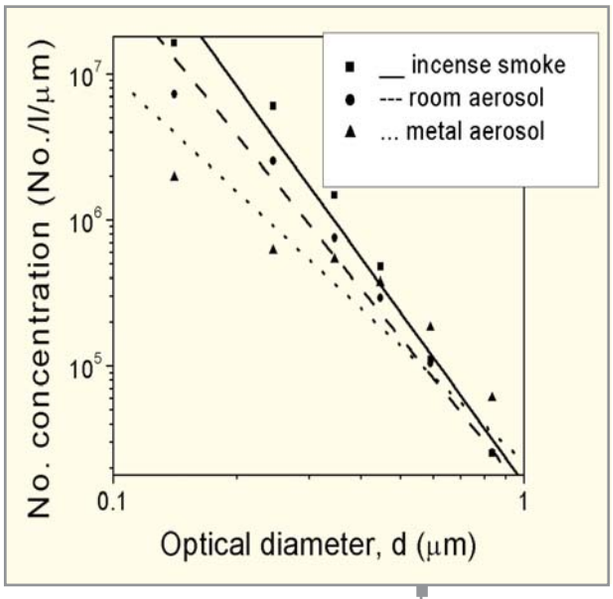

Number-size distribution

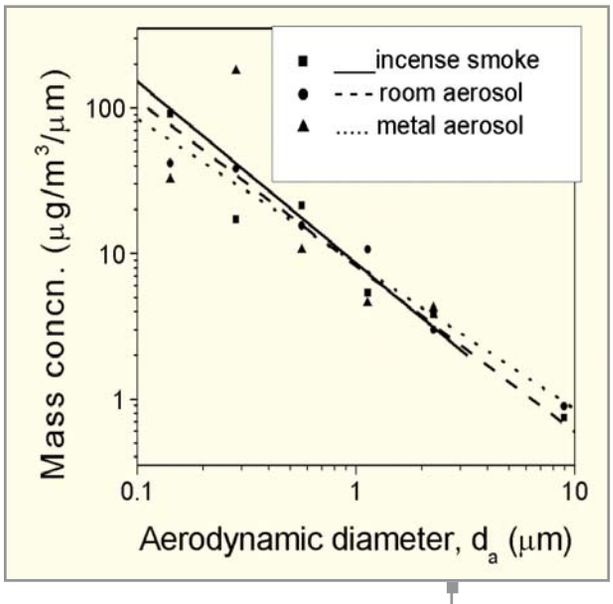

Mass-size distribution

The power-law fits were quite satisfactory. From these, the fractal dimensions and the density parameters were calculated for each of the cases using Eq.(7). The results are shown in the following table:

Optical dia. (μm)	Particle density (g/cc) for Room Aerosols	Incense stick aerosols	Metal Aggregates
0.2	2.0	1.4	2.7
0.5	1.2	1.1	0.7
1.0	0.9	0.9	0.3
Fractal dim.	2.5	2.7	1.6

Discussions and conclusions

The incense stick-smoke and room aerosols yield fractal dimensions of 2.7 and 2.5 respectively indicating nearly compact structures. In contrast, the metal aggregates showed low fractal dimension (1.6) and hence a rapid decrease of densities with size. This is as expected from the cluster-cluster aggregation models generally employed to describe metal aerosol coagulation. In fact, classical theories predict particle fractal dimensions close to 1.8 for cluster-cluster aggregates.

The apparent densities of aggregate particles decrease to as low as a value of 0.3 g/cc for 1 μm particles. It was found that these densities were consistent with the crude densities of deposited materials obtained by collecting deposits in known volume and weighing.

The study has provided valuable input in validating aerosol behaviour codes in Nuclear Aerosol Test facility studies. It was found that the use of these realistic densities coupled with accounting for all the known deposition mechanisms agreed with experimental behaviour than the use of material densites. The technique appears to be suitable when the size distributions follow good power-law variations. Studies are in progress for validating the method through electron microscopy based measurements of size.

Le Bronec, E., Renoux, A., Boulaud, D. and Pourprix, M. (1999). **Effect of gravity in differential mobility analysers. A new method to determine the density and mass of aerosol particles.** J. Aerosol Sci. 30, 89-103.

Schmidt-Ott, A. and Wustenberg, J. (1995). **Equivalent Diameters of non-Spherical Particles.** J. Aerosol. Sci. 26, S923-S924.

Kutz, S. and Schmidt-Ott, A. (1993). **Experimental study of the influence of flow-conditions on the size distribution and structure of agglomerates.** J. Aerosol Sci. 24, S553-S554.

4.6 INDIGENOUS DEVELOPMENT OF PARTICLE AERODYNAMIC SIZE SEPARATOR (PASS)

Measurement of aerosol particle size distribution is important in a host of fields such as evaluation of inhalation hazard from radioactive and chemical pollutants, climate effect of air pollution, characterization of drug delivery systems to the lung and material synthesis. Although several techniques have been developed for size distribution measurements, the most widely used technique is based on inertial separation of particles using cascade impactors. Their popularity stems from the fact that they are quite rugged and require minimum supervision during field use; they directly yield information on aerodynamic diameters which are the required parameters for inhalation hazard evaluation. However, most commercially available impactors are expensive and in order to render them cost-effective for large scale use in environmental studies across the country, a unit referred to as the Particle Aerodynamic Size Separator (PASS), has been designed and developed. It is based on the principle of inertial impaction and separates particles according to their aerodynamic diameters in the range of 0.53-10 μm in seven class intervals. Being indigenous in design, it may be fabricated on a commercial scale at a cost much less than that of the imported units. This instrument will be of help to several national laboratories and universities for carrying out studies on atmospheric pollution and aerosol characterization.

■ Advantages of this system

Apart from the cost factor, PASS has the following few additional useful features over the imported impactors:

1) It operates at a higher flow rate thus enabling a quicker collection of samples for analysis.

2) It can be loaded with any desired number of stages other than the maximum of seven, depending upon the requirement of the user.

3) It has a new design for the collection plates to reduce inter-stage losses.

Assembled view of Particle Aerodynamic Size Separator

It may be easily assembled by the use of stud-wing nut arrangement.

■ Working principle

In an impactor, the particle-laden air emerging from an orifice strikes a collection surface and is forced to take a 90° turn around it. Particles having their aerodynamic diameters above a certain critical value (cut-off diameters) tend to proceed straight towards the impaction plate due to inertia (collection plate) and get deposited on it, whereas particles with lower inertia will remain in the air stream. Thus the impactor separates the particles into two specific groups; viz., the deposited particles of aerodynamic diameters larger than the cut-off diameter and the airborne particles of aerodynamic diameters lower than the cut-off diameter. The dependence of the collection efficiency of an impactor stage on particle size may be expressed uniquely as a function of a dimensionless parameter, known as the Stoke's number (*Stk*), defined as

$$Stk = \frac{\rho_p C_c d_p^2 U}{9\eta W}$$

Where

ρ_p = particle density
d_p = particle diameter
Cc = Cunningham slip correction factor
U = average air velocity at the nozzle exit
W = nozzle diameter
η = air viscosity

In the present system, the stage cut-off aerodynamic diameters ($D_{50} = d_p \sqrt{\rho_p}$) for each of the stages are specified by a Stokes number (Stk_{50}) that yields 50% collection efficiency. The other governing parameters such as the flow rate (Q), nozzle sizes (W) and number of nozzles (N), throat length (T) and plate to nozzle spacing (S), etc. are determined by using an elaborate system of conservation and constraint equations to optimize the deposition characteristics of the particles. The design takes into account optimization w.r.t cross flows from adjacent nozzles, both jet and particle Reynolds numbers and bounce off considerations.

Specifications

The PASS assembly consists of:

1) Base plate with three rods for tightening the full assembly and three wing nuts.

2) Inlet cone.

3) Stages 1-7, reckoned serially from the top.

4) Back-up filter stage.

5) Impaction substrate holder- 7.

6) Solid collection substrates - 7.

7) Air mover pump fixed at a suction rate of 45 lpm.

Components of PASS Unit

Performance testing and calibration

The unit has been calibrated both for its integral performance and the cut-off characteristics. The integral performance evaluation is assessed by comparing the size distribution parameters of various test aerosols obtained by this unit with that obtained by other available impactors. To standardize the cut-off characteristics, a simple calibration method using well characterized, nebulizer generated polydisperse aerosols has been evolved. The unit has also been tested for its sharpness of stage response, i.e. variation of the collection efficiency with particle size.

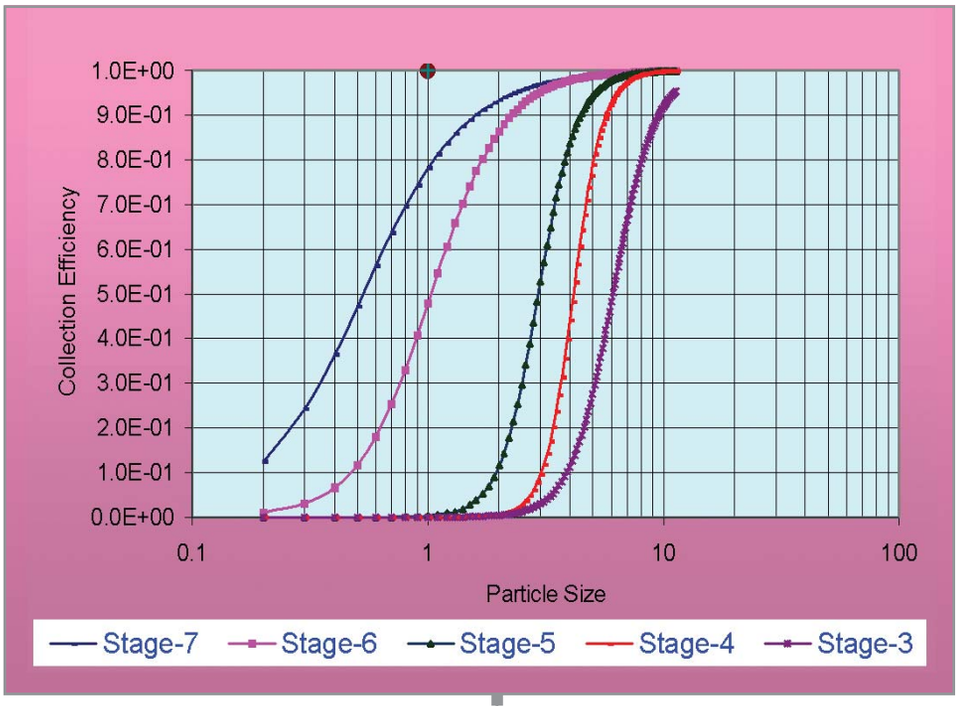

Response functions for the Impaction stages of PASS

Stage No.	Cut-off diameter (μm)
1	8.95
2	7.91
3	6.09
4	4.15
5	2.94
6	1.03
7	0.53

Stage Cut-off diameters of PASS

Based on the experience of PASS, a low pressure size separator known as PASS-LP, that can separate particles in the range of 0.1-25 mm in 11 size classes has been designed and fabricated. This operates at a flow rate of 10 lpm and is suited for determination of size distribution of radioactivity and chemical composition in the environment. The unit has shown satisfactory overall performance and detailed experiments are being conducted to examine its suitability for practical applications.

Sanjay Singh, Arshad Khan, Tanmoy Das, B. K. Sapra, Pushparaja and Y.S.Mayya (2005), **Indigenous Development of an aerodynamic size separator for aerosol size distribution studies,** Current Science, vol 88, no. 8, pp 1426-1433.

Sanjay Singh, Arshad Khan, R. Balasubramaniam, B.K. Sapra and Y.S. Mayya (2003), **Indigenous development of a dual configuration cascade impactor,** Proceedings of the conference at IIT, Bombay, Advances in Environmental Sciences and Engineering, AE-08.

4.7 ELECTROSTATIC CHAMBER FOR MEASURING THORON IN EXHALED BREATH OF THORIUM WORKERS

Measurement of internal contamination of occupational workers engaged in handling radioactive materials is a challenging task in radiological protection. Thoron In Breath Measurement (TIBM) is a sensitive technique for estimating ^{232}Th body burden with which a small fraction of the Annual Limit of Intake (ALI) value of internally deposited thorium can be detected free of any external contamination. The measurement procedure is simple as it involves sampling the exhaled breath of the subject for say 10 to 20 mins. Thoron formed from Ra-224 in the thorium decay series is a short-lived gas having 55 sec. half life. Thorium being in secular equilibrium with its daughter products, estimating thoron activity in the body directly leads to the activity of thorium in the body. Thoron produced in the body can be estimated from the measured concentration in breath and from the knowledge of an average breathing rate of a subject and the fraction of thoron that is exhaled of that produced in the body. Double Filter techniques were used for thoron-in- breath measurement earlier which are now replaced by the more sensitive Electrostatic methods. This simple technique can also be used for assessing the internal deposition of ^{233}U by assessing the deposition of ^{232}U which is always present at ppm levels in ^{233}U.

■ Description of the system

The ElectroStatic Chamber (ESC) is an aluminum cylinder of 35 litres capacity (height 52 cm, diameter 29.2 cm) with an air-tight lid and an electrode suspended at 10 cm from top which is maintained at negative potential. The subject breathes thoron-free air from a delay chamber and breathes out into the electrostatic chamber through a nose–cum face mask. This air enters the chamber through an inlet at the bottom and decays in the transit volume and exits through the outlet at the top. A replaceable thin aluminium plate of 5 cm diameter is held tightly below the electrode facing the inlet stream for collection of positively charged thoron daughter products. The progeny atoms mainly constituting ^{212}Pb and ^{212}Bi, collected at the electrode are later counted for its alpha activity using a ZnS scintillation counter for about 18 hrs after a delay of 5 hrs after sampling. The 5 hr delay ensures the decay of short lived radon daughter products which form the background and also an adequate build up of ^{212}Bi from the decay of ^{212}Pb which has a half life of 10.6 hrs. The concentration of thoron-laden air entering the chamber (thoron in exhaled breath) is estimated from this measured activity by using appropriate calibration factors. The activity of ^{224}Ra and that of Thorium are estimated from the measured thoron concentration by assuming that about 9% thoron is exhaled from the body into human breath.

Thoron-in-breath measurement system

■ Calibration procedure

Although simple in principle, the calibration of the system is a challenging task in view of the complications arising out of the short-lived nature of thoron and its consequent spatial inhomogeneity in the chamber. It is necessary to examine various issues relating to flow dynamics, radioactive decay and electrostatics in order to arrive at a reliable calibration factor. For this, several systematic experiments at various flow rates and electric fields were carried out.

A steady concentration of thoron source was produced online by passing room air through a ^{228}Th Pylon source with the help of a vacuum pump. The air flow rate through the source during sampling was monitored accurately with the flow meter, as any fluctuation in the flow rate would alter the concentration of thoron generated. The concentration of thoron during the entire sampling duration was measured online using a Lucas scintillation cell and its associated counting electronics.

Though classical Thomas's formula provides a relationship between the observed alpha counts and the mean chamber concentration, it is not of practical use as the chamber concentration cannot be directly measured during sampling. Hence, an appropriate mathematical formulation based on mixed flow model was evolved to establish a relationship between the chamber concentration and the inlet concentration. This provides a working formula linearly relating the inlet concentration to the observed alpha counts. The mixing model was experimentally validated by simultaneously measuring the inlet and the outlet concentration of thoron during sampling. It is seen that the measured values are close to the predictions of the mixing model and they are totally at variance with the values predicted by the commonly assumed stream lined flow model.

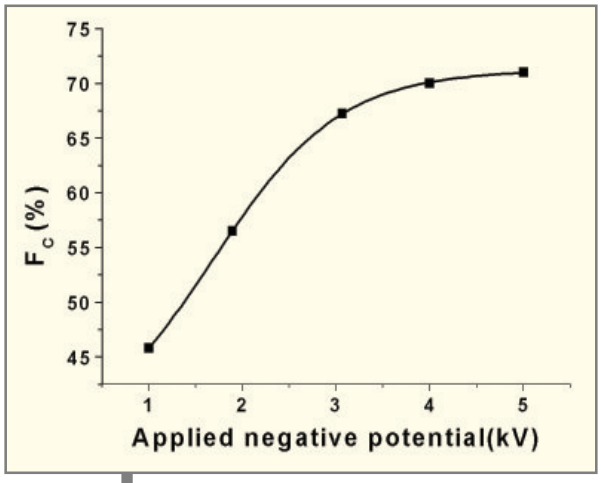

Collection efficiency vs. Voltage

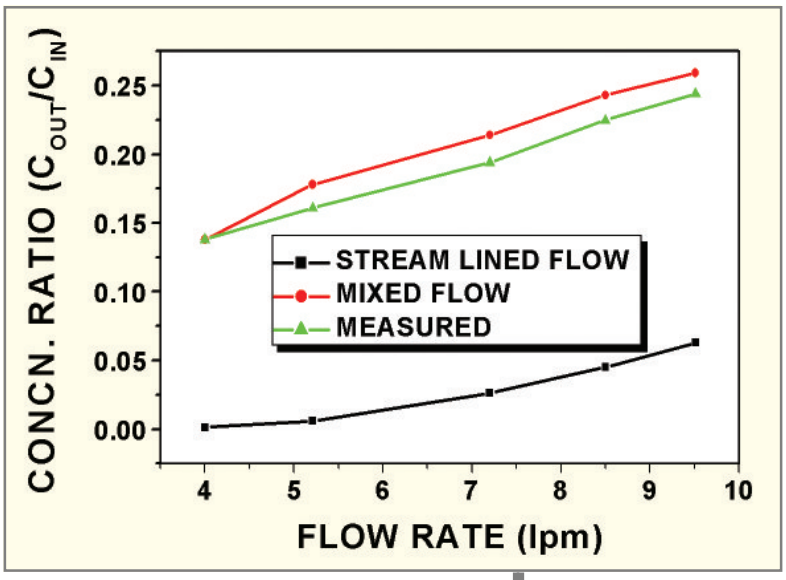

Validation of the mixing model used in calibration of the system

The electrical collection efficiency of the chamber, which is a fraction of ThB atoms collected on the plate to the total produced in the volume, was determined as a function of applied voltage ranging from -1 kV to -4 kV. It increases with voltage and saturates at a value of about 70 % at –4 KV.

A working formula is derived for the constant of proportionality *K* which linearly relates the inlet concentration to the total observed alpha counts and is an explicit function of the collection efficiency, flow rate, the counting schedule and alpha counter efficiency. *K* may be evaluated by the user as per experimental conditions. Minimum detectable activity of equivalent Ra-224 for this system has been estimated to be about 0.36 Bq.

Conclusion

This system is being used for estimating the thorium body burden of occupational workers in the thorium reprocessing facilities and in gas mantle industries. As India's nuclear programme envisages making use of our vast thorium reserves, it is expected that the present thoron body burden measurement system will have wide utility in the future.

Mayya, Y.S., Prasad, S.K., Nambiar, P.P.V.J.,Kotrappa, P. and Somasundaram, S., **Measurement of Rn^{220} in Exhaled Breath of Thorium Plant Workers.** Health Phys. 51(6), 737-744 (1986).

Mehta, D.J and Sharma, R.C. **An electrostatic apparatus for measurement of thoron in breath.** Radiat.Prot.Dosimetry 83, 249–256 (1999)

Thomas, J.W. **Thoron determination by Two Filter Method.** Health & Safety Laboratory Report No. HASL-TM-71-1 (1971)

Sathyabhama N., Eappen K.P. and Mayya Y.S. (2005), **Calibration of an electrostatic chamber for thoron measurements in exhaled breath.** Radiat. Prot. Dosimetry. Vol. 118, 61 - 69, 2005.

4.8 BIOPROCESS FOR DE-CONTAMINATION OF POOL WATER CONTAINING ^{60}Co

Bioremediation is gaining importance as an alternative technology for treating heavy metal and radionuclide waste and also for use in conjunction with the existing methods. The use of biopolymers especially the microbial exopolysaccharides which are often rich in hexuronic acids, are of current interest, as they display properties which make them attractive for use in bioremediation. On these lines, a bioresin termed as 'BARC bioresin' has been developed at Nuclear Agriculture & Biotechnology Division, BARC, which has an average diameter of 1 mm and can be prepared in bulk.

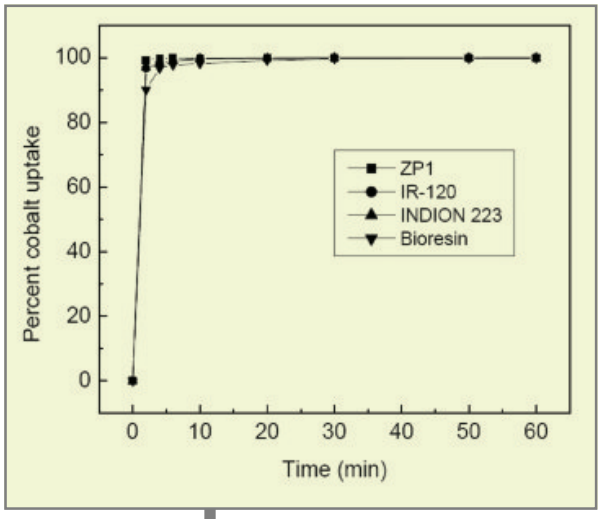

Kinetics of ^{60}Co uptake by different sorbents

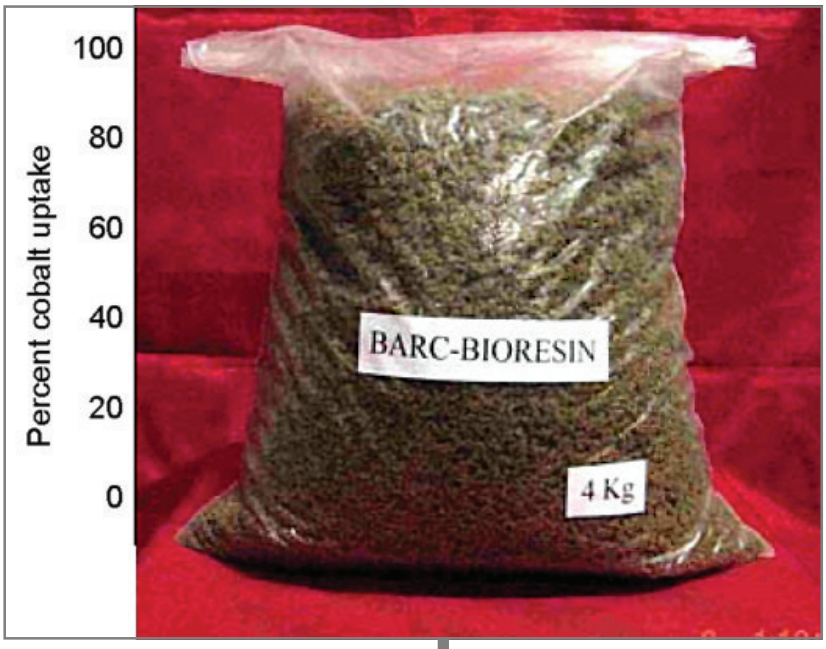

Packet containing BARC bioresin

BARC bioresin has been tested for remediation of ^{60}Co. A comparative study was carried out using different chemical ion-exchangers viz. zirconium phosphate (inorganic ion exchanger) IR-120 and Indion 223 (organic ion exchanger) and the bioresin, for the removal of ^{60}Co from aqueous solution. The kinetics was investigated and the uptake of Cobalt was found to be rapid and equilibrium was reached almost instantaneously.

■ Performance evaluation

In the presence of other cations like sodium ions, the chemical exchangers exhibited lower specificity for Cobalt than the bioresin. Another advantage in using the bioresin is the possibility for its incineration considering its biological nature/composition, unlike the chemical exchangers which are prone to toxic fumes. It is observed that on incinerating the bioresin loaded with ^{60}Co, it showed no loss in activity in the residue. Performance of the bioresin was then tested both at lab and pilot scale. A number of trials were carried out using different amounts of the bioresin packed in filters and perfused with the pool water at different flow rates. In the preliminary stages the bioresin was initially packed in one filter and then scaled up to three filters, pool water was perfused using a peristaltic pump. Finally the bioresin (2.1 kg) was tested on-line with the under water filtration system at flow rates of 5.5 m^3 / h to decontaminate 30 m^3 of pool water.

Set up using one filter

Set up using 3 filters

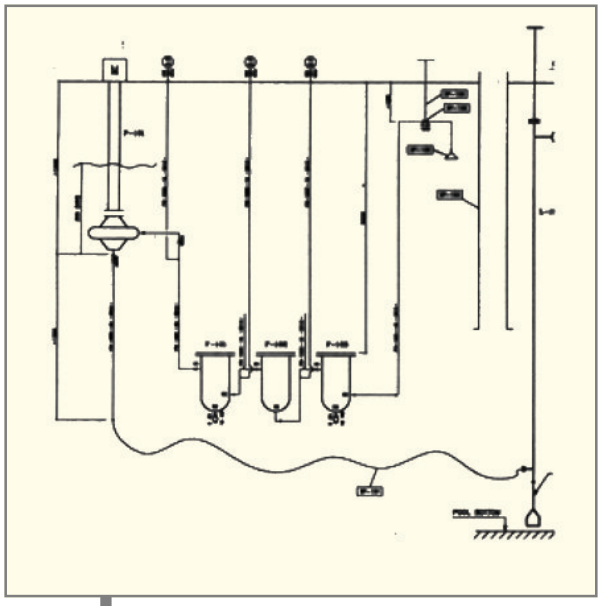

Schematic of the water filtration system

Filter used under water

Conclusions

The results indicated that saturation capacity of the bioresin for ^{60}Co was ~ 5.18 MBq /g. After circulating 30 m^3 of pool water through the filter under water, activity in pool reduced by 20 percent thus proving the efficiency of the bioresin even at high flow rates.

D'Souza S. F., Sangurdekar P. R., Melo J. S. and Pimputkar D. P. (2003) **Biosorption of 60Co: decontamination of pool water,** proceedings of the conference at BARC, Mumbai. Nuclear and Radiochemistry Symposium 2003.

Sangurdekar P. R., Melo J. S. and D'Souza S.F. (2005) **The behaviour of radioactive cobalt from aqueous solution on inorganic, organic ion exchanger and biosorbent: A preliminary study,** proceedings of the conference at BARC, Mumbai. Nuclear and Radiochemistry Symposium 2005.

4.9 APPLICATION OF ISOTOPE TRACER TECHNIQUES FOR GROUND WATER PROTECTION

Isotope tracer techniques provide valuable tools in protecting groundwater from pollutants. Pollutants from industrial and/or agricultural activities, enter through the unsaturated zone before ultimately joining the saturated zone. Once a groundwater is polluted it is rather difficult or impossible to take remedial measures for its protection. Groundwater being an important natural resource, it is essential to have clear understanding of the complex processes (physical, biological, chemical) occurring in the unsaturated zone, in order to protect it from pollution. A sizable population of national capital area Delhi is dependent on groundwater for their potable water requirement. Delhi also uses many landfills for domestic and industrial garbage disposal, which are potential contributors of pollutants to the groundwater in their vicinity. Environmental as well as artificial tracer techniques provide better insight in to the pollutant behavior in unsaturated or saturated zones. Herein two case studies are presented to illustrate the tracer techniques. First is the study at the Indian Agricultural Research Institute (IARI) farm site at New Delhi, wherein emphasis is given on the pollutants generated from agricultural activities, such as NO_3, pesticides etc. Tritiated water (^3H), ^{60}Co (a gamma emitting tracer in the cyanide complex form) and LiBr were used as tracers for this study. The second study illustrates the use of hydrochemistry and environmental isotopes for investigating contamination in groundwater near landfills sites in Delhi.

■ Case studies

Case study-1: Farm Site at Delhi

The artificial radioactive and chemical tracers were injected at 60 cm depth and depth profile of ^{60}Co tracer obtained after 5 irrigation events. In-situ measurement of ^{60}Co tracer displacement, helped in determining the depth of the soil core to be taken out for Li^+, Br^- and ^3H tracer displacement analysis. For the measurement of Li^+, Br^- and tritium tracer displacement, soil cores up to 3 m depth were taken after 5 irrigation events. Soil moisture was extracted from the soil core by vacuum distillation technique. Tritium tracer concentration in the moisture was measured by liquid scintillation method. In 1:1 soil extract Li^+ and Br^- ion concentrations were measured by ion chromatography.

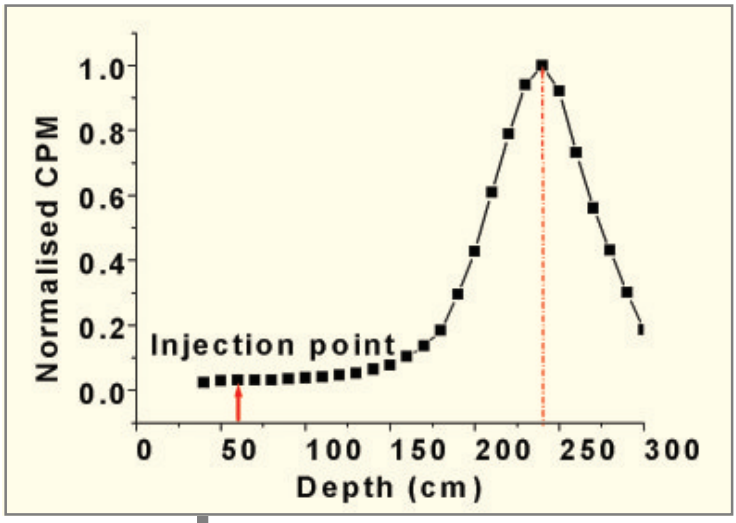

^{60}Co tracer profile in the unsaturated zone

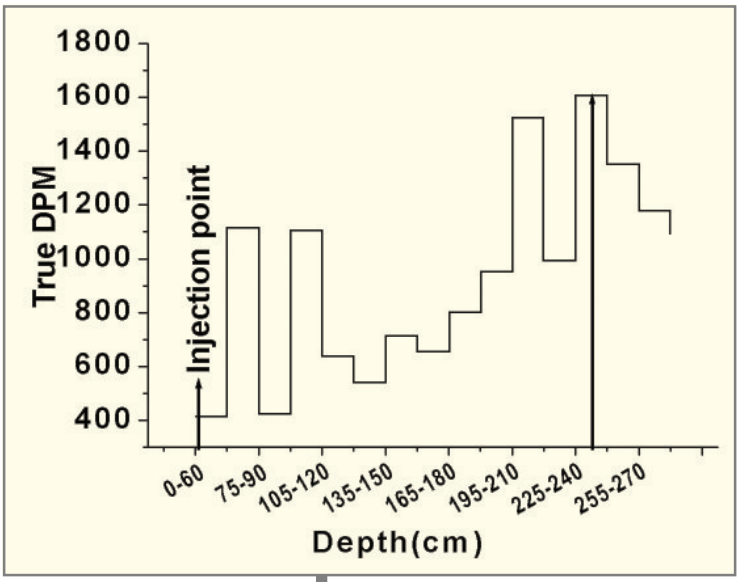

Tritium tracer profile

Tracer results indicated that pollutants move at different rate. Li^+ tracer (0.9m/6 month) lags behind other tracers indicating its increased interaction with the soil. As at 1.5 m depth the clay percentage is more in the formation, cations are retained by ion exchange process. Part of the ^3H tracer also gets exchanged with immobile water of the soil as 3 distinct peaks are seen in the tritium profile. After 5 irrigation events, tracer has displaced up to 1.8 m in six months. These results are based on 5 irrigation events, which are normally required for single crop cultivation.

Thus, the present study shows that, assuming steady state movement of the pollutant, the agricultural pollutants generated at IARI farm site would reach the water table in ~4 years. ^{15}N of NO_3^- is being employed to study the possible retardation of the nitrates due to any denitrification taking place in the unsaturated zone.

Case study-2: Landfill site

This study was carried out in collaboration with Central Groundwater Board, New Delhi, at two active landfill sites and one old landfill site in Delhi area. The objective of the study was to identify the extent of pollution of groundwater from the above landfill leachates. Hydrochemistry and environmental isotopes were used as evidence of contamination from landfills.

Samples collected from two active landfill sites Bhalsawa and Gazipur and one old landfill site I.P. Depot in the month of December 2003 and June 2004 were analyzed for isotopes ^{18}O, ^2H, ^3H and ^{13}C. Bhalsawa and Gazipur landfill sites are active landfills, which became operational in 1992 and 1994 respectively. The sites are underlain by thick clay layer mixed with sand and small stones. Water table is about 5 to 9 m bgl. Groundwater is brackish in the shallow zone and becomes saline with increasing depth. IP Depot is an old landfill site with a beautiful park developed on it.

Results

Landfill leachate sample shows 100 to 175 TU (1TU = 3.2 pCi/L) indicating the elevated levels of tritium in the landfills. Groundwater samples in the vicinity of landfill show tritium concentration varying from 5 to 20 T. Higher tritium concentration in the groundwater could be due to leachate contribution to the groundwater. As we move away from the landfills site, tritium concentration in ground water decreases, which indicates that leachate contribution to the groundwater, is localized.

Carbon-13 content of groundwater samples from main landfill site is enriched further indicating the contribution of landfill leachate to the groundwater. ^{13}C content also shows the direction of the spread of pollutant plume from the Gazipur landfill. Pollutant plume appears to be spreading towards northeast direction of the landfill site in Gazipur study area.

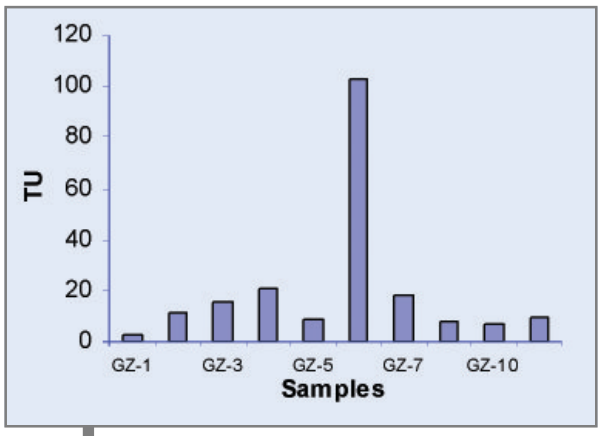

Tritium content of Gazipur samples

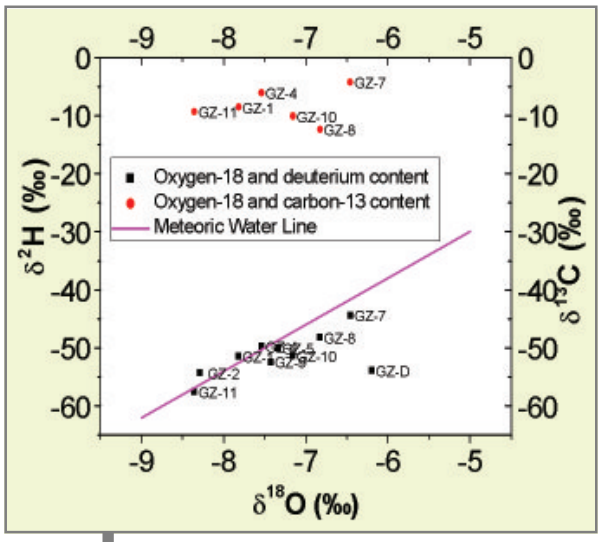

Plot of oxygen-18 vs Carbon-13 of samples from Gazipur landfill site

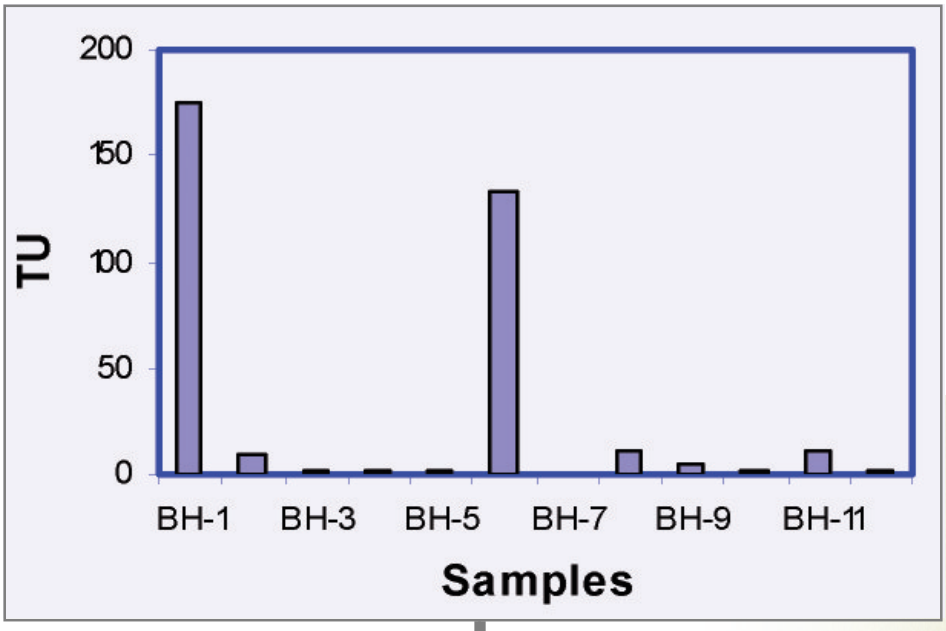

Tritium concentrations Bhalsawa samples

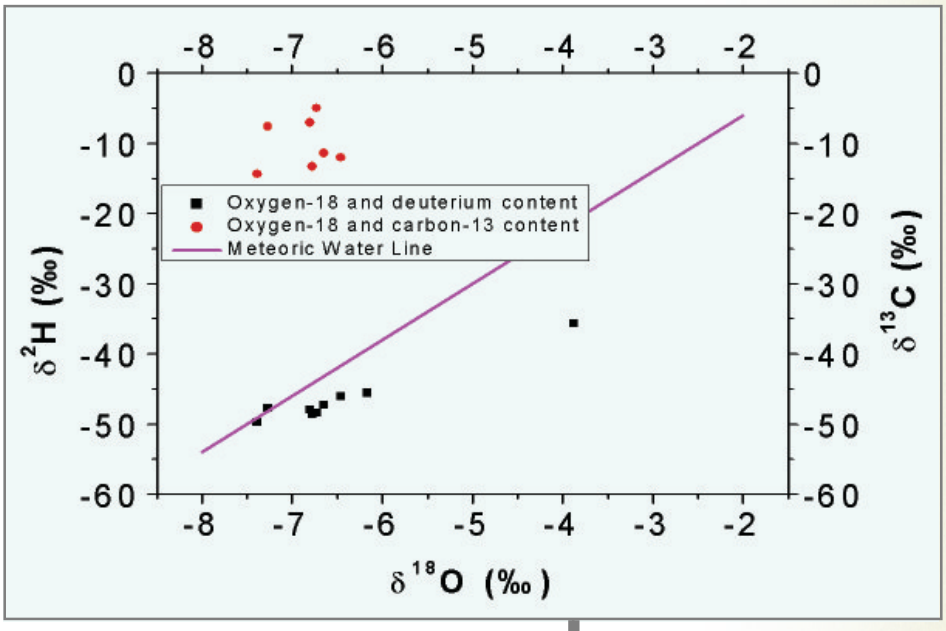

Plot of Oxygen-18 vs. Deuterium and Carbon-13 of samples from Bhalsawa landfill site

Conclusions

Assuming steady state movement of the migration of the pollutants in the unsaturated zone, the agricultural pollutants generated at IARI farm site would reach the water table in ~ 4 years. There is a minor contribution of landfill leachates to the groundwater in the vicinity of landfill sites studied. This contribution is localized and has an effect on shallow aquifer only.

Soil and groundwater pollution from agricultural activities, IHP-V, Technical documents in Hydrology, No.19, UNESCO, Paris, 1998.

Kulkarni, U.P., Navada S.V., Sinha, U.K., Datta, P.S., Sud, Y.K., Kulkarni, K.M., Aggarwal, P., **Stable isotopes and hydrogeochemical approach to understand mechanism of groundwater pollution in IARI farm, New Delhi,** Proc. Int. Conf. On Soil, Water and Environment quality, 2005.

Kulkarni, U.P., Navada S.V., Sinha, U.K., Datta, P.S., Sud, Y.K., Kulkarni, K.M., Aggarwal, P., **Radiotracer technique to study pollutant behavior in the vadose zone for groundwater protection,** Proc. INSAC-2004.

Kulkarni, U.P., Navada S.V., Sinha, U.K., Datta, P.S., Sud, Y.K., Kulkarni, K.M., Aggarwal, P., **Multi tracer technique to study pollutant behavior in the unsaturated zone.** Proc. Int. Conf. On Soil, Water and Environment quality, 2005.

Sinha, U.K., Kulkarni, K.M., Sharma, S., Ray, A., and Bodhankar, N., **"Assessment of Aquifer System Using Isotope Techniques in Urban Centers Raipur, Calcutta and Jodhpur, India",** IAEA-TECDOC-1298, 2002, pp. 77-94.

Lansdown, J.M., Quay, P.D. and King, S.L., **CH_4 production via CO_2 reduction in a temperate bog: A source of ^{13}C depleted CH_4.** Geochimica Cosmochimica Acta, 56: 3493–3503, 1992

4.10 INDIGENOUS DEVELOPMENT OF ISOTROPIC RF RADIATION MONITOR

High-power sources, including high-frequency (HF) sealers and TV/Radio broadcast stations, produce potentially hazardous radio-frequency (RF) fields in the frequency range from 1 MHz to 300 MHz. Potential hazard is evaluated in terms of the electric (E) and magnetic (H) field measurements and the induced body current measurements. Measurements of electric and magnetic fields in the near fields are difficult. The distribution of the fields is non-uniform and the polarization and the magnitude of the field vectors vary as a function of position without any correlation between the two fields. Thus, the electric and magnetic fields should be measured separately with the electrically small isotropic probes whose output voltages do not depend on the direction of the fields. The isotropic response is usually achieved by using three mutually orthogonal small-sized antenna elements (dipoles or loops). However, to achieve overall symmetry for the probe, additional sensor elements are mounted on the opposite sides of the cube. The increased complexity of this solution is justified by the clear advantages associated with a well defined electrical center and the cancellation of the mutual couplings. This probe has been developed for simultaneous measurements of electric and magnetic fields which facilitate the measurement of complex near fields, whereas, conventional RF radiation hazard meters are equipped with separate probes for electric and magnetic fields.

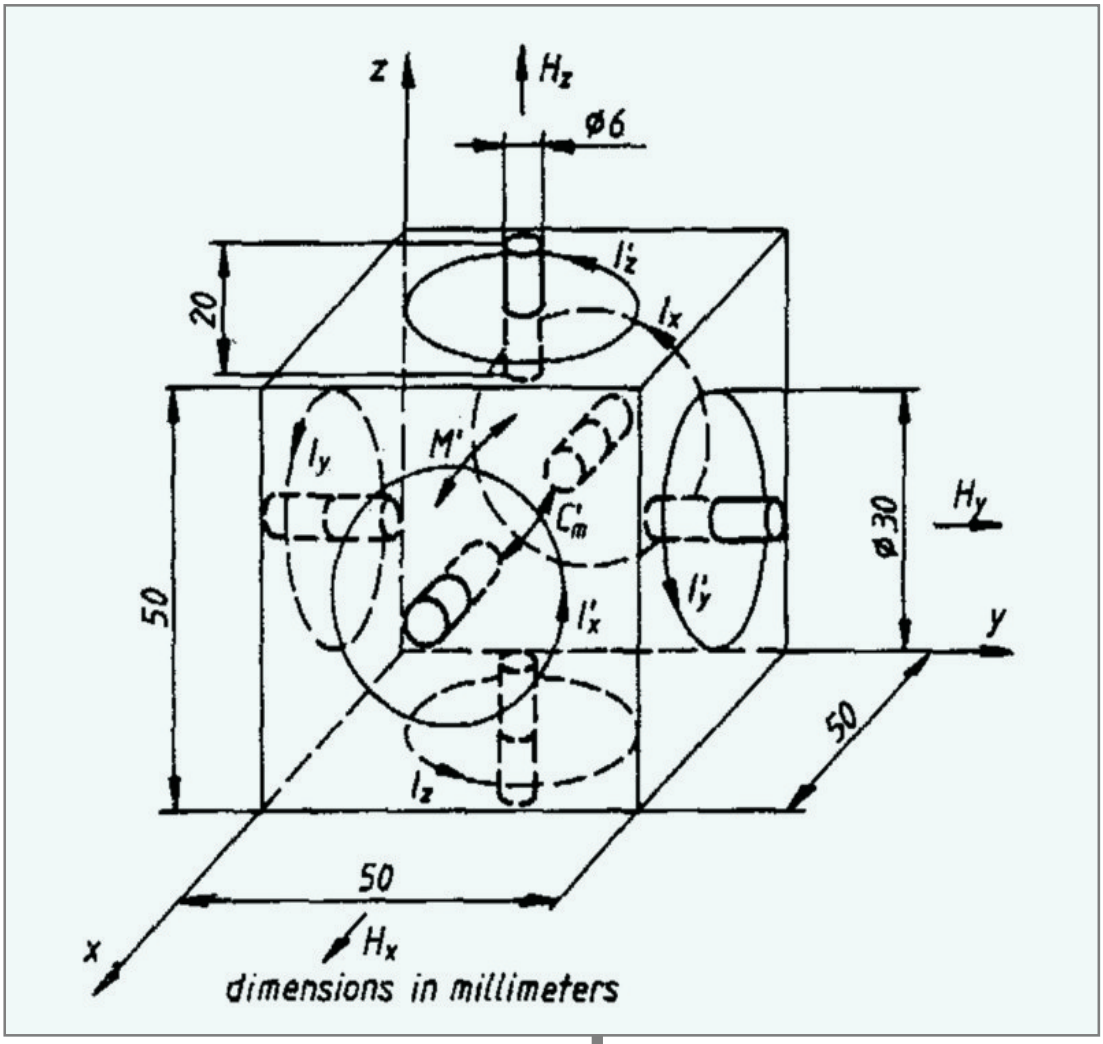

Six-face arrangement of dipole and loop antenna elements

The complete arrangement of the RF radiation monitoring instrument is located inside a thermocol structure.

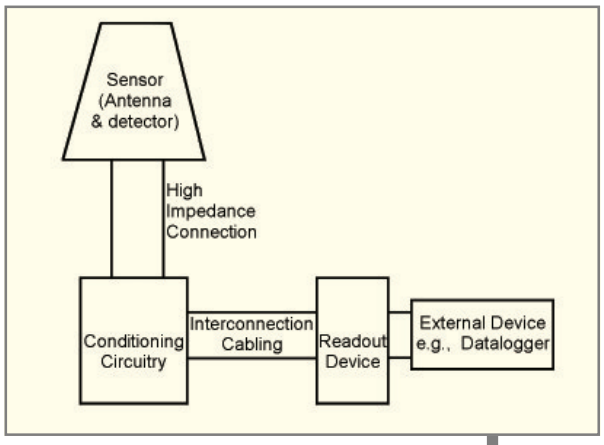

Main building blocks of the RF radiation monitoring instrument

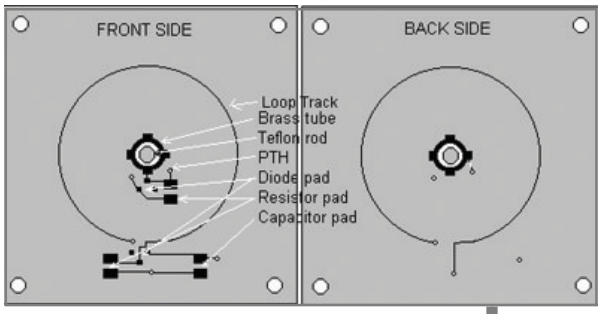

PCB layout for electric dipole and magnetic loop antenna

All the dipoles and loops are properly terminated with the detector diodes. The SMD diodes are mounted on the PCB with suitable surface mounted capacitors and resistors. Low-barrier zero-bias Schottky diode is used to rectify the small voltage appearing across it. Since the detector diode works in square-law region, small dc voltage is proportional to the square of amplitude of incident field. The electrically-induced voltages, from two opposite dipole sensors, are summed. High resistive lines of Nichrome (~1kΩ/m) transmit the detected signals inside the hollow probe handle to a distance of about 20 cm, where the lines coming from the opposite loop/dipole detector pairs are connected to the amplifying and conditioning circuit. The high resistance transmission lines attenuate and reduce the scattering of the incident field. The lines behave as a "Pi" low-pass filter network.

The signals from all the instrumentation amplifiers are added after passive filtration and displayed. The small size of the dipole and loop antenna results in a small output signal and the high output impedance results due to high impedance transmission lines. The signal conditioning and amplification system is built in order to ensure good DC performance. It has been designed for low quiescent current components, which are required to operate even at low supply voltage, thus making the electronics suitable for battery operation. Input stage of the conditioning circuit is carefully designed to achieve low offset and low drift errors.

Preliminary testing of the probe has been carried out using a TEM cell facility. The initial results are very encouraging. The sensing probe has shown expected sensitivity for both electric and magnetic fields with near field response.

This experimentation has resulted in the construction of a probe where dipole and loop sensors are placed at all sides of a cube, allowing simultaneous measurements of RF electric and magnetic fields in non-uniform near fields. An amplification and signal conditioning system for radiofrequency monitoring probe has been developed. The TEM cell is found to be useful for calibrating the RF probes. In particular, the preliminary measurement results demonstrate a relatively uniform field region in the cell where the effect of position error is small and accurate calibration is possible.

R.H. Chilkulwar, G. Joshi, C. I. Sujo , Shyam Mohan
<sujo@barc.gov.in>

4.11 SOLID-STATE SENSORS FOR TRACE GAS MONITORING IN THE ATMOSPHERE

Monitoring and control of toxic and combustible gases such as H_2S, NH_3, CO, NO_2, CH_4 and hydrogen etc. is necessary in laboratories and industrial areas where these are used as process gas or are generated as a byproduct. Some of these gases are also used for research and production facilities in DAE and therefore development of sensors for these gases is important. TPPED had taken up the development of several such gas sensors and sensors for H_2S and hydrogen have been developed. Further work on ammonia, CO, and NO_2 gas sensors is being carried out.

H_2S gas sensors: Hydrogen sulphide is a toxic gas with threshold limit value (TLV) of 10 ppm. Department of Atomic Energy has two heavy water plants based on H_2S and over 300 sensors are required at different locations in these plants. Solid state H_2S sensors based on SnO_2:CuO thin films deposited on polycrystalline alumina substrates have been developed for monitoring gas concentration in 0-50 ppm range. The films need high temperature for operation and for this purpose platinum heaters are fixed on the backside of the substrate. Platinum heater element also helps in monitoring the sensor temperature that is maintained at about 200°C using a temperature controller circuit.

Operating principle: The sensor film contains n-type SnO_2 and p-type CuO grains that form a large number of p-n junctions in the composite film. As a result, the sensors show a very high resistance (~1 GΩ) in air. In presence of H_2S, CuO cnoverts to metallic CuS (via $CuO + H_2S \rightarrow CuS + H_2O$), destroying the p-n junctions and the resistance of the film drops to low values (<10 kΩ, in 50 ppm H_2S). In clean air, CuS converts back to CuO (via $2CuS + 3O_2 \rightarrow 2CuO + 2SO_2$), and the resistance of the film restores to its high value. Thus, concentration of H_2S in air can be determined by measuring the electrical conductivity of the sensor film.

Hydrogen gas sensors: Hydrogen is a hazardous gas with Lower Explosive Limit (LEL) of 4 % in air. Pellistor-type sensors based on Pd:Al_2O_3 thick films have been developed. The sensors consist of two platinum wire heaters wound on polycrystalline alumina substrates and embedded with a glass coating. While one of these heaters (sensor element), is further coated with a Pd:Al_2O_3 thick film, the other is used as a compensating element. The Pd:Al_2O_3 film on the sensing element is also coated with a protecting teflon layer.

Specifications of H_2S sensor with control unit

Range: 0-50 ppm

Operating temperature: 200°C

Accuracy: 10% of reading

Response time: 3-5 mins

Recovery time: 1-3 mins

Alarm: Settable in full range

H_2S sensor with electronic display unit

Specifications of hydrogen sensor

Operating temperature: 100°C

Range: 0-4% of hydrogen

Accuracy: 0.1% hydrogen

Response time: 1 min

Recovery time: 1 min

Alarm: Settable at any concentration

Hydrogen sensor with electronic display unit

Operating principle: Sensor and compensating elements are connected in series and a current is passed so as to control the compensating element temperature at about 100°C. In absence of hydrogen, temperature of sensor element is nearly same. In the presence of hydrogen gas, palladium (on sensor element) acts as catalyst for exothermic reaction between hydrogen and oxygen leading to formation of water. This results in increase in temperature of sensing element and difference in temperature of sensing and compensating elements is a measure of hydrogen concentration.

Conclusions

Further studies on development of materials for toxic gas sensors are being carried out. Tellurium films have been found to show high sensitivity to various gases and have the advantage of room temperature operation. Polymer-based sensors for ammonia have also been developed. These are being investigated for long-term stability. Studies on composites of oxide semiconductors (such as ZnO and CuO) and conducting polymers are also being carried out.

Katti V.R., Debnath A.K., Muthe K.P., Kaur Manmeet , Dua A. K., Gadkari S.C., Gupta S. K. and Sahni V.C., **Mechanisms of drifts in H_2S sensing properties of SnO_2:CuO composite thin film sensors prepared by thermal evaporation,** Sensors and Actuators B 96 (2003) 245.

Kaur Manmeet, Gupta S. K., Betty C. A., Saxena Vibha, Katti V. R., Gadkari S. C., and Yakhmi J. V., **Detection of reducing gases by SnO_2 thin films: an impedance spectroscopy study,** Sensors & Actuators, B B 107 (2005) 360.

Katti V. R., Debnath A. K., Gadkari S. C., Gupta S. K. and Sahni V. C., **Passivated thick film catalytic type H_2 sensor operating at low temperature,** Sensors & Actuators, B 84 (2002) 219.

Saxena Vibha, Choudhury Sipra, Gadkari S. C., Gupta S. K. and Yakhmi J. V., **Room temperature operated ammonia gas sensors using polycarbozole Langmuir-Blodgett films,** Sensors & Actuators B 107 (2005) 277.

Sen Shashwati, Muthe K. P., Joshi Niraj, Gadkari S. C., Gupta S. K. , Jagannath, Roy M., Deshpande S. K. and Yakmi J. V. , **Room temperature operating ammonia sensor based on tellurium thin films,** Sensors & Actuators B 98 (2004) 154.

4.12 LUMINESCENCE TECHNIQUES : APPLICATIONS IN EARTH SCIENCES AND ARCHAEOLOGY

The phenomenon of luminescence, particularly Thermoluminescence (TL) and Optically Stimulated Luminescence (OSL), is extensively used in dating the kiln-fired objects/potteries (archaeological dating) or sun-bleached soil/sediment samples (geological dating). The basic premise of this technique is as follows:

1. Primordial radioactivity in the nature irradiates the soil continuously and causes luminescence signal in some minerals like quartz or feldspar found in the soil.
2. This luminescence signal, generated over the centuries, is erased either by heating (kiln firing) or exposure to the sunlight.
3. Luminescence signal, generated thereafter due to the dose (Gy) by primordial radioactivity, can be measured after calibration using TL or OSL techniques. Determining the soil radioactivity and the resultant dose rate (Gy/ka), the age of the sample can be estimated.

Methodology

1. A suitable mineral, quartz or feldspar, known to preserve the luminescence signal for millions of years, is extracted from the sample using physico-chemical procedures.
2. The dose received by the sample is determined by calibrating the luminescence signal using known doses using TL/OSL reader.
3. Radioactivity present in the sample is determined by gross alpha counting with Pairs technique, gamma spectrometry or Atomic Absorbance Spectrometry to evaluate the dose rate.
4. The ratio Gy/(Gy/ka) gives the age of the sample.

TL/OSL system routinely used in BARC for luminescence dating applications.

Gross alpha Counter with Pairs Technique, routinely used in BARC for determination of dose rate.

■ Applications

1. Dating of fossilised human skull

Ferricrete sample, collected from the surrounding of a well fossilised human skull found at a depth of about 6 meters from horizon at Bommayarpalayam, Tamil Nadu, was dated by geological dating techniques using blue light OSL. Quartz was extracted from the sample and the naturally accrued dose was evaluated by regeneration technique using Riso TL-OSL set-up. The natural dose rate was evaluated using the gross alpha counting technique and the age was found to be 166 ± 30 ka. This makes the finding of fossilised human skull the second oldest human fossil in India.

The age showed that in the human evolutionary stage Laterite Baby from Odai belonged to Homo sapiens of the Middle Pleistocene period.

The age of the skull also showed the age of ferricretisation — the process of clay changing into laterite — of the fluvial deposit on the East coast of India. It is believed by the geologists that this period represents the stage between Homo erectus and Homo sapiens or modern man.

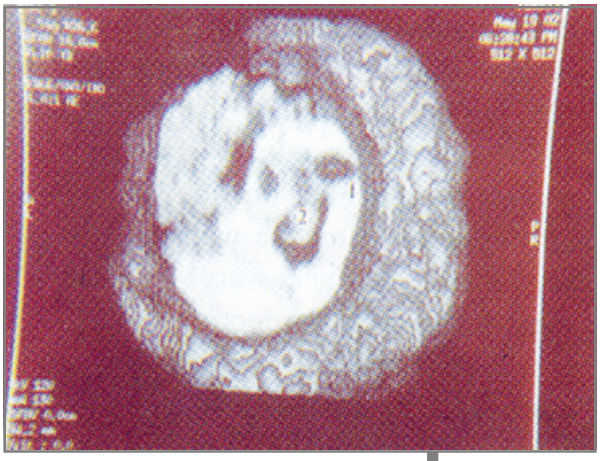

CAT Scan of the fossilised skull found in Tamil Nadu.

2. Dating of Desert sand from Sand dunes in Rajasthan

One sequence of two sand dunes near Jaipur Rajasthan was dated using feldspar extracted from twelve sand samples collected at different depths. Infra Red Stimulated Luminescence (IRSL) technique was used for dating the samples under a DST sponsored multi-disciplinary multi-organisational project. The age of the samples ranged between 7 (at 0.5m depth) –22 (at 4.5m depth) ka indicating that the desert in eastern margin of Rajasthan to be stabilised over past 7000 years. The sequences near Jaisalmer, western Rajasthan, dated under the project indicated the age of the samples to be as low as 70 years at

Two sand dunes at Amarsar, Jaipur where twelve samples were collected for dating.

0.5m depth indicating active sand migration in the western margin of the Rajasthan desert. It also indicated the desert not migrating towards Delhi. The age of the samples dated by BARC, when plotted against their depths also highlighted the past history of the dune building at Amarsar thereby giving an important input to geologists on the past history of paleoclimate, viz. the past arid and wet periods in the region. The solid line with lower slope indicates lesser time span for more deposition and hence dry period resulting increased desertification whereas dotted lines with higher slope indicates more time for lesser deposition and hence stabilised desert conditions.

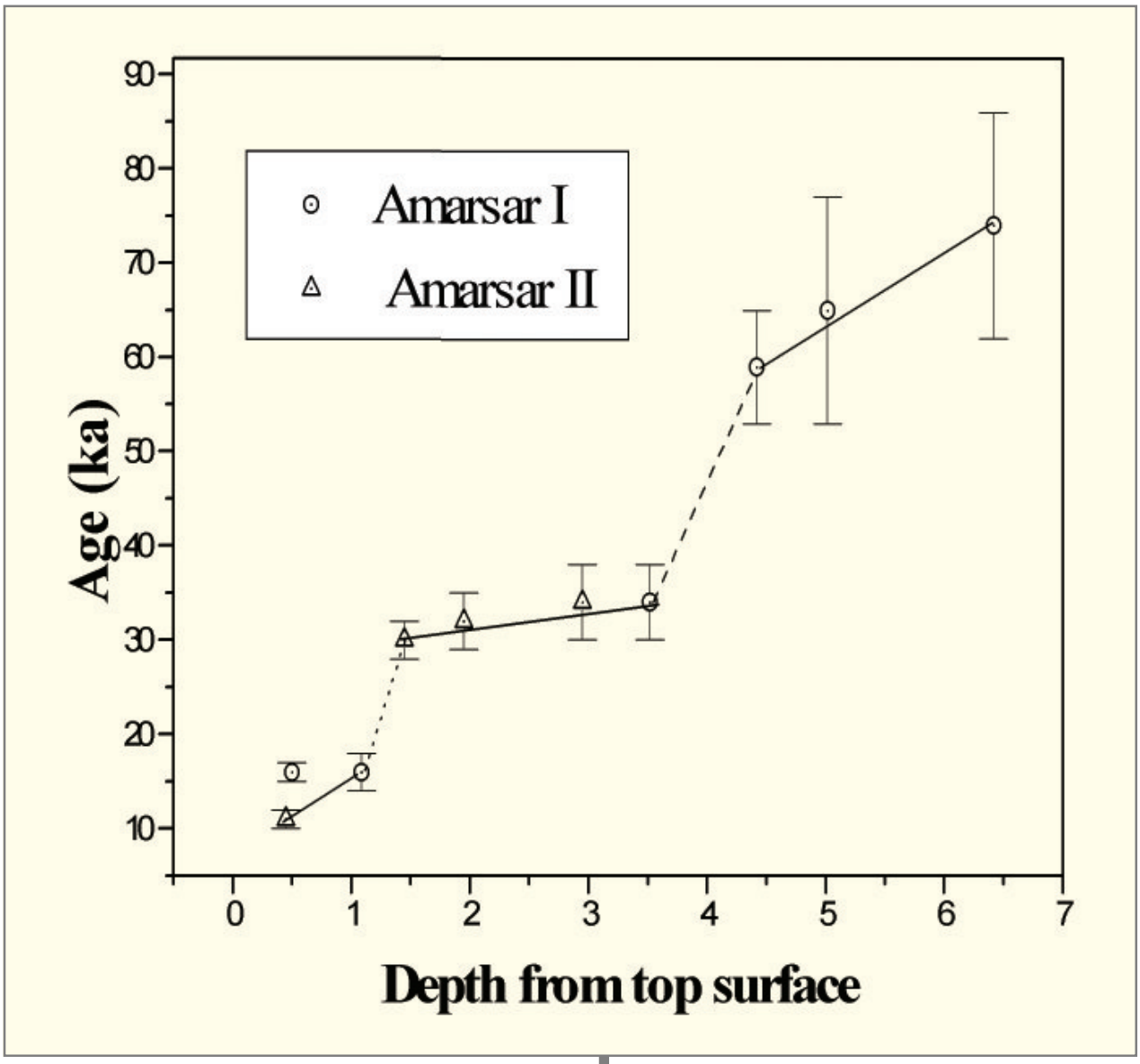

A plot of age of the sample vs depth shows the past history of the desertification in the region.

Dr. M.P. Chougaonkar, <puranik@barc.gov.in>